ISTANBUL TECHNICAL UNIVERSITY ★ GRADUATE SCHOOL

NOZZLE GUIDE VANE COOLING DESIGN FOR THE GAS TURBINE ENGINES

M.Sc. THESIS

Alparslan HALAÇ

Department of Mechanical Engineering

Heat - Fluid Programme

NOVEMBER 2024

ISTANBUL TECHNICAL UNIVERSITY ★ GRADUATE SCHOOL

NOZZLE GUIDE VANE COOLING DESIGN FOR THE GAS TURBINE ENGINES

M.Sc. THESIS

Alparslan HALAÇ
(503201103)

Department of Mechanical Engineering

Heat - Fluid Programme

Thesis Advisor: Prof. Dr. Hasan GÜNEŞ

NOVEMBER 2024

İSTANBUL TEKNİK ÜNİVERSİTESİ ★ LİSANSÜSTÜ EĞİTİM ENSTİTÜSÜ

GAZ TÜRBİNLİ MOTORLARDA TÜRBİN SABİT KILAVUZ KANADINDA SOĞUTMA TASARIMI

YÜKSEK LİSANS TEZİ

Alparslan HALAÇ
(503201103)

Makina Mühendisliği Anabilim Dalı

Isı Akışkan Programı

Tez Danışmanı: Prof. Dr. Hasan GÜNEŞ

KASIM 2024

Alparslan HALAÇ, a M.Sc. student of ITU Graduate School student ID 503201103 successfully defended the thesis entitled “NOZZLE GUIDE VANE COOLING DESIGN FOR THE GAS TURBINE ENGINES ”, which he prepared after fulfilling the requirements specified in the associated legislations, before the jury whose signatures are below.

Thesis Advisor :	**Prof. Dr. Hasan GÜNEŞ** Istanbul Technical University	.....
Jury Members :	**Prof. Dr. Aliihsan KOCA** Istanbul Technical University	.....
	Prof. Dr. Ali Bahadır OLCAY Yeditepe University	.....

Date of Submission : 26 November 2024
Date of Defense : 3 December 2024

To my family,

FOREWORD

I would like to thanks to my thesis advisor, guided and supported me throughout the thesis process, Professor Doctor Hasan Güneş.

I am thankful to Adem Yılmaz and Ali Akça for their support and guidance. Finally, I would like to say that I have dedicated this thesis to my family.

November 2024

Alparslan HALAÇ
(Mechanical Engineer)

TABLE OF CONTENTS

ABBREVIATIONS

NGV	**:** Nozzle Guide Vane
M	**:** Mach Number
R	**:** Specific Gas Constant
HTC	**:** Heat Transfer Coefficient
CFD	**:** Computational Fluid Dynamics
TBC	**:** Thermal Barrier Coating
RTDF	**:** Radial Temperature Distribution Factor
OTDF	**:** Overall Temperature Distribution Factor
GDT	**:** Geometric Dimensioning and Tolerancing
PS	**:** Pressure Side
SS	**:** Suction Side

SYMBOLS

r_p : Pressure Ratio
k : Thermal Conductivity
$\frac{dT}{dx}$: Temperature Gradient
h : Convection Heat Transfer Coefficient
T_s : Surface Temperature
T_∞ : Environment Temperature
L : Characteristic Length of the Surface
$\dot{Q}$: Radiation Heat Transfer Rate
ε : Surface Emissivity
σ : Stefan-Boltzmann constant
A : Heat Transfer Area
Nu : Nusselt Number
Re : Reynolds Number
w : Channel Width
L : Channel Length
T_{aw} : Adiabatic Wall Temperature
T_r : Recovery Temperature
T_j : Jet Temperature
T_∞ : Ambient Temperature
ρ_f : Density of the Film Cooling Air
ρ_∞ : Density of the Main Flow
V_∞ : Velocity of the Main Flow
P_{S_c} : Coolant Air Pressure
P_{T_g} : Gas Side Pressure
T_m : Mainstream Temperature
T_w : Wall Temperature
T_c : Coolant Gas Temperature
E^3 : Energy Efficient Engine

LIST OF TABLES

LIST OF FIGURES

NOZZLE GUIDE VANE COOLING DESIGN FOR THE GAS TURBINE ENGINES

SUMMARY

Compressor, combustion chamber, and turbine are main parts of gas turbine engines. Air enters from the compressor. The compressor works on the air. The pressure and temperature of the air is increased. Air has high temperature and high pressure enters the combustion chamber. Combustion occurs and the temperature of the gas is increased. After the combustion chamber air enters the turbine section. The first stop is the nozzle guide vane which is stationary airfoil in the high-pressure turbine location after the combustion chamber. Using the high pressure and temperature of the flow, the turbine drives the compressors. Gas turbine engines work with the Brayton cycle. According to the Brayton cycle, when the turbine entering temperature that is named with T_4 is increased, the efficiency of the Brayton cycle is increased. Therefore, T_4 temperature should be increased as possible as. High temperatures have negative effects on the nozzle guide vane in terms of strength, and life. Besides, the material service temperature limits the T_4 temperatures. Therefore, engineers thought of another solution. They found cooled vane and blade design. Compressed and relatively colder air according to the turbine section is used for the cooling of the vane. This air is provided by compressors at different stages. There are different ways of cooling of vane. Also, vane can be cooled inside or outside. The main philosophy of cooling is managing the heat transfer coefficient. Heat transfer coefficient distribution differs pressure side and suction side of the outside of the vane. Therefore, the location of film cooling holes is important in terms of the outside heat transfer coefficient distribution. The heat transfer coefficient is proportional to the increase of the Nusselt number. The increase in the heat transfer coefficient in the external flow, and therefore the increase in the Nusselt number, causes the gases coming from the combustion chamber to increase the temperature of the metal. Therefore, if the location of the film cooling holes is designed to locations where the heat transfer coefficient increases, better cooling is achieved. In order to increase the performance of the coolant flow inside the vane, it is necessary to increase the heat transfer coefficient. Moreover, as the turbulence of the coolant flow increases, heat transfer coefficient of increases for the inside of the nozzle guide vane. That's way various turbulator geometries are used inside of the nozzle guide vane. In this study, sample nozzle guide vane coolant geometry is designed. Part has film cooling holes for outside of the cooling. Also, impingement holes are located in leading edge of the part. Also, pin-fins are located in trailing edge of the part. That pin-fins increase the turbulence of air. Geometry is designed and checked with computational fluid dynamics software. Temperature distributions are found.

GAZ TÜRBİNLİ MOTORLARDA TÜRBİN SABİT KILAVUZ KANADINDA SOĞUTMA TASARIMI

ÖZET

Kompresör, yanma odası ve türbin bir gas türbinli motorun temel komponentlerindendir. Hava kompresörden girer. Kompresör akışkan üzerine iş yapar. Kompresörden geçen havanın basıncı ve sıcaklığı artar. Sıcaklığı ve basıncı kompresörde artmış olan hava yanma odasına girer. Yanma odasında meydana gelen yanmadan sonra gazın sıcaklığı artar. Yanma odasından sonra hava türbin bölümüne girer. Yanma odasından sonraki türbindeki ilk durak yüksek basınç türbininin sabit kılavuz kanadıdır (nozzle guide vane). Akışkanın enerjisini kullanan türbin, kompresörleri sürer. Gaz türbinli motorlar Brayton çevrimi ile çalışır. Brayton çevrimine göre T_4 ile adlandırılan türbin giriş sıcaklığı arttığında Brayton çevriminin verimi de artmaktadır. Bu nedenle T_4 sıcaklığın mümkün olduğu kadar arttırılması gerekmektedir. Yüksek sıcaklıkların türbin sabit kılavuz kanadı üzerinde mukavemet ve ömür açısından olumsuz etkileri vardır. Ayrıca malzeme servis sıcaklığı da T_4 sıcaklıklarını sınırlar. Bu nedenle mühendisler başka bir çözüm düşündüler. Türbin sabit kılavuz kanadını soğutacak tasarımlar buldular. Kanadın soğutulması için türbin bölümünden daha basınçlı ve daha soğuk hava kullanılır. Bu hava kompresörün farklı kademelerinden sağlanır. Türbin sabit kılavuz kanadını soğutmanın farklı yolları vardır. Kanat, içeriden veya dışarıdan soğutulabilir. Soğutmanın ana felsefesi ısı transfer katsayısını yönetmektir. Kanadın dışında basınç ve emme tarafında ısı transfer katsayısı dağılımı farklılık gösterir. Kanadın dışındaki ısı transfer katsayısı dağılımı, film soğutma deliklerinin lokasyonuna karar verirken önemlidir. Isı transfer katsayısı, nusselt sayısının artışı ile orantılıdır. Dış akıştaki ısı transfer katsayısının artması, dolayısıyla nusselt sayısının artması, yanma odasından çıkan gazların metalin sıcaklığını artırmasına sebep olur. Bu yüzden film soğutma deliklerinin lokasyonu, ısı transfer katsayısının arttığı lokasyonlara açılırsa daha iyi soğutma sağlanır. Kanadın içinde dolaşan soğutucu akışkanın performansını artırmak için ısı transfer katsayısını artırmak gereklidir. Soğutucu akışının türbülansı arttıkça, türbin sabit kılavuz kanadının iç kısmı için ısı transfer katsayısı da artar. Bu yüzden türbin sabit kılavuz kanadının içinde çeşitli türbülatör geometrileri kullanılır. Bu çalışmada bir türbin sabit kılavuz kanadı için soğutma geometrisi tasarlanmıştır. Parçada soğutma için film soğutma delikleri kullanılmıştır. Ayrıca parçanın hücum kenarında çarpma delikleri bulunur. Ayrıca parçanın firar kenarında pin-finler bulunur. Bu pin-finler havanın türbülansını arttırır. Geometri tasarlandıktan sonra hesaplamalı akışkanlar dinamiği yazılımı ile kontrol edilmiştir. Sonuç olarak sıcaklık dağılımları bulunmuştur.

1. INTRODUCTION

Humanity has always had a significant demand for energy. Humanity has looked for a number of ways to fulfil this energy requirement. They initially profited from nature because of this. Water resources and wind energy were used. New searches started when these resources ran out. The Industrial Revolution led to the greatest energy demand in recorded history. Coal, natural gas, oil, nuclear energy, and renewable energy sources have grown in significance in the modern era. Gas turbines also contribute to meeting this energy need.

High temperature creates problems in the operation of machines in many different areas. Elevated temperatures are critical in terms of degrading the mechanical characteristics of materials and reducing their lifespan.

Therefore, it was intended to reduce the adverse effects of this temperature in order to extend the parts' lifespan. This has been attempted to be accomplished in certain machines by cooling with water, in other machines by cooling with oil, and in other systems by cooling with air.

The thermodynamic Brayton cycle serves as the foundation for the operation of gas turbines. The compressor compresses and increases the pressure before sending the air to the combustion chamber in the Brayton cycle. The air in the combustion chamber gains energy from the fuel and is transported to the turbine at a high temperature. The turbine uses this fluid energy to create mechanical energy, which drives the compressor.

In gas turbines, high-energy air from the combustion chamber is introduced to the turbine stages in order to acquire this energy. This place has temperatures of about 2000K according to modern measurements. Creating efficient cooling technology is the answer to dealing with these temperatures, which are higher than the material limitations in the turbine.

Designing an effective and competitive gas turbine requires the ability to withstand these high temperatures. For this reason, the significance of cooling is highlighted. In order to maintain the mechanical qualities of the parts at high temperatures, it is crucial to develop suitable cooling systems.

Material technology is another factor that helps extend the life of parts that are used in hot environments. It seems that turbine intake temperatures have increased when comparing historical data to current data. Further advancements in cooling and material technologies are also critical to offset the rise in turbine temperatures.

High temperatures have disadvantage for materials in terms of structural criterias. High temperature resistant materials can overcome this problem. However, development of material technology takes long times that's why cooling configurations gain importance.

2. GAS TURBINE ENGINES

2.1 General Informations

As seen in Figure 2.1, the open cycle gas turbine system is comprised of the compressor, combustion chamber, gas turbine, and generator. Despite this, the inclusion of other compressors, turbines, reheaters, intercoolers, and fuel preheater exchangers can effectively improve both efficiency and capacity.

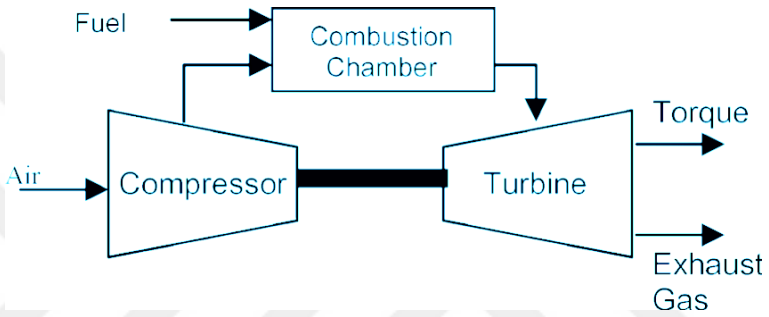

Figure 2.1 : Open Cycle Gas Turbine [2]

Gas turbine cycles can be classified under several headings: [19]

1. In terms of energy input
   (a) Constant volume gas turbines
   (b) Constant pressure gas turbines
2. Based on the type of cycle
   (a) Open system gas turbines
   (b) Closed system gas turbines
   (c) Combined system gas turbines
3. In terms of mechanical layouts;
   (a) Gas turbines with single shaft

(b) Gas turbines with multiple shafts

(c) Gas turbines with serial flow

(d) Gas turbines with parallel flow

4. Based on the used parts

(a) Simple gas turbines

(b) Gas turbines with regenerator

(c) Gas turbines with intercooler

(d) Gas turbines with reheater

5. Depending on the usage

(a) Stationary plant gas turbines

(b) Industrial gas turbines

(c) Electrical generator gas turbines

(d) Pump gas turbines

(e) Gas turbines used in vehicles

i. Gas turbines used in automotive

ii. Gas turbines used in railways

iii. Gas turbines used in marine

iv. Gas turbines used in aviation

A. Ramjet

B. Pulsejet

C. Turbojet

D. Turboshaft

E. Turboprop

F. Turbofan

A sample of gas turbine works based on a combined cycle is shown in 2.2.

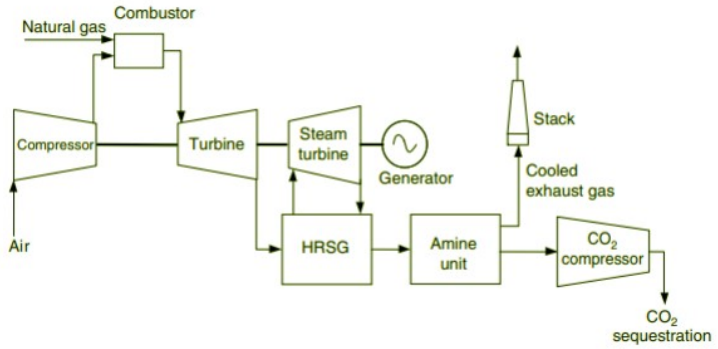

Figure 2.2 : Gas Turbine Combined Cycle [20]

Gas turbines are smaller machines compared to internal combustion engines in terms of specific mass and dimensions, which allows for high rotation speeds. Gas turbines are commonly employed in the fields of propulsion and electrical energy generation. The thrust power occurs from exhaust gases coming out of the turbine at high speed. These gas turbines are commonly used in aviation. An example gas turbine schematic is shown in Figure 2.3.

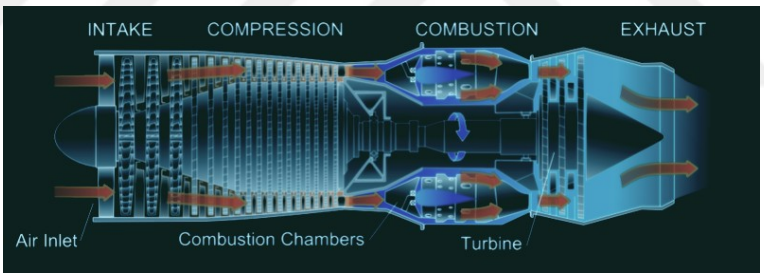

Figure 2.3 : Gas Turbine Working Principle [3]

Gas turbines operate in accordance with the Brayton cycle. Basically, mechanism of gas turbine engine which is turbojet engine can be said that;

- The compressor pressurizes the air from the atmosphere and the compressed flow goes to the combustion chamber.
- The combustion chamber is filled with fuel composed of air. Then burnt gases move to the turbine section.
- The thermal energy of gases at high temperatures and pressures is turned into mechanical energy in the turbine section. The final gases are sent into exhaust.

The heat energy of gas has a high temperature and pressure are coming from the combustion chamber to the turbine is used for obtaining the mechanical energy. The finished gases are released to the exhaust.

2.2 Historical Development of Gas Turbines

The idea of a turbine as a power source and the principle of reaction go back to the 130s BC when the philosopher Heron of Alexandria designed a simple reaction turbine. Figure 2.4 shows the first steam turbine from Heron. A turbine is a hollow sphere with two tubes that point in opposite directions. When water is boiled in a sphere, steam come out of the pipes and caused the sphere to turn.

Figure 2.4 : Heron's Gas Turbine [3].

Similarly, Giovanni Branca also designed such a turbine that is shown in Figure 2.5 in 1629. The turbine rotated as a result of the steam coming out of the steam jet hitting the turbine blades. The reduction gears also rotated cause of the rotating turbin.

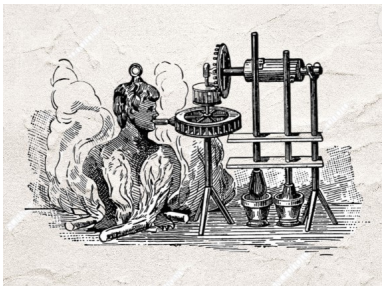

Figure 2.5 : Giovanni Branca Steam Turbine [3].

Sir Isaac Newton stated the possibility of jet reaction with his third law of motion, which he put forward in 1680. He also made a horseless chariot project in the same period. Picture of Newton's Horseless Carriage is shown in Figure 2.6.

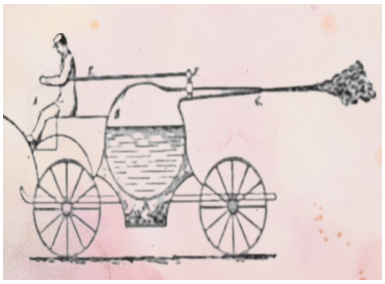

Figure 2.6 : Newton's Horseless Carriage [3].

The aforementioned engines, which utilize steam power, later served as benchmarks for gas turbines that operate with gases derived from the burned fuel with air. The Englishman John Barber devised and patented an innovative form of gas turbine in 1791. This engine, seen in Figure 2.7, is known as the first patented gas turbine. This design engine included a gas generator, a gas device, gas and air compressors, a combustion chamber, a turbine, and speed reduction parts.

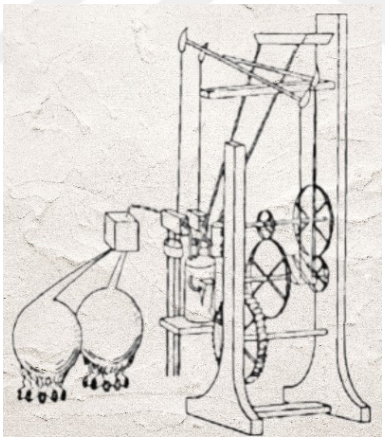

Figure 2.7 : The first gas turbine patent was granted to John Barber [3].

Many scientists made efforts to develop this type of engines in the following years. These names can be found in the following order: English W. F. Fernibough, French Armengaud and Lemale designed initial gas turbine examples. Stolze built an engine with a heat exchanger and a multi-blade turbine between 1900 and 1904, but the engine was not successful due to the very low efficiency of the turbine and compressor.

The inventor of steam turbines, Sir Charles Parson, patented an engine that resembled the design of today's modern gas turbines in 1884. The German H. H. Holzwarth created a constant-volume combustion gas turbine in 1905, and the Brown Boveri firm produced it in 1911.

After that, Brown Boveri operated commercial engines of the stationary or continuous combustion type for stationary installations, land, sea, and air vehicles.

British scientist Frank Whittle explained that a gas turbine could be used to provide jet propulsion for an aircraft in 1920. He used a axial turbine and a centrifugal compressor to provide power by compressing the air into the turbojet part in 1930. He also patented the first turbojet it's schematic view is located in Figure 2.8.

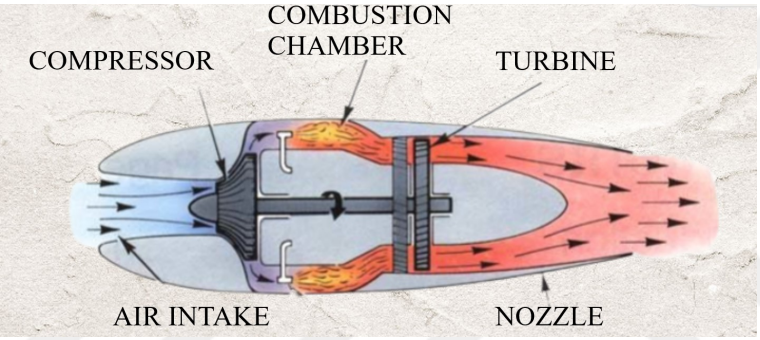

Figure 2.8 : Whittle turbojet engine schematic view section [3].

Currently, gas turbine engines are developed utilizing superior technologies. Currently, studies are being conducted to enhance efficiency. An example of modern gas turbines is located in Figure 2.9.

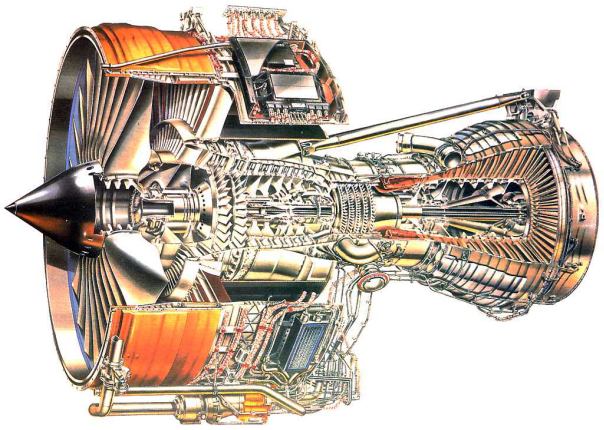

Figure 2.9 : Rolls-Royce Trent 800 Engine [4].

2.3 The Basic Principles of Gas Turbines

2.3.1 Brayton cycle

A simple gas turbine is combined of a compressor, turbine, combustion chamber, and output power connection assembled on a common shaft. A simple gas turbine schematic is located in Figure 2.10.

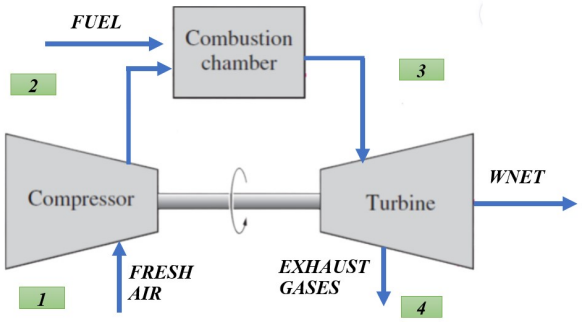

Figure 2.10 : An Open Cycle Gas Turbine Engine [2].

The Brayton cycle, consisting of four internal reversible processes, is the ideal condition for working fluid to go through in this closed loop:

- 1-2 Isentropic compression (in a compressor)
- 2-3 Constant-pressure heat addition
- 3-4 Isentropic expansion (in a turbine)
- 4-1 Constant-pressure heat rejection

The compressor takes atmospheric air from point 1 and increases it to the pressure at point 2 before sending it to the combustion chamber. Fuel enters the combustion chamber from a second location.

At constant pressure and continuously, the fuel sprayed into the atmosphere is burned. The gases that leave the turbines are discharged into the atmosphere from section 4 or disposed of to waste heat boilers as soon as combustion products have entered the turbine in section 3.

Theoretically, the exhaust gas pressure has to be at atmospheric pressures. Pv and Ts diagrams of this cycles are located in Figure 2.11 and Figure 2.12.

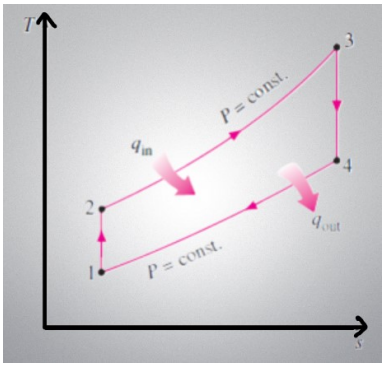

Figure 2.11 : T-s Diagram for the ideal Brayton cycle [2].

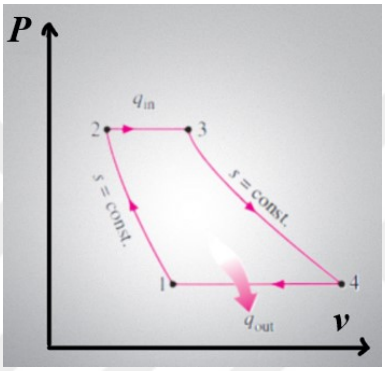

Figure 2.12 : P-v Diagram for the ideal Brayton cycle [2].

Brayton cycle efficiency is directly proportional to the pressure ratio. The pressure ratio is also proportional to the temperature ratio. The maximum temperature in the Brayton cycle is T_3 , which is at the end of the combustion chamber.

Therefore, increasing temperature of T_3 increases the Brayton cycle efficiency. The Brayton cycle efficiency is shown in between Equations (2.1) and (2.7).

$$(q_{in} - q_{out}) + (w_{in} - w_{out}) = h_{exit} - h_{outlet} \tag{2.1}$$

$$q_{in} = h_3 - h_2 = (c_p)(T_3 - T_2) \tag{2.2}$$

$$q_{out} = h_4 - h_1 = (c_p)(T_4 - T_1) \tag{2.3}$$

$$\eta_{th,Brayton} = \frac{w_{net}}{q_{in}} = 1 - \frac{q_{out}}{q_{in}} = 1 - \frac{(c_p)(T_4 - T_1)}{(c_p)(T_3 - T_2)} = 1 - \frac{T_1(T_4/T_1 - 1)}{T_2(T_3/T_2 - 1)} \quad (2.4)$$

$$\frac{T_2}{T_1} = \left(\frac{P_2}{P_1}\right)^{(k-1)/k} = \left(\frac{P_3}{P_4}\right)^{(k-1)/k} = \frac{T_3}{T_4} \quad (2.5)$$

$$r_p = \frac{P_2}{P_1} \quad (2.6)$$

$$\eta_{th,Brayton} = 1 - \frac{1}{r_p^{(k-1)/k}} \quad (2.7)$$

pressure ratio is r_p

The gas engines operate with the Brayton cycle principle. The efficiency of the engine is increased by increasing the temperature of the gases at the exit of the combustion chamber.

The life and durability of the hot parts of the gas turbines determine the maximum temperature of gases output of the combustion chamber. Main gas flow can be allowed to exceed the material's strength temperature by means of various cooling techniques for the hot parts such as blades and vanes.

2.3.2 Brayton cycle with regeneration

Burned gas temperature is higher than the temperature of the air leaving the compressor. Therefore, a counterflow heat exchanger called a regenerator can heat the high pressure air coming out of the compressor with the exhaust gases coming out of the turbines. Regenerative Brayton cycle is shown in Figure 2.13.

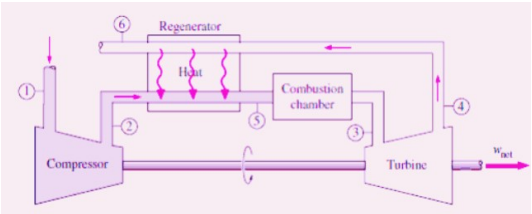

Figure 2.13 : Regenerative Brayton cycle [2].

A portion of the heat given to the environment by the exhaust gases is used to heat the air in used cycle. By utilizing the regenerator, heat provided to the combustion chamber for the same net work decreases and cycle efficiency increases. In ideal conditions, the highest temperature in the regenerator can be T4, which is the temperature at which exhaust gases are thrown out of the engine.

The processes performed in the Brayton cycle with regenerator are as follows:

- 1-2 In the compressor, air is compressed isentropically.
- 2-5 Compressed air is energized at stable pressure in the regenerator.
- 5-3 The system is energized at constant pressure in the combustion chamber.
- 3-4 Combusted gases expand isentropically in the turbine.
- 4-6 At constant pressure, energy is given from the exhaust gas to the compressed air in the regenerator.
- 6-1 At constant pressure, energy is given to the environment from the system.

T-s diagram of brayton cycle with regenerator is located in Figure 2.14.

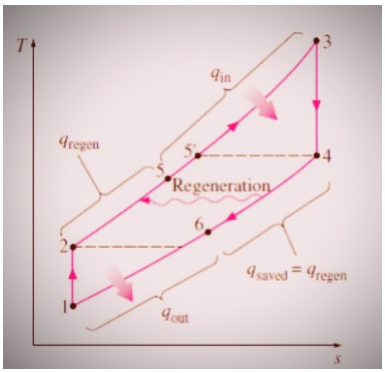

Figure 2.14 : T-s Diagram for the ideal Brayton cycle with regeneration [2].

Brayton cycle efficiency is related to the ratio of the min and max values of temperature and pressure is shown in Equation 2.8.

$$\eta_{th,Brayton} = 1 - \left(\frac{T_1}{T_3}\right) r_p^{(k-1)/k} \tag{2.8}$$

2.3.3 Brayton cycle with reheat and intercooling

To calculate the cycle net work, subtract compressor work from the turbine work. As a result, expanding net work can be accomplished by bringing down turbine and compressor temperatures.

The work required to compress the air can be limited by compressing in stages and cooling it between them. This is often known as the intercooled multistage compression strategy. Additionally, the work done by a turbine working can be improved by extending in stages and heating the gas between them.

When intercooling and interheating are performed, compressor exit temperature is decreased and turbine exit temperature is increased as opposed to the simple cycle. In this case, it would be beneficial to add a regenerator to the cycle as the difference between the compressed air coming out of the compressor and the exhaust gas temperatures coming out of the turbine rises.

It occurs during the Brayton cycle, with intercooling and interheating regenerators. Schematic view is located in Figure 2.15

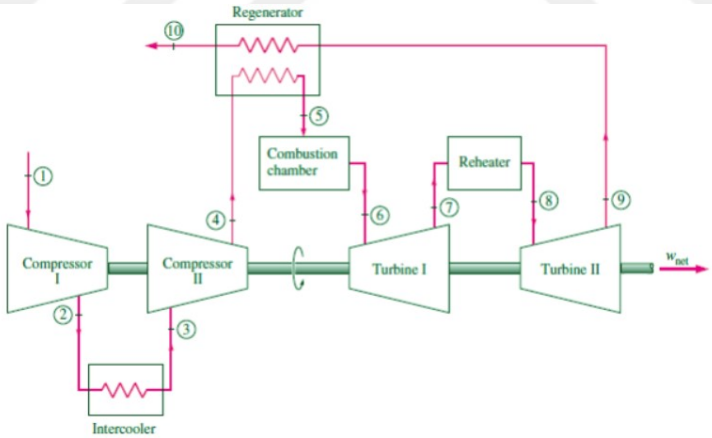

Figure 2.15 : A gas-turbine engine with intercooling, reheating, and regeneration [2].

Processes are as follows:

- 1-2 The compressor compresses the air isentropically.
- 2-3 Air is cooled under steady pressure.
- 3-4 Air is compressed isentropically.
- 4–9 Compressed air is energised at constant pressure in the regenerator
- 9-5 Energy is provided at a constant pressure in the combustion chamber.
- 5-6 The combustion gases expand isentropically in the turbine.
- 6-7 Energy is delivered at constant pressure in the combustion chamber.
- 7-8 The gases expand isentropically in the turbine.
- 8-10 At constant pressure, exhaust gas energy moves to the compressed air in regenerator.

Intercooling and interheating have a beneficial effect on the gas turbine cycle's work rate. However, this does not imply a rise in thermal efficiency. In actuality, when regeneration is not combined with intercooling and interheating, thermal efficiency always drops. The average temperature at which heat is delivered to the cycle is lowered by intercooling, whereas the average temperature at which heat is extracted from the cycle is raised by interheating. Thus, if intercooling and interheating are used, a regenerator must be added to the system for gas turbine applications.

3. IMPORTANCE OF COOLING FOR GAS TURBINE ENGINES

3.1 Advantages of Cooling for Gas Turbine Engines

The best characteristic for determining the life of turbine components as well as the efficiency and output power of the turbine is the turbine inlet temperature. The strength of the turbine parts directly affects how much the turbine inlet temperature.

The durability of turbine parts depends on the material composition used, the manufacturing method and the temperature they are exposed to. Due to their exposure to both mechanical and thermal stress, turbine parts are the most critical components. Especially, rotor blades are exposed to both the mechanical stress caused by the pressurized gas and the centrifugal forces caused by rotation.

The way to minimize the thermal stresses caused by the temperature effect to which these parts are exposed is to cool the turbine blades. The following advantages can be achieved by cooling the turbine blades.

- Material life can be increased: If the turbine blades are properly cooled, they will have a significantly longer life with the same combustion chamber inlet temperature.
- It is possible to lower maintenance expenses and raise the capacity utilisation factor: By keeping the turbine blades colder, it will be feasible to perform regular maintenance on the turbines and replace the blades more frequently. This will reduce maintenance durations, which will enhance the units' working times and capacity utilisation factors. Costs can also be decreased by extending the usage period.
- Turbine output power can be increased: The turbine can be operated at greater turbine inlet temperatures by using an appropriate technique to cool the turbine

blades. The working of the gas and the heat energy supplied to the turbine will both rise with temperature, and the turbine output power will rise in tandem.

- Turbine efficiency will increase: Turbine efficiency may also be raised by cooling the turbine blades and running the turbine at higher turbine inlet temperatures.

3.2 The Importance Of Cooling

Enhancing the cooling efficiency of gas turbines not only reaches higher thermal efficiency levels for the system but also has a significant impact on material strength.

The Nozzle Guide Vane material needs to work at high temperatures because of the high temperatures at which the turbine inlet is located. Fuel consumption is directly decreased by gas turbine engines' increased efficiency.

Reducing gas turbine engine size and weight is achieved by increasing thrust, or specific work, and these are critical aspects in aviation applications. Recent advancements in material technologies have led to the application of ceramics and thermal protective coatings on turbine blades. The life of a turbine blade or vane limits its working temperature [21].

Between the hot gases, ceramics are utilised as insulation for turbine vane material. Therefore, for rising gas temperatures or falling cooling air temperatures, a constant metal operating temperature can be employed [22].

In order for a new material can resist high temperatures to be desinged and become usable in an engine, it must go through a series of tests. This process also takes many years [22].

The materials that are going to be used to make gas turbine blades have to be able to resist high temperatures mechanically, as well as oxidation and thermal fatigue [23].

Effective cooling is achieved by a variety of techniques in addition to research done to improve the temperature resistance of the materials used in turbine blades. Figure 3.1 illustrates the variations in material operating temperatures and turbine inlet temperatures over time. Turbine cooling becomes more important as turbine intake temperatures rise.

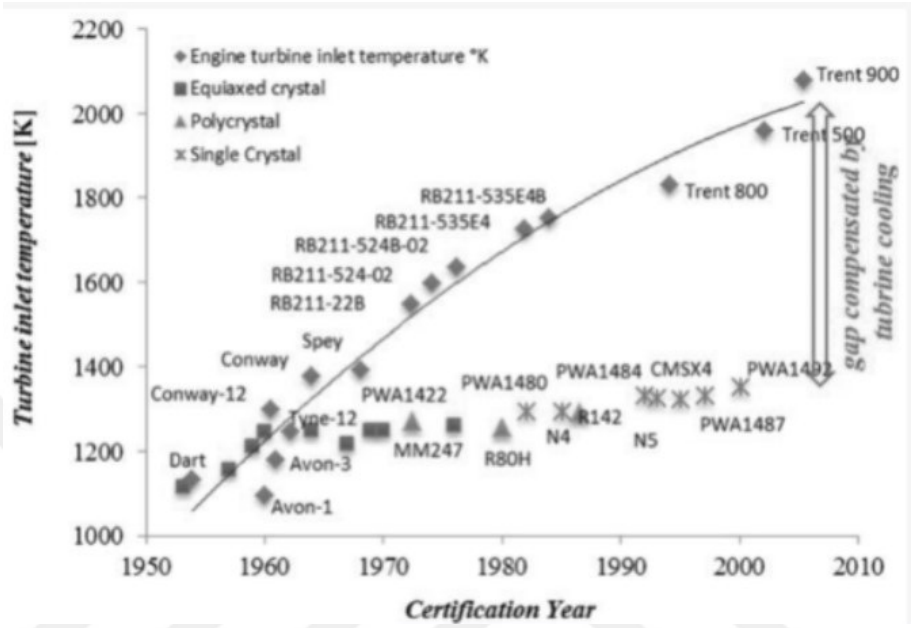

Figure 3.1 : Turbine Inlet Temperature vs Certification Year [5].

By enhancing cooling systems, optimised turbine cooling allows for even higher turbine input temperatures. Using different cooling techniques can improve cooling performance.

Cooling air for air-cooled turbines is taken from the compressor. Alloys based on nickel, thermal barrier coating (TBC) considerably raises the material limit temperature. Additionally, it permits a significant improvement in resistance to corrosion and oxidation. The effects of cooling techniques on turbine inlet temperature over the years are seen in Figure 3.2.

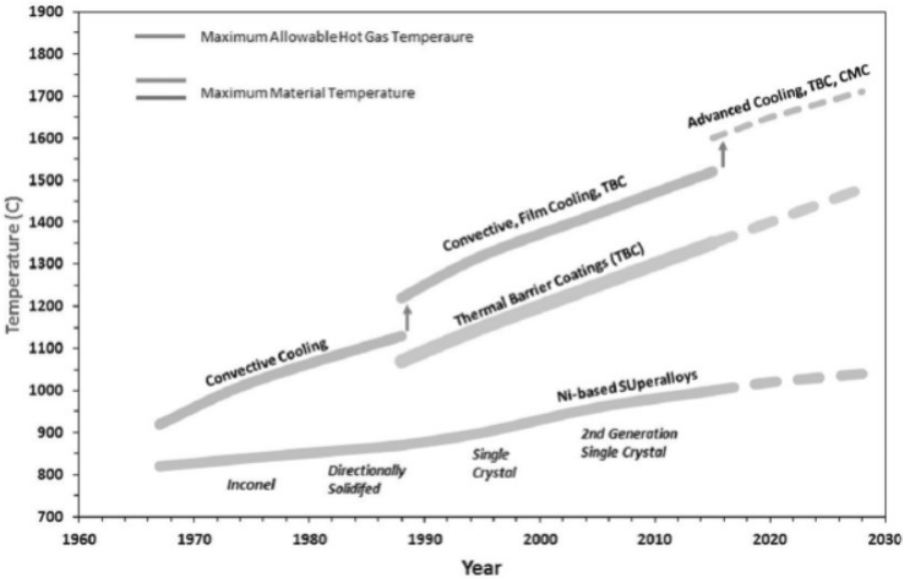

Figure 3.2 : Turbine Inlet Temperature vs Cooling Techniques [6].

From an alternative viewpoint, the primary reasons why turbines are air-cooled rather than water-cooled are that air has a more cost-effective structure, reduces the impact of chemical reactions, and makes it easier to provide the necessary cooling surface area.

Turbine cooling is primarily accomplished through internal and exterior cooling methods. Film cooling and transpiration cooling are the two main categories into which external cooling techniques can be separated. As the temperature of the turbine inlet rises, using this kind of cooling gets harder [24].

Conversely, jet impingement cooling and effusive cooling are two types of internal cooling techniques. In addition to this, there are techniques called rib cooling and pin-fin cooling.

Figure 3.3 illustrates the turbine cooling techniques and their corresponding efficiencies.

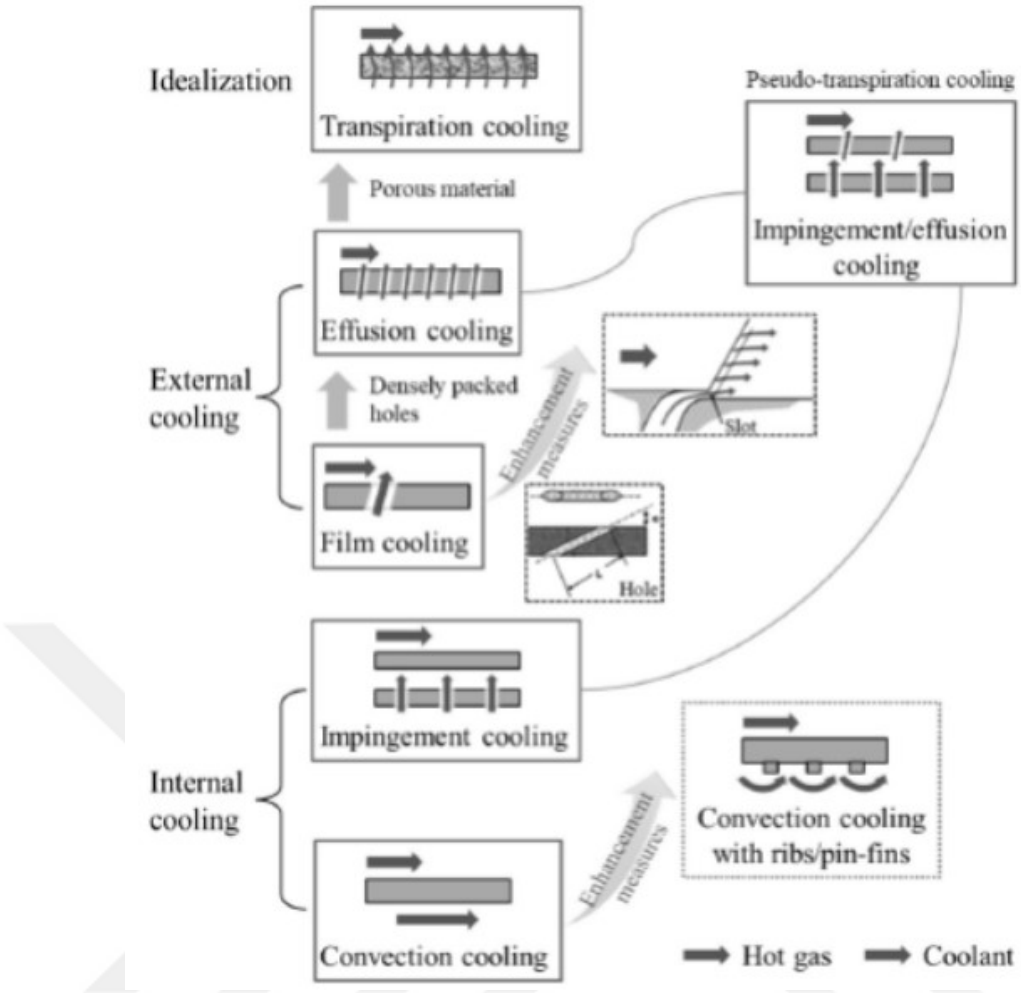

Figure 3.3 : Advances in NGV cooling Schemes [7].

There are some important issues for cooling of vanes are located in below lines:

- The life requirements of the gas turbine's blade and vane components as well as its overall efficiency and power output
- Depending on the features of the surrounding environment, engine starting and stopping situations
- Air profiles from the combustion chamber's temperature, pressure, and velocity
- Temperature, pressure and velocity profiles of air from the combustion chamber
- For the duration of the engine's operation, the cooling air extracted from the compressor can satisfy the needs.

- The operating temperatures of the blade and vane materials are crucial.
- Turbine blades' front stages are cooled by film and jet impingement, which have a higher cooling efficiency, because they are subjected to higher pressure and temperature. However, the temperature distribution originating from the combustion chamber is irregular. In cooling design, it is crucial to consider the radial temperature distribution factor (RTDF) and overall temperature distribution factor (OTDF) of this temperature profile. These profiles are crucial for designing details like blade and vane tips. Figure 3.4 depicts temperature profiles at the combustion chamber output.

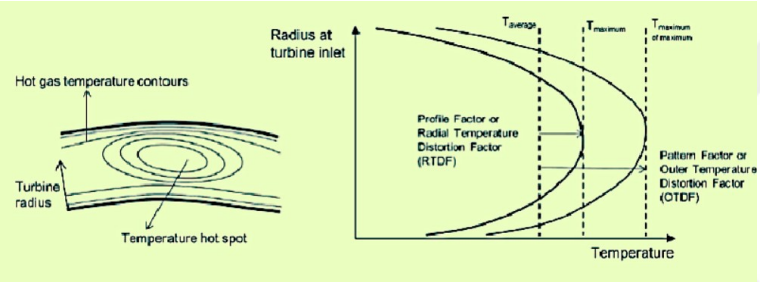

Figure 3.4 : Combustor Hot Gas Temperature Profiles [6].

For every vane, the metal temperature can be lowered by 200–300 K by utilising 1.5–2 % of the compressor's mass flow rate [25].

3.3 Heat Transfer Mechanism for Vane and Blade in Gas Turbines

There is a heat transfer mechanism if there is a temperature differential between the objects. There are three ways in which heat transfer can happen:

3.3.1 Conduction

Conduction heat transfer occurs when a stationary solid or fluid has a temperature difference. Schematic view for conduction can be seen in Figure 3.5.

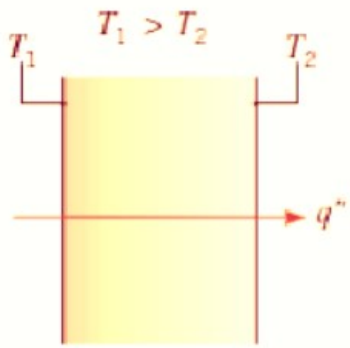

Figure 3.5 : Conduction Heat Transfer [8].

Conduction heat transfer mechanism is defines with Fourier's Law. The expression for one-dimensional conduction heat transfer is located in Equation 3.1;

$$q'' = -k\frac{dT}{dx} \tag{3.1}$$

Where;

- q" is the heat flux
- k is thermal conductivity
- $\frac{dT}{dx}$ is temperature gradient.

The direction of heat transfer to the decreasing side is indicated by a minus sign.

Equation 3.2 expresses the temperature gradient in the case of a linear temperature distribution.

$$\frac{dT}{dx} = \frac{T_2 - T_1}{L} \tag{3.2}$$

3.3.2 Convection

When two objects are at different temperatures, and there is moving fluid in the environment, heat transfer occurs between them. Convection is the name of that mechanism. Schematic view for convection can be seen in Figure 3.6.

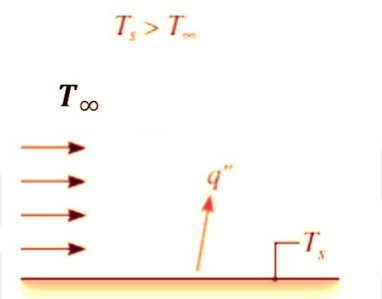

Figure 3.6 : Convection Heat Transfer [8].

Convection heat transfer is another heat transfer type for internal and external blade and vane cooling. Convection heat transfer formula is represented by the Equation 3.3.

$$q'' = h(T_s - T_\infty) \tag{3.3}$$

Where;

- q" is the convective heat flux
- h is convection heat transfer coefficient
- T_s is surface temperature
- T_∞ is environment temperature

Another crucial factor in convective heat transfer is the Nusselt Number. Convective heat transfer divided by conductive heat transfer is the definition of the Nusselt number. Formula for Nusselt numbers is displayed in Equation 3.4.

$$Nu = \frac{hL}{k} \tag{3.4}$$

Where;

- h is the convection heat transfer coefficient
- L is the characteristic length of the surface
- k is thermal conductivity

3.3.3 Radiation

Electromagnetic waves are the form of energy emitted by all surfaces with finite temperatures. Thus, there is net heat transfer by radiation between two surfaces at differing temperatures in the absence of an intervening medium. Schematic view for radiation can be seen in Figure 3.7.

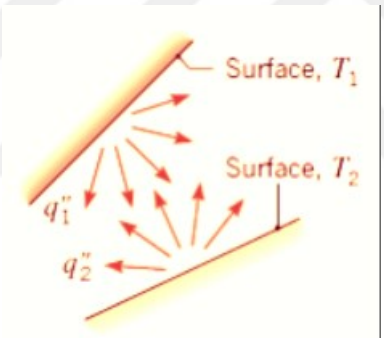

Figure 3.7 : Radiation Heat Transfer [8].

The radiation heat transfer from a grey surface is controlled by the Stefan-Boltzmann's law is shown in Equation 3.5:

$$\dot{Q} = \varepsilon \sigma A T_s^4 \tag{3.5}$$

Where;

- $\dot{Q}$ is Radiation heat transfer rate
- ε is surface emissivity.
- σ is Stefan-Boltzmann constant
- A is Heat transfer area
- T_s Surface temperature

For high temperatures, one driven factor heat transfer technique is radiation heat transfer. Consequently, radiation works well for a gas turbine engine's turbine side.

4. COOLING TECHNIQUES FOR GAS TURBINE ENGINES

Over the years, numerous cooling methods have been put, including fuel, water, steam, and air cooling. Nonetheless, air cooling is the most widely utilised cooling method, particularly for gas turbines utilised in the aviation sector. The necessary secondary air system air is taken from the compressor and used to decrease the metal temperatures of the turbine's hot parts. The engine performs less well since the fluid that the compressor worked on is utilised for cooling. Nevertheless, because of the cooling design, it is possible to raise the turbine inlet temperature, offsetting this loss and boosting engine performance [26].

Cooling methods for turbine blades and vanes can be classified as follows [27]:

- Air Cooling
  - Internal Cooling
    - Channel cooling
    - Rib turbulated cooling
    - Pin-fin turbulator cooling
    - Closed system vapor cooling
    - Impingement cooling
  - External Cooling
    - Transpiration cooling
    - Film cooling
- Liquid Cooling

By moving the coolant fluid around inside the blade and vane and absorbing the heat, the internal cooling technique described in the categorization above achieves cooling. With the coolant fluid outside the wing, a layer is formed between the burned gas and the blade and surface to provide cooling in the external cooling technique.

4.1 Thermal Barrier Coating

To lessen heat transfer to the internal cooling flow, a thermal barrier coating (TBC) with extremely low thermal conductivity is frequently applied to the blade surface exposed to hot gases. It may be tempting to use a heat transfer design solution that uses a TBC with significantly lower thermal conductivity or one that increases TBC thickness in order to minimize the internal cooling flow to increase turbine efficiency. Due to the temperature differential between the hot gases and the vane, heat transfer will undoubtedly take place and, in a steady state, eventually heat the whole blade or vane to the temperature of the hot gases [28].

Two categories of coating methods exist [29]:

1. Air plasma spray
2. Electron beam physical vapor deposition

The coating thickness and previously described coating processes determine the TBC characteristics. Research is being done to find improved coating materials, better coating procedures, controlled coating thickness, excellent bond coat, and hot corrosion testing for TBC life determining by the industry. Determining how TBC roughness affect the aerodynamic and heat transfer performance of turbines is crucial [1].

4.2 Air Cooling

Air is typically used as a cooling gas for the high pressure turbine side of gas turbines. Nozzle guide vane cooling is accomplished by using compressed and coolant air. Figure 4.1 shows the path of the coolant air.

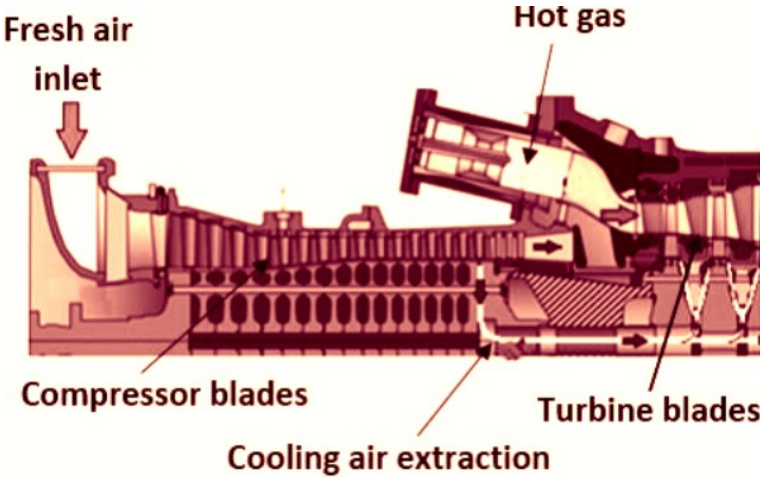

Figure 4.1 : Cooling Air Direction [9]

4.2.1 Internal cooling

Coolant air is used from the compressor for internal cooling. Air is used to cool the inside of the blade or vane. There are different types of internal cooling type.

4.2.1.1 Channel cooling

The inner walls of the turbine blades and vanes are cooled by the cooling fluid in the channels within the blade. Regardless of whether this is the first cooling technique used, the defects are constructed in a single pass and the walls are flat. The design of cooling connections has evolved into multi-pass channels as production technology and cooling efficiency have both risen. Channel cooling picture can be seen in Figure 4.2.

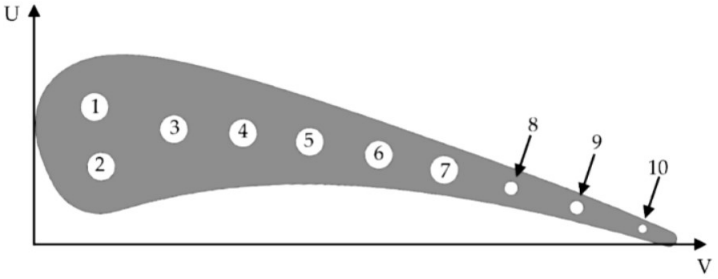

Figure 4.2 : Simple Cooling Channels [10].

4.2.1.2 Rib turbulated cooling

Turbulence-generating ribs are positioned on two opposing walls of internal cooling channels in modern gas turbine engines in order to increase heat transfer [30]. Internal cooling channels are frequently represented as square or rectangular channels with various geometries. The channel geometry on which the turbulators are positioned, as well as the protrusion size, form, distribution, flow incidence angle, and flow Reynolds number, all affect the increase in heat transfer in rectangular channels with turbulators. Pressure drops are caused by turbulators. Repeated projections for ducted heat sinks are typically square in shape and have channel size ratios between 0.25 and 4. Turbulators with a square profile are generally used on blades with duct size ratios between 0.25 and 4. Protrusion heights typically range from 5 to 10% of the hydraulic diameter of the coolant channel. Protrusion height to protrusion spacing has a ratio of 5 to 15. The protrusion's angle with respect to the flow is between thirty and sixty degrees [30].

Sample rib turbulated cooling geometry can be seen in Figure 4.3.

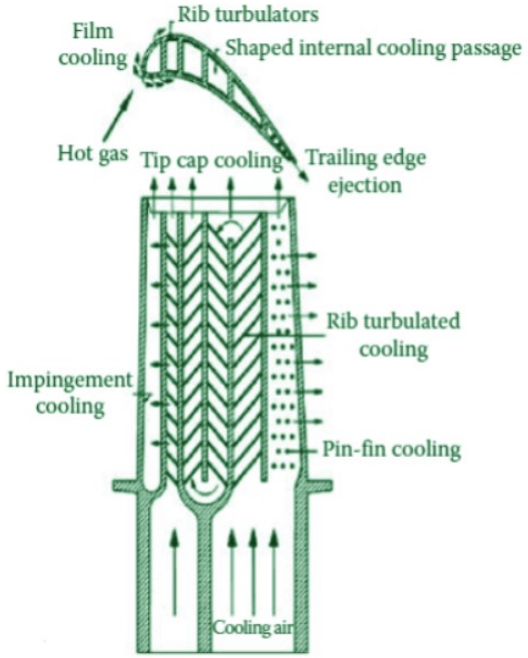

Figure 4.3 : Inside cooling with protrusion turbulators [1]

2-4 times more turbulence and heat transfer occurs in the flow around the protrusion than in a channel cooling system with a flat wall [31].

As the flow passes over protrusions, flow separation can be happen and flow rejoins in the space between them. Increased heat transfer results from boundary layer separation. The flow becomes more turbulent due to separation and combining, causing the coolant flowing in the centre of the flow to mix with the coolant flowing at the flow's edge. At the junction, each protrusion is followed by a new thin boundary layer [32].

4.2.1.3 Pin-fin turbulator cooling

There are little dimples that are named as pin-fins are located in the interior passageways for cooling. The flow's turbulence is increased by these pin-fins. Inside the channels, HTC rises for the reason that increased turbulent flow. The inside of the channels cools more effectively due to increased HTC. An example to pin-fin turbulator cooling is located in Figure 4.4

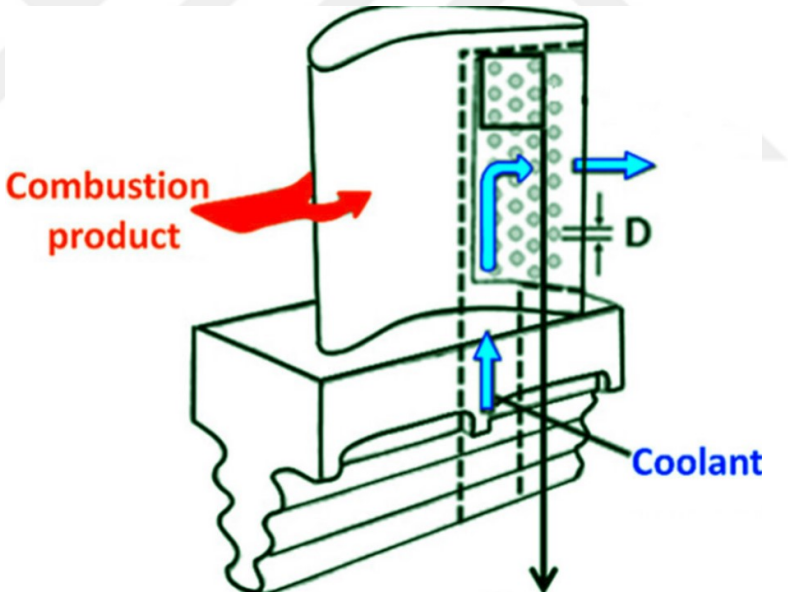

Figure 4.4 : Channel cooling with pin fin turbulator [11].

Pins are used on the narrow trailing edge of the vane, where there is not enough space for protruding channels, as they are difficult to manufacture [1]. Pins with a height to diameter ratio of 0.5 to 4 are typically used in pin-fins for turbine cooling [30]. Numerous studies assess how the form, size, distribution, and pin-fin cooling affect the distribution of HTC [1].

The coolant air moves through the set of pins, removing heat from the blade and vane. Heat transfer in the cooling channel is enhanced and extra structural support is given by the pins connecting the pressure and suction sides of the channel.

Pin positioning within the blades or vanes might be either inline or staggered. The pins are positioned diagonally in the staggered arrangement. On the other hand, the pins are placed in a single row in the inline design. These two designs are located in Figure 4.5.

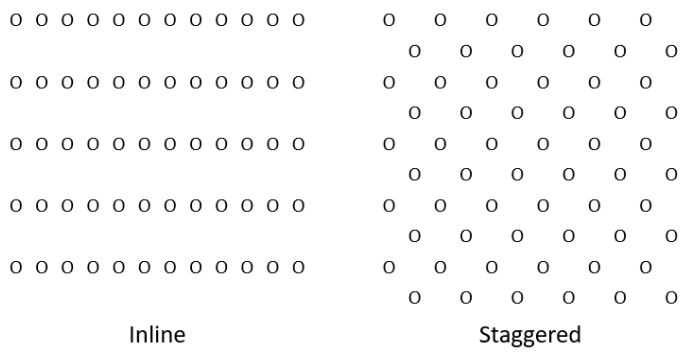

Figure 4.5 : Staggered and Inline Pin-fin Distribution [1].

Nusselt number differs according to pin-fin design. Calculations details are located in Equation 4.1 [1].

$$Nu = a(Re)^b \left(\frac{S_z}{w}\right)^c \left(\frac{S_x}{L}\right)^d \tag{4.1}$$

Where;

- Nu is the Nusselt number in the thermally developed region
- Re is the Reynolds number based on pin diameter
- Sz and Sx are the spanwise and stream wise pin spacing

- w and L are channel width and length
- The constants a, b, c, and d are correlation constants

Table 4.1, 4.2, and 4.3 shows the a, b, c, and d coefficients for inline and staggered design;

Table 4.1 : Pin-Fin Nusselt Number Correlation Constants for C/H=0.0. [1]

Constant	Inline	Staggered
a	0.45	0.3
b	0.71	0.98
c	0.4	0.35
d	0.51	0.24

Table 4.2 : Pin-Fin Nusselt Number Correlation Constants for C/H=0.5. [1]

Constant	Inline	Staggered
a	0.36	0.21
b	0.56	0.68
c	0.47	0.06
d	0.13	0.08

Table 4.3 : Pin-Fin Nusselt Number Correlation Constants for C/H=1.0. [1]

Constant	Inline	Staggered
a	0.58	0.31
b	0.51	0.92
c	0.18	0.2
d	0.21	0.23

- For table 4.1, C/H = 0.0 indicates the there is not any clearance top of pin,
- For table 4.2, C/H = 0.5 indicates the there is half of pin height clearance,
- For table 4.1, C/H = 1.0 indicates the there is full of pin height clearance,

Additionally, pin-fins can be designed in diamond and cubic forms as much as manufacturing capabilities allow.

Various pin-fin designs are available with inline or staggered distribution using cubic or diamond shaped pin-fins. It is possible to increase the HTC with various distributions.

4.2.1.4 Closed system steam cooling

The closed system cooling method is one of the convection-based cooling techniques. Through the inner vane's channels and perforations, the cooling air enters from the vane root and combines with the burned gases outside on the vane. In this transitional phase, the air attempts to remove the heat that the burning gas had imparted to the vane by absorbing it. Another design technique that is commonly used in this cooling approach is designing turbulators to provide turbulence inside the air for improved cooling. This convection method is mostly used in landing gas turbine engines.

Some gas turbine manufacturers have begun to replace the air used in vane cooling techniques with steam in a closed-loop system. Usually, this method is used with stationary vanes. It is possible to raise gas turbine efficiency even in the absence of either the turbine input temperature, or the combustion chamber exit temperature. Because air cooling involves mixing the burned gas flow with the air that exits the vane after internal cooling. Because in air cooling, after internal cooling, the air comes out of the vane and mixes with the burnt gas flow.

Figure 4.6 appears the burnt gas stream sometime recently and after the 1st organize stationary vane of GE company H system turbines, and the picture of the open system air-cooled vane and the closed system steam-cooled vane.

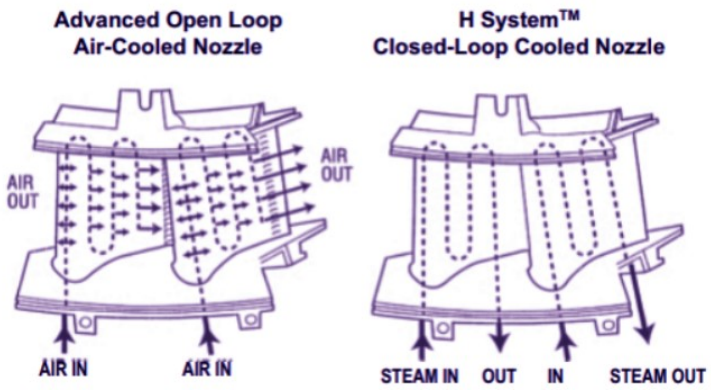

Figure 4.6 : Steam Cooled NGV Design Examples [12].

Cycle efficiency rises because these structures use steam for cooling. Simultaneously, compressed air is reduced for cooling. Compressed air is increased; therefore, turbine power is increased.

In modern gas turbines, steam may be utilized in place of this air to raise cycle efficiency by up to 2% and produce a significant increase in output power. To sum up, all of the compressor air is directed onto the turbine and effectively utilized.

4.2.1.5 Impingement

Impingement jets are frequently used in gas turbines to cool different parts. Impingement jets have a very high cooling efficiency, especially in high pressure turbines. At the leading edge of the blade or vane, this cooling is frequently a very effective localized cooling technique. Compressed and cold air according to turbine section move to the inside of the turbine blade or vanes from the perforated plate. Air strikes the vane's inner surface as an air jet, the surface cools. Regular arrays of impinging jets are used to provide uniform and controlled cooling of turbine blades and shrouds. The jet-to-jet gap distance, the orifice diameter, the flow route, and the distance between the jet orifice and the target plate are important parameters for the impingement cooling design. The boundary layer that produces the extremely high heat transfer coefficient is extremely thin, and the flow is extremely turbulent where the jets strike the target plate. When extremely high heat transfer is required, impingement cooling is used. Impingement jet design example can be seen in Figure 4.7.

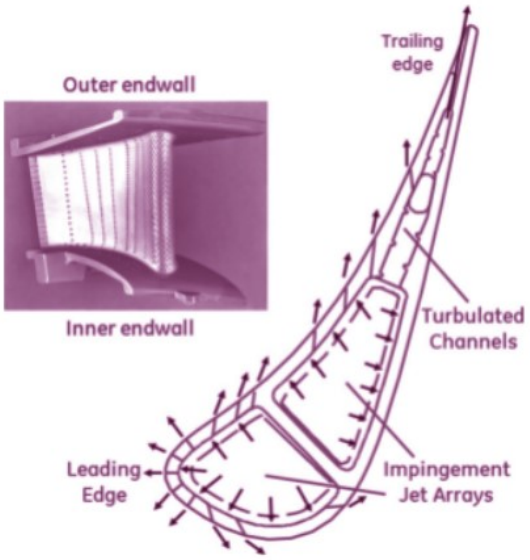

Figure 4.7 : Impingement Jet Design [13].

Among all the cooling techniques; Impinging jet cooling is the highest potential to increase the regional HTC. Since the structure of the impinging jet cooling holes are weaken structural integrity, impinging jet cooling should be used in places where thermal loads are high. For example, it is a very applicable method for the front part (leading edge) because the thermal load is highest in this part.

Equation 4.2 shows that the effectiveness of the impingement cooling:

$$\eta = \frac{T_{aw} - T_r}{T_j - T_\infty} \tag{4.2}$$

Where;

- T_{aw} is the adiabatic wall temperature
- T_r is the recovery temperature
- T_j is the jet temperature
- T_∞ is the ambient temperature

The impinged jet enhances heat transfer by creating a very turbulent flow after impingement. Theoretically, no heat transfer is possible in the stationary area with zero velocity. Nonetheless, in reality, the still area is not very orderly and there is

always movement. Because of the thin laminar boundary layer, there is a very high HTC in the stationary zone. The HTC decreases as the distance from the stagnation point increases. On the other hand, maximal heat transfer can happen briefly at a certain Re number and z/d ratio when the wall jet transitions from laminar to turbulent flow.

4.2.2 External cooling

Coolant air is used from the compressor during external cooling. Coolant air moves to the outside of the blade. On the vane's outside wall, this air creates a thin layer of cooling layer. By offering protection, this method lengthens the blade's life [27].

4.2.2.1 Transpiration cooling

The most effective cooling technique is frequently said to be transpiration cooling. A continuous film layer that protects the surface is formed when the coolant is driven through the porous vane or blade surface. However, transpiration cooling do not realized still due to issues with manufacturing and materials.

This amount was intended to be used to construct a gas turbine that would operate at 60% efficiency. In addition, the cage arrangements of the blades used in this method do not sufficiently resist mechanical and thermal stresses of the blade. Transpiration cooling schematic is located in Figure 4.8.

Figure 4.8 : Transpiration Cooling Figure [14].

In this type of cooling, the coolant reduces the internal temperature of the part as it passes through the walls. As the coolant fluid passes from the inside to the outside of the part, it also affects the convection. Transpiration cooling can be used with porous and perforated cooling [33].

4.2.2.2 Film cooling

The fundamental idea behind this kind of cooling is to release air via the channels by holes in the blade surface at specific angles. The pumped and coolant air causes a film layer to build on the blade's surface. This film layer significantly prevents highly hot gases in the main flow from coming into direct contact with the surface.

High temperature gas turbines can be designed thanks to the development of the film cooling technique. The hottest areas of the gas turbine, such as the HPT NGV and blades, are often designed with film cooling. A turbine blade with designed with film cooling holes example is shown in Figure 4.9.

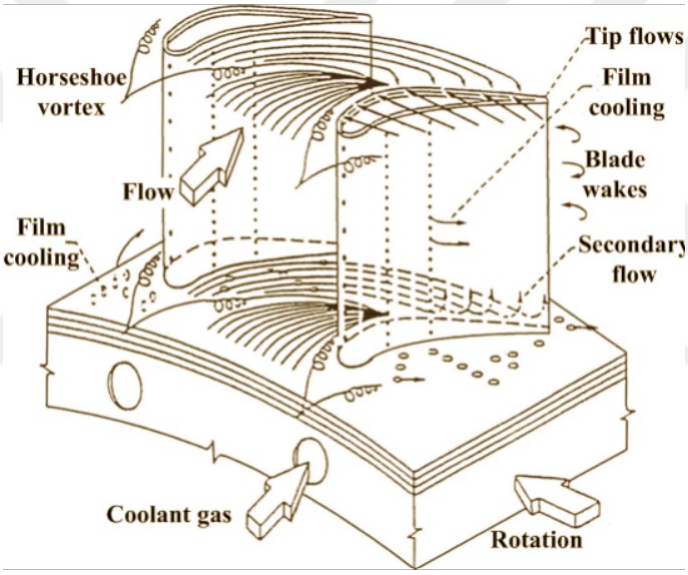

Figure 4.9 : Film Cooling Coolant Design for the Turbine Blade [15].

Basic studies and information found from the literature for film cooling are as follows:

1. The impact of the depth and diameter of the film cooling holes on the cooling efficacy is crucial for optimising the efficiency of film cooling. Equation 4.3 is defines the cooling efficiency [34]. In this equation, d stands for depth and D for hole diameter. Furthermore, failure scenarios should be taken into account while choosing the hole diameter.

$$d = 0.8D \tag{4.3}$$

2. The maximum cooling efficiency in film cooling using a single row of jets inclined at 30 or 35 degrees on a flat plate was reported [35].

3. Effectiveness of this cooling technique varies with the shape of the holes, which can be round, rectangular, elliptical, or oval and have varying cross sections. Rectangular cross-section holes have a higher film cooling effectiveness than circular cross-section holes [36]. But strength and manufacturability are also taken into account when choosing a film cooling form.

4. A vane's suction and pressure side have different HTC distribution. On the suction side, where the turbulent flow occurs, the stationary turbine vane's heat transfer coefficient rises. Consequently, the vane can cool by opening film cooling holes on the suction side to cool the flow's transition region. Furthermore, the gases at the combustion chamber's exit make direct touch with the vane's surface on the pressure side. On the pressure side compared to the suction side, there will be less flow separation. Consequently, increasing the frequency of film cooling holes on the pressure side guarantees more efficient vane cooling. Consequently, Figure 4.10 is useful for determining where the film cooling holes should be placed. Cooling efficiency rises when film cooling holes are positioned where HTC is at its maximum. Cooling flow rate extracted from the compressor decreases as cooling efficiency rises. Performance of the engine is increased by using less worked air.

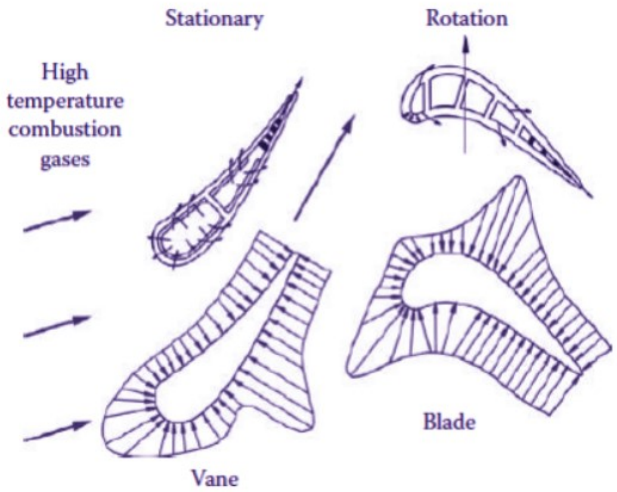

Figure 4.10 : HTC Distribution on the Stationary Vane and Rotationary Blade [1].

5. Another crucial factor in the design of the film cooling system is the blowing ratio (M). The blowing ratio has the ability to alter the HTC [1]. HTC is directly proportional to the blowing rate as can be seen in Equation 4.4.

$$M = \frac{\rho_f V_f}{\rho_\infty V_\infty} \tag{4.4}$$

Where;

- ρ_f is density of the film cooling air
- ρ_∞ is density of the main flow
- V_f is velocity of the film cooling air
- V_∞ is velocity of the main flow

Film cooling design should also account for potential failure scenarios. The failure mode of this design is not cooling air moving through the outside of vane, but hot gas leaking within. The gas temperature at the turbine intake of gas turbine engines is higher than the nozzle guide vane metal's service temperature.

There are problems satisfying the criteria for creep, low-cycle fatigue, and component strength if the hot gas within seeps through the film cooling holes. Air must be discharged from the cooling holes under all operating conditions. This requires that the backflow margin be computed as shown in Equation 4.5. Even in the hole with the greatest pressure loss, backflow margin (BFM) criteria should be satisfied [18].

$$BFM = 100x\frac{P_{S_c} - P_{T_g}}{P_{T_g}} \tag{4.5}$$

Where;

- P_{S_c} is coolant air pressure
- P_{T_g} is gas side pressure

The effectiveness of film cooling is a crucial design factor. The effectiveness is defined with the Equation 4.6 ;

$$\eta = \frac{T_m - T_w}{T_m - T_c} \tag{4.6}$$

Where;

- T_m is mainstream temperature,
- T_w is wall temperature,
- T_c is coolant gas temperature.

There are a lot of parameters that specify the effectiveness of film cooling:

- Angle at which the fluid sprays from the holes to produce the film layer
- Diffusion of the cooling air producing a film layer after leaving the holes
- Count of film cooling holes on the blade and their distance from each other
- Turbulences occurring in main gas and film cooling air
- Blade surface curves

These above parameters are important for accurate film cooling design. Additionally, one of the factors that needs to be chosen carefully is the cooling air's blowing ratio.

Also, another failure scenario is filling with foreign objects such as sand for not only film cooling but also impingement cooling. When the engine mostly turboshaft engines operate in dusty and sandy areas such as deserts, sand particles may enter the engine. If sand particles pass the particle separator, sand particles go to the main flow. Coolant air that comes from the compressor may contain these sands. Sand particles may fill the impingement and film cooling holes. Cause of hot air, these sand particles may convert to glass. The total cooling hole area decreases due to sand particles close the holes. Therefore, coolant performance decreases and vane and blade life requirements may not be satisfied. Thus, field data feedback is really important for the choosing the minimum hole diameter.

4.3 Liquid cooling

In industrial gas turbines, this kind of liquid cooling system was utilized. A liquid tank is also necessary when choosing to use liquids as the cooler. On the other hand, it is not favored in aviation for this reason, among others. Additionally needed for the cooling water is a tank valve pump. The weight of the gas turbine is increased by these systems. Since weight is not an issue, it was utilized in industrial gas turbines. A schematic view is shown in Figure 4.11.

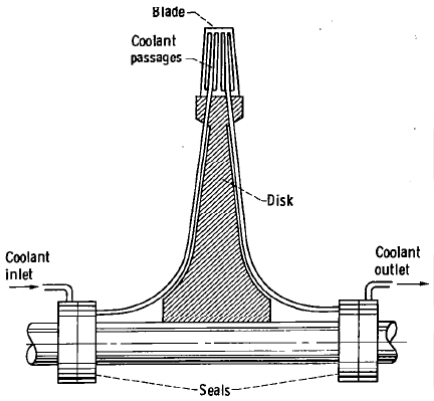

Figure 4.11 : Simple Forced Convection [16].

Air cooling is a more popular cooling technique. One of the main challenges to the general application of this technology is the sealing issues between the stator and rotor. Air and liquid HTC values are located in the Figure 4.12.

Process	h ($W/m^2 \cdot K$)
Free convection	
Gases	2–25
Liquids	50–1000
Forced convection	
Gases	25–250
Liquids	100–20,000
Convection with phase change	
Boiling or condensation	2500–100,000

Figure 4.12 : Heat Transfer Coefficients of Fluids [8].

4.3.1 Forced convection

This kind of cooling works by circulating liquid through the rotor blade's internal channels while going through the seals. Convection therefore provides cooling.

The cooling performance of this system is its primary benefit. It lowers the metal's temperature considerably. The metal temperature in a liquid-cooled blade in an engine with a turbine inlet temperature of 1422K was measured in a test at the NACA Lewis Flight Propulsion Laboratory, and it was found to be 470K [16]. Blade image is shown in Figure 4.13.

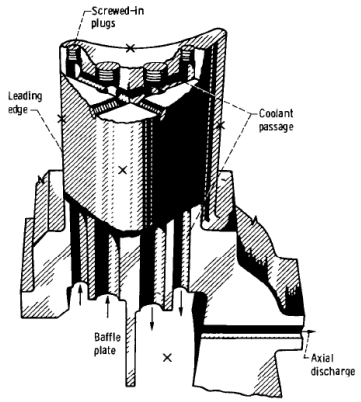

Figure 4.13 : NACA forced-convection water-cooled turbine [16].

Corrosion is among this system's disadvantages. The appropriate blade material must be chosen in order to use this method. Furthermore, high-pressure coolant liquid and high-flow coolant are required for this kind of cooling. Boiling water can lead to issues.

There are various configurations available for this cooling type where the cooling water is released through the holes from the trailing edge.

4.3.2 Thermosyphon

The aim of this cooling method is to create a closed-circuit cooling system in order to cool the blades. The fluid's flow removes heat from the environment.

In the transition zone between the area where heat is delivered and received, hot and cold fluids collide. Heat exchange occurs between fluids in this collision area. Example of closed thermosyphon cooling method is located in Figure 4.14.

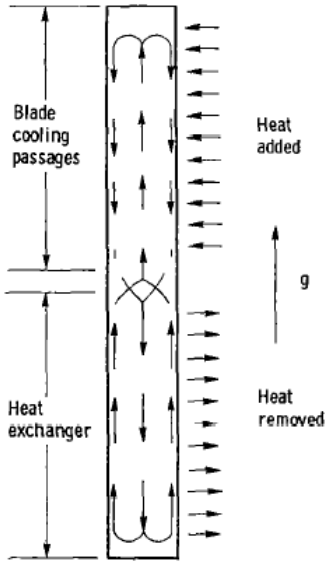

Figure 4.14 : Closed Thermosyphon Cycle [16].

Additionally, the thermosyphon cooling system is used as open cycle. For this kind of cooling, a reservoir system is used. The reservoir cavity may see through the open blade cooling channels. Cold water in the reservoir and hot water coming from the blades are combined during operation. A diagram of open thermosyhon cooling is presented in Figure 4.15.

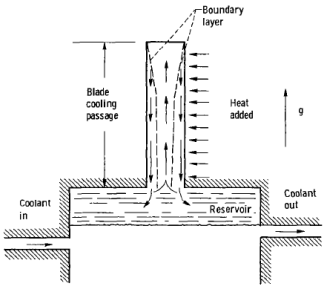

Figure 4.15 : Open Thermosyphon Cycle [16].

5. DESIGN, NUMERICAL CALCULATION DETAILS AND RESULTS

5.1 Design Details

The NASA Energy Efficient Engine (E^3) program design is closely examined during the NGV design phase. In the 1970s, NASA supported a program called the Energy Efficient Engine, which produced technologies for turbofan engines. Reducing thrust-specific fuel consumption was the aim.

According to the NGV design of the NASA E^3 program, it has been observed that the first turbine stage NGV contains film cooling, internal cooling trailing edge discharge holes [17]. E^3 turbine vane pictures can be seen in Figure 5.1.

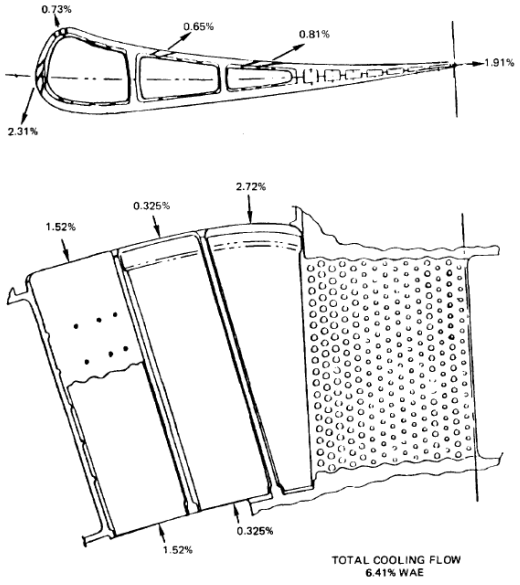

Figure 5.1 : NASA Energy Efficient Engine Turbine Vane Cooling Design [17].

The vane structure has segmented structure and consists of 20 pieces in the tangential direction. As will be mentioned in detail later, for ease of solution, only the 18-degree part was modeled periodically instead of the entire model. It is essential to choose materials that can withstand high temperatures in turbine fixed parts.

These are the important parameters in internal channel design:

1. To design internal channels that will keep the cooling efficiency at the maximum level.
2. Keeping vane life as high as possible

By focusing on these components, the design takes on the following forms:

1. In the design, it was chosen appropriate to apply internal channel cooling, film cooling and cut back methods.
2. Two main channels were designed according to vane geometry and dimensions.
3. The coolant air exits both the trailing edge of the vane and the film holes, but the flow entering the channel in the front duct only escapes through the film holes.

5.1.1 About analysis program

Analyses are performed with CTAADS program. The Concepts NREC Windows program CTAADS (Cooled Turbine Airfoil Agile Design System) lets the users create cooled axial turbine blades and vanes. Lead time for cooled turbine design decreases thanks to CTAADS.

Users benefit from the following abilities [37]:

1. Documentation and analysis parameter specification
2. Defining the aerofoil core
3. 3-D auto meshing
4. Modelling the internal cooling airflow
5. Creating exterior airfoil boundary conditions
6. Film effectiveness calculations
7. Thermal analysis and steady-state solution

8. Post-processing

In order to arrange and organize the numerous detailed parameters that need to be characterized in order to form a cooled turbine airfoil design, CTAADS is divided into parameter segments, also known as modules. The user can easily access these modules by using the wizard utility or by choosing a command from the setup menu. The following table highlights key points for every module [37]:

1. Analysis Parameters: The user can configure analysis parameters, profiles, and materials with this module. The parameters that are available in this module can also be specified by choosing analysis parameters from the setup menu.

2. Airfoil Center: The user can create complex airfoil cooling arrangements and characterize the airfoil core with this module. The film cooling models, internal cooling airflow, and 3D auto mesh data is gathered in this module. Parameters available in this wizard module can also be specified by choosing airfoil core from the setup menu.

3. Internal Cooling Airflow: The user can create and display a one-dimensional fluid flow network that addresses the entire cooling system. Additionally, parameters available in this wizard module can be indicated by selecting internal cooling airflow from the setup menu.

4. 3D Mesh: This module allows the user to model the ParaSolid "closed passage" airfoil geometry as a three-dimensional finite element model. The ParaSolid "closed passage" airfoil geometry at each show segment is examined by the TAS solver, which imports all model areas that have been characterized for inner segments. After that, it compiles the geometry data into an impartial TAS record. Additionally, parameters available in this Wizard module can be indicated by choosing 3-D Auto Mesh - TAS Generate Mesh from the Setup menu.

5. External Boundary Conditions: The user can arrange the enternal airfoil boundary conditions in this module, which incorporates the adiabatic wall temperature and the outside airfoil heat transfer coefficients. This module uses for outside boundary

conditions utilizing the STAN7 program. The establishment of STAN7 could be a 2D model. CTAADS runs at different airfoil sections for both the pressure and suction sides, performing a numerical arrangement of boundary layer speed and temperature profiles utilizing the STAN7 show. Parameters available in this Wizard module can be indicated by choosing External Boundary Conditions from the Setup menu.

6. Film Effectiveness and Heat Transfer Augmentation: With the help of this module, the user can define the parameters for the film effectiveness and heat transfer, as well as show the film curves and film coverage for each section of the vane. Parameters that are accessible in this Wizard module can also be indicated by choosing Film Effectiveness from the Setup menu.

7. Thermal Analysis: The user can create and solve the Thermal Analysis System (TAS) model with the help of this module. The parameters that are available in this Wizard module can also be specified by choosing Thermal Analysis System from the Setup menu.

8. Steady-State Solver: Performing a steady-state solution is a crucial step that needs to be taken before finishing a thermal analysis. Although the steady-state solver arranges all of the solvers in CTAADS iteratively, before running this solver, you must have previously run the Closed Passage solver and created a 3D mesh using the TAS solver.

5.1.2 3D geometry

As seen in Figure 5.2 NGV geometry has 3 internal cooling ducts, also there is film cooling holes and cut backs.

Film cooling holes are designed inline for base model. Every diameter 0.3mm and there is 9 film cooling columns on the geometry. 5 columns are located in leading edge side channel and 4 of them are located in middle channel.

There are 18 holes for leading edge side first 5 columns and others have 12 film cooling holes in every columns.

Leading edge Wall thickness is designed 0.5 mm with nominal thickness and suction side and pressure side wall thickness are designed with 0.25mm nominal thickness.

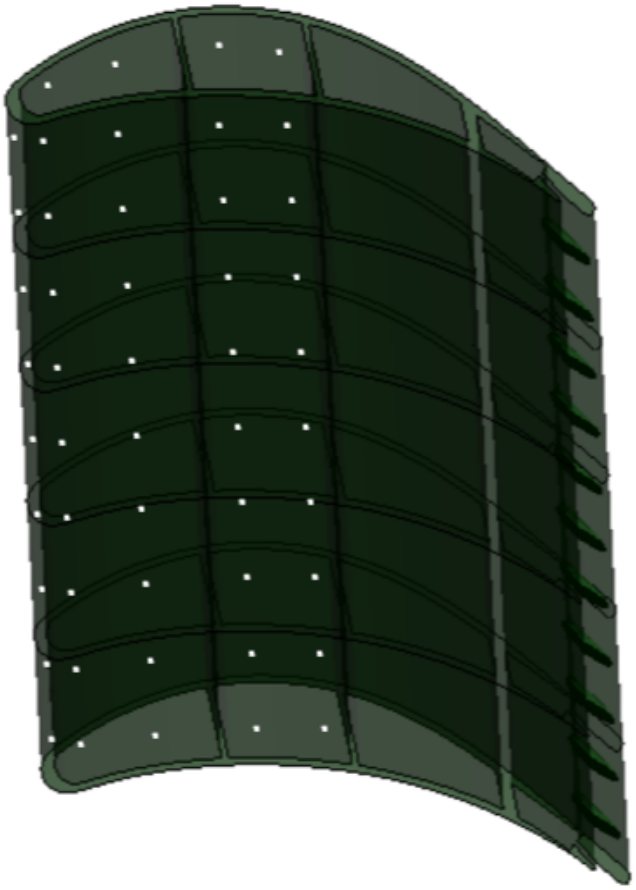

Figure 5.2 : Designed NGV

5.1.3 Material data

The NGV material is chosen as Mar-M247 material. This material is a superalloy based on nickel. This material is applied to the hot sections of the HP blades and HP vanes of gas turbines. In high temperatures, the material is a good chose in terms of creep, life, and strength characteristics.

Material data of Mar M247 is shown in figure , A.1, A.2, A.3, and A.4.

5.1.4 Mesh details

Geometry is meshed with hex elements. The geometry is divided into 2 elements along the thickness as it can be seen in Figure 5.3.

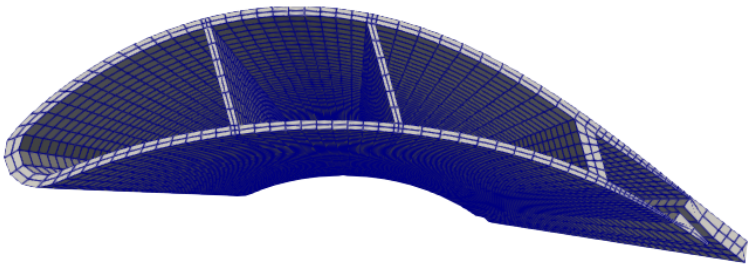

Figure 5.3 : Mesh View of the Geometry

5.1.5 Turbulence model

$k-\omega$ model is used for shear flow behaviour, compressibility, and low Re number effects. This model gives accurate solutions for not only radial but also circular jets. Thus, it predicts free shear flow velocities for both wall-confined and free shear flows.

According to the literature research, the $k-\omega$ SST turbulence model produces results that are more consistent with the experiments [38], [39], [40], [41].

5.1.6 Boundary conditions

Coolant flow temperature is chosen as 900K and pressure is 525 kPa. Turbine inlet temperature is taken 1100K and pressure is taken 400 kPa. Total mass flow rate for engine 19.5 kg/s.

5.2 Results for Base Model

1D temperature results for base model are shown in Figure 5.4.

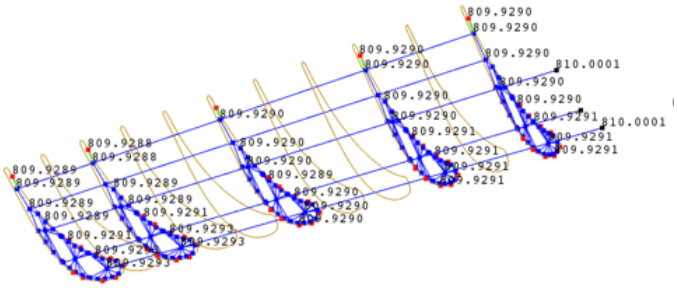

Figure 5.4 : 1D Temperature Results

Also 3D temperature distributions can be seen in Figure 5.5 and 5.6.

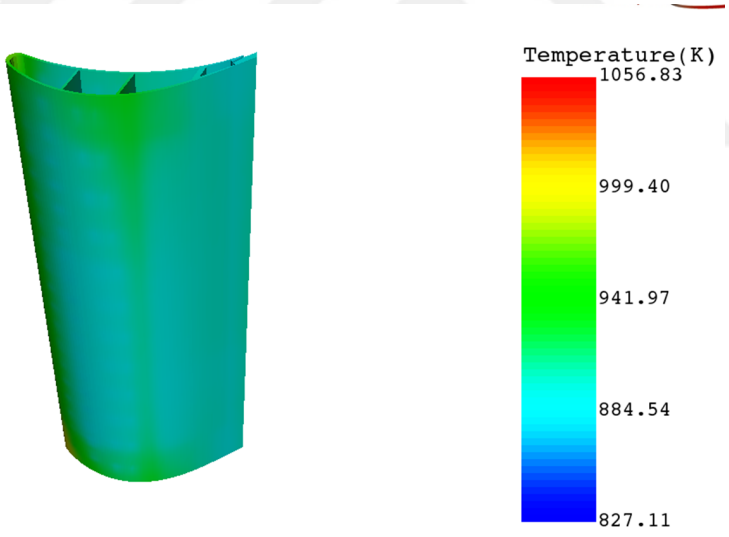

Figure 5.5 : 3D Suction Side Temperature Results

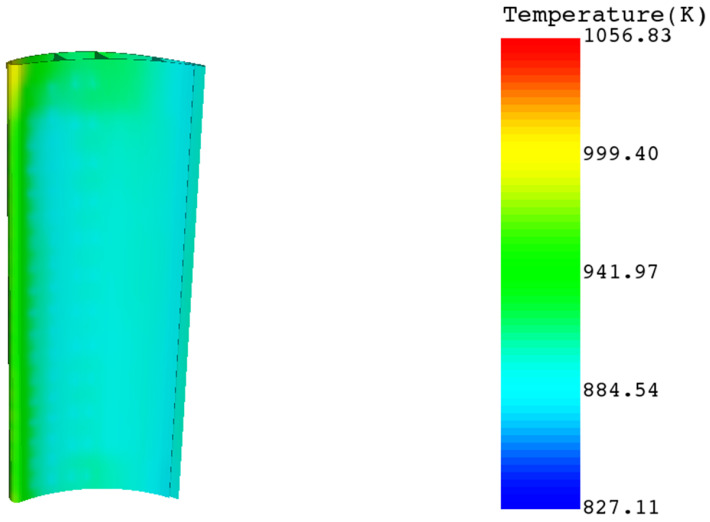

Figure 5.6 : 3D Pressure Side Temperature Results

5.3 Mesh Independency Study

Using the same boundary conditions and the same geometry, the mesh dimensions were changed and the results were obtained from the analysis. Base model has 2 thickness division. Division number of the thickness is changed.

5.3.1 3 division

Mesh view especially thickness division view can be shown in Figure 5.7.

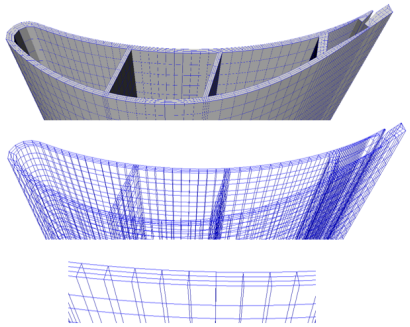

Figure 5.7 : 3 Division Mesh View

3D Temperature results for the pressure and suction side are shown in Figure 5.8.

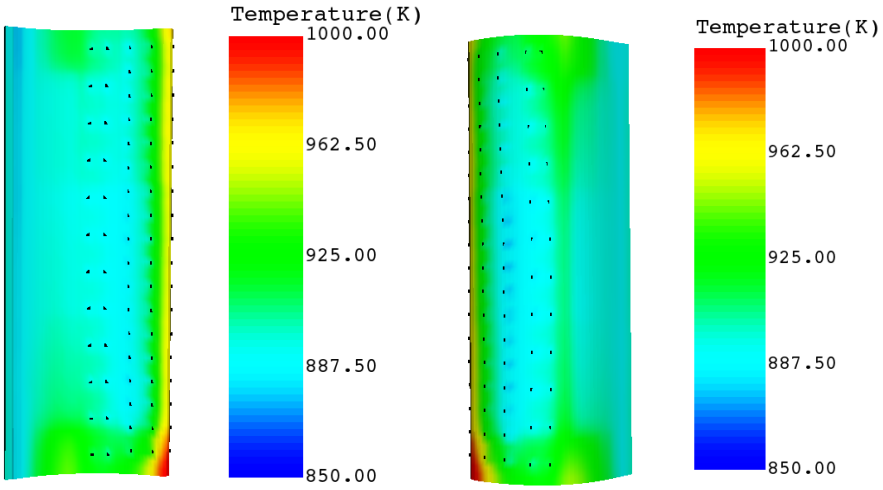

Figure 5.8 : Temperature Distribution for 3 Division

5.3.2 4 division

Mesh view especially thickness division view can be shown in Figure 5.9.

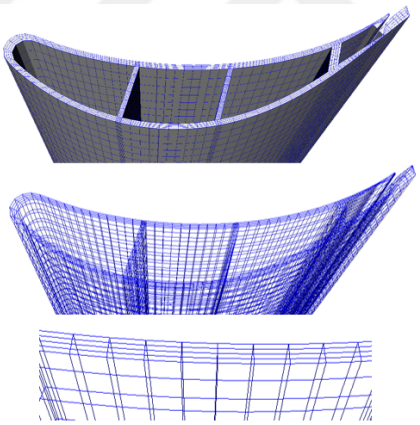

Figure 5.9 : 4 Division Mesh View

3D Temperature results for the pressure is shown in Figure 5.10.

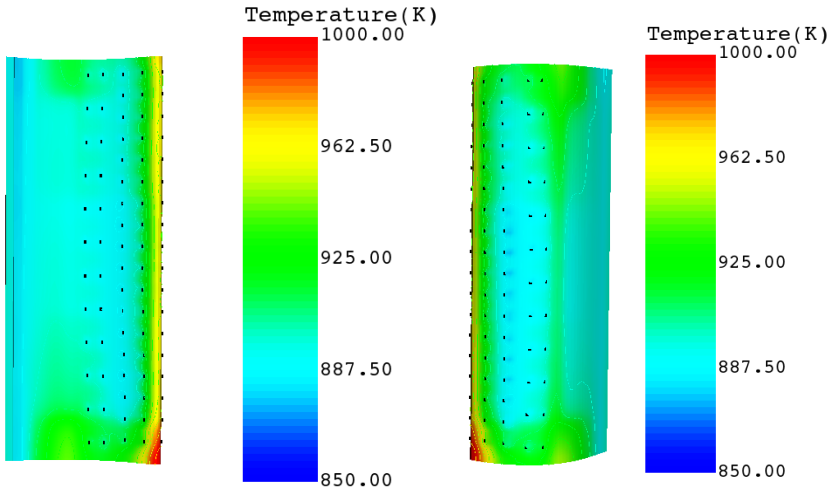

Figure 5.10 : Pressure Side Temperature Distribution for 4 Division

5.3.3 Summary of mesh independency study

When the temperature results are evaluated, there is minor temperature difference between the results both pressure and suction sides. Therefore, results are appropriate in terms of mesh frequency.

5.3.4 Safety validation study

NASA's second stage of NGV of the E^3 engine was used for the safety validation study. Metal temperature results of the NGV of the second stage of the ECU engine at 65% span are given in Figure 5.11.

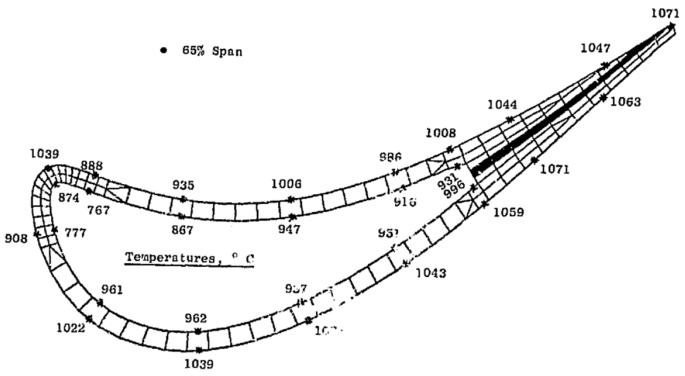

Figure 5.11 : 2nd Stage of HPT NGV Results for E^3 Engine [18]

Test details and metal temperature results are located in Figure 5.12.

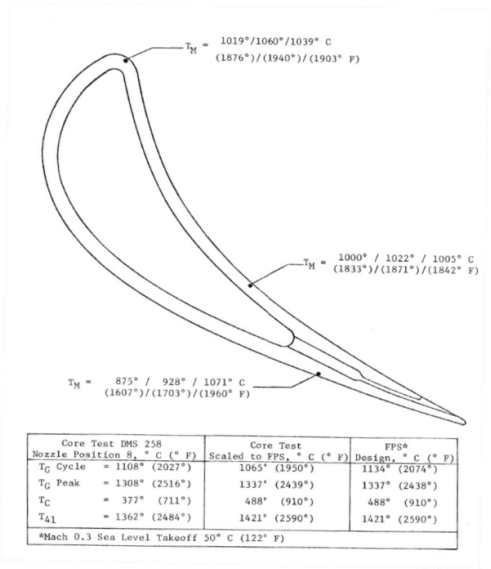

Core Test DMS 258 Nozzle Position 8, ° C (° F)	Core Test Scaled to FPS, ° C (° F)	FPS* Design, ° C (° F)
T_G Cycle = 1108° (2027°)	1065° (1950°)	1134° (2074°)
T_G Peak = 1308° (2516°)	1337° (2439°)	1337° (2438°)
T_C = 377° (711°)	488° (910°)	488° (910°)
T_{41} = 1362° (2484°)	1421° (2590°)	1421° (2590°)

*Mach 0.3 Sea Level Takeoff 50° C (122° F)

Figure 5.12 : 2nd Stage of HPT NGV Results for E^3 Engine [18]

This geometry is modeled in CTAADS program and analysis are done. Similar temperature results are found with NGV 2nd stage. Temperature results are located in Figure 5.13.

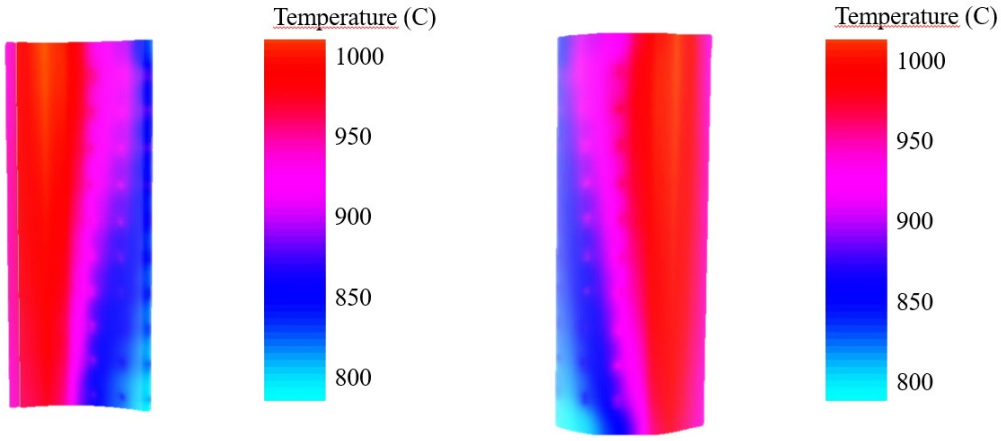

Figure 5.13 : Validation Study Results for E^3 Engine

5.4 Thickness Variation Study

Airfoil LE Wall Thickness is designed 0.5mm and nominal wall thickness is designed as 0.25mm as defined in Figure 5.14.

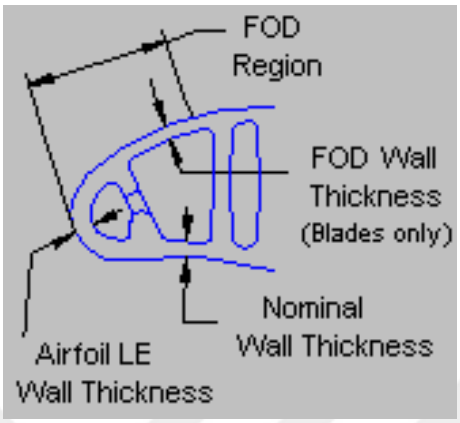

Figure 5.14 : Leading Edge and Wall Thickness Definiton

The effect of the thickness variation in the vane on temperature is studied in this section of study. Leading edge thickness is increased according to the base model and the suction side and pressure side wall thickness of the vane is designed 0.25mm with nominal thickness.

Different size of wall thicknesses are studied in this section.

5.4.1 0.6mm leading edge thickness and 0.25mm wall thickness

Temperature distribution plots and temperature spans of the geometry with 0.6mm leading edge thickness and 0.25mm wall thickness are in Figure 5.15 and 5.16.

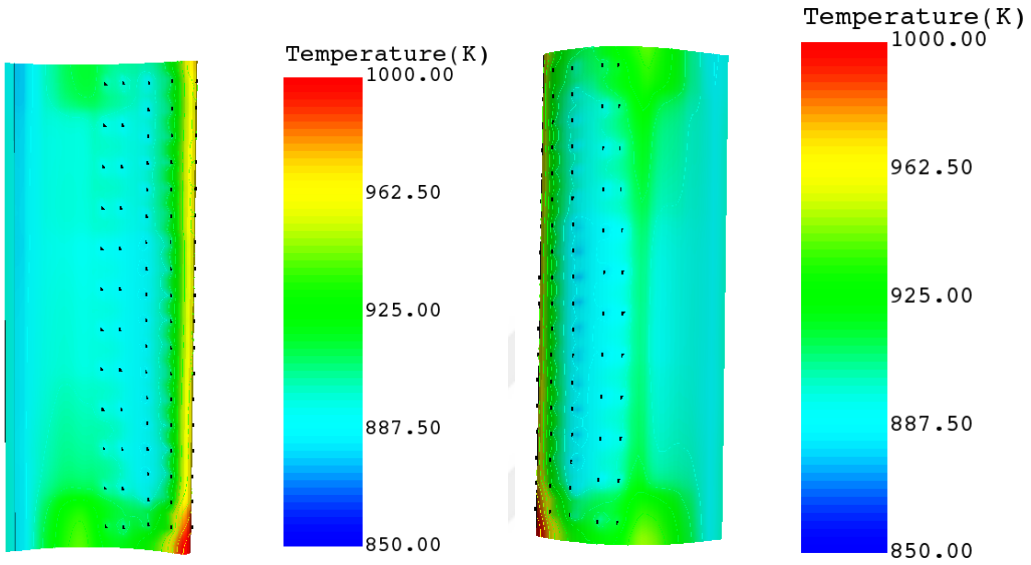

Figure 5.15 : Temperature Distribution for 0.6mm Leading Edge Thickness 0.25mm Wall Thickness

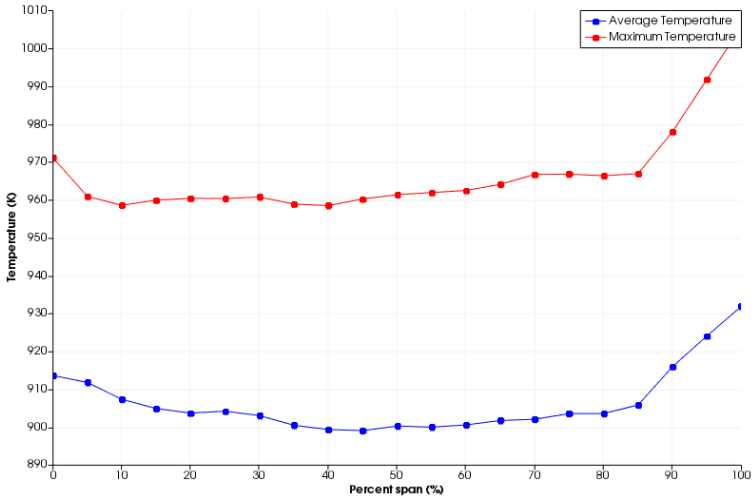

Figure 5.16 : Average and Maximum Temperature Span for 0.6mm Leading Edge Thickness 0.25mm Wall Thickness

Film effectiveness plots for tip, mid, and hub section of the geometry with 0.6mm leading edge thickness and 0.25 wall thickness are in Figure 5.17.

Red line shows the pressure side combined film effectiveness, blue line shows the pressure side of the showerhead film effectiveness, green line suction side combined film effectiveness, purple line shows the suction side of the showerhead film effectiveness.

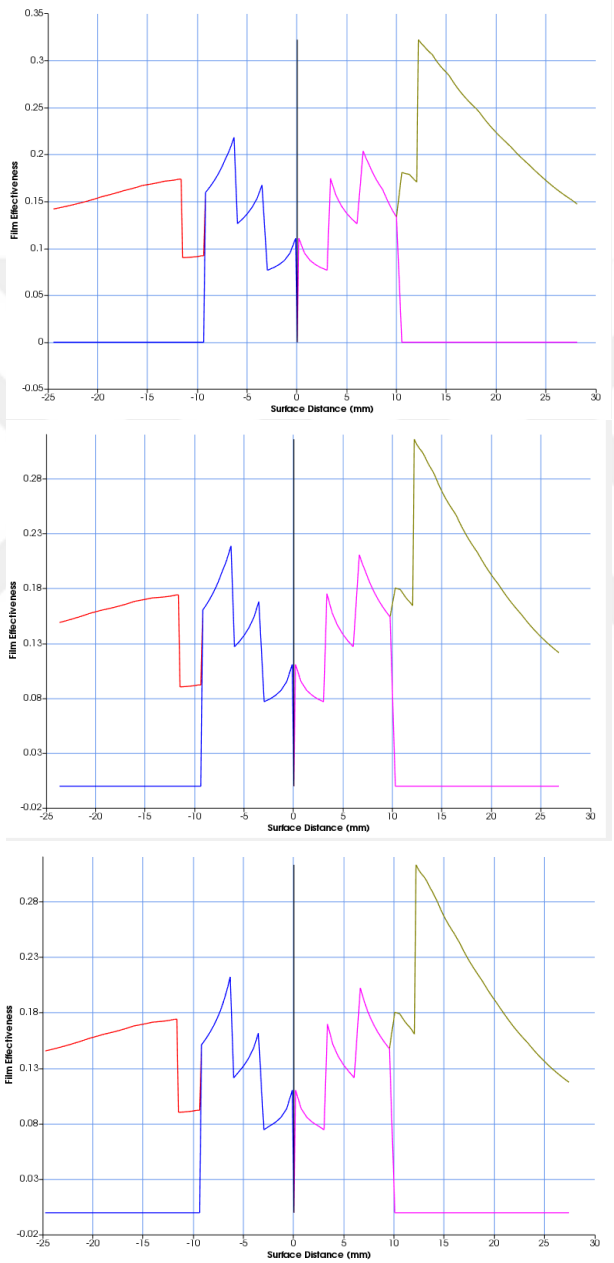

Figure 5.17 : Film Effectiveness of Tip Mid and Hub Section of The Span for 0.6mm Leading Edge Thickness 0.25mm Wall Thickness

5.4.2 0.7mm leading edge thickness and 0.25mm wall thickness

Temperature distribution plots and temperature spans of the geometry with 0.7mm leading edge thickness and 0.25mm wall thickness are in Figure 5.18 and 5.19.

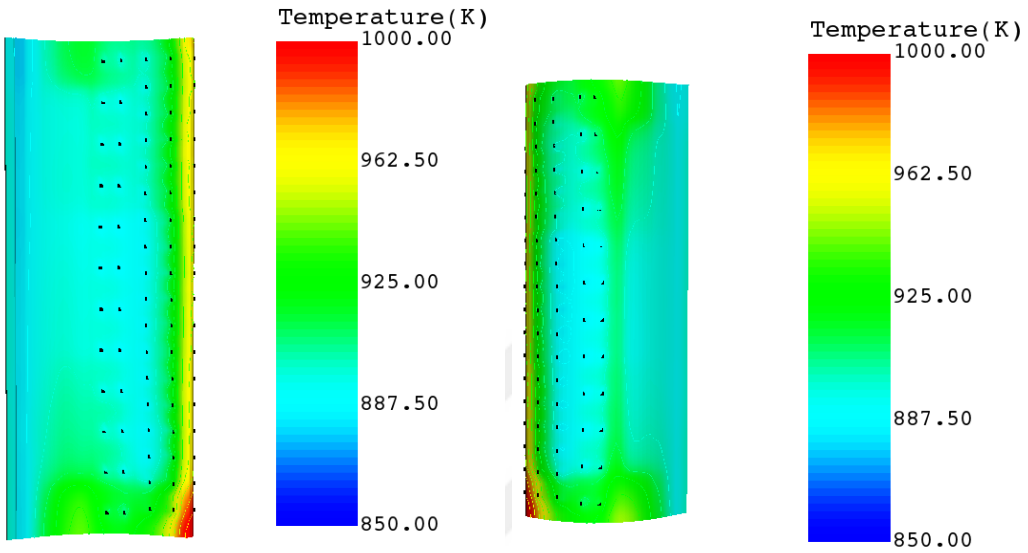

Figure 5.18 : Temperature Distribution for 0.7mm Leading Edge Thickness 0.25mm Wall Thickness

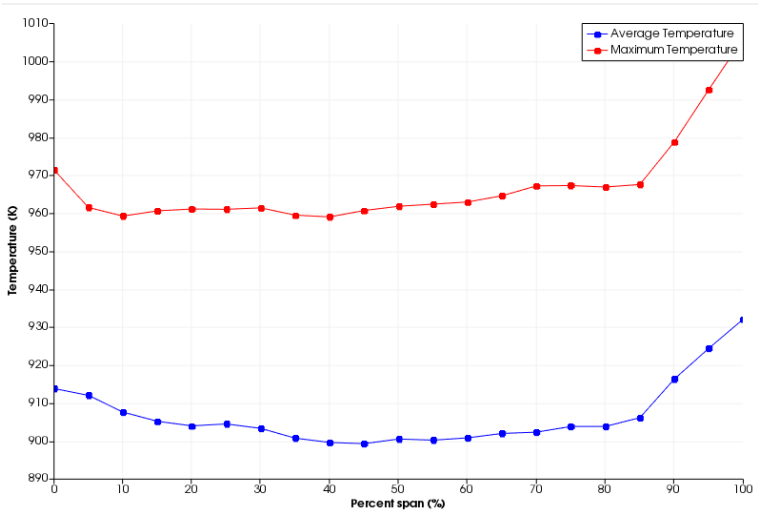

Figure 5.19 : Average and Maximum Temperature Span for 0.7mm Leading Edge Thickness 0.25mm Wall Thickness

Film effectiveness plots for tip, mid, and hub section of the geometry with 0.7mm leading edge thickness and 0.25 wall thickness are in Figure 5.20.

Red line shows the pressure side combined film effectiveness, blue line shows the pressure side of the showerhead film effectiveness, green line suction side combined film effectiveness, purple line shows the suction side of the showerhead film effectiveness.

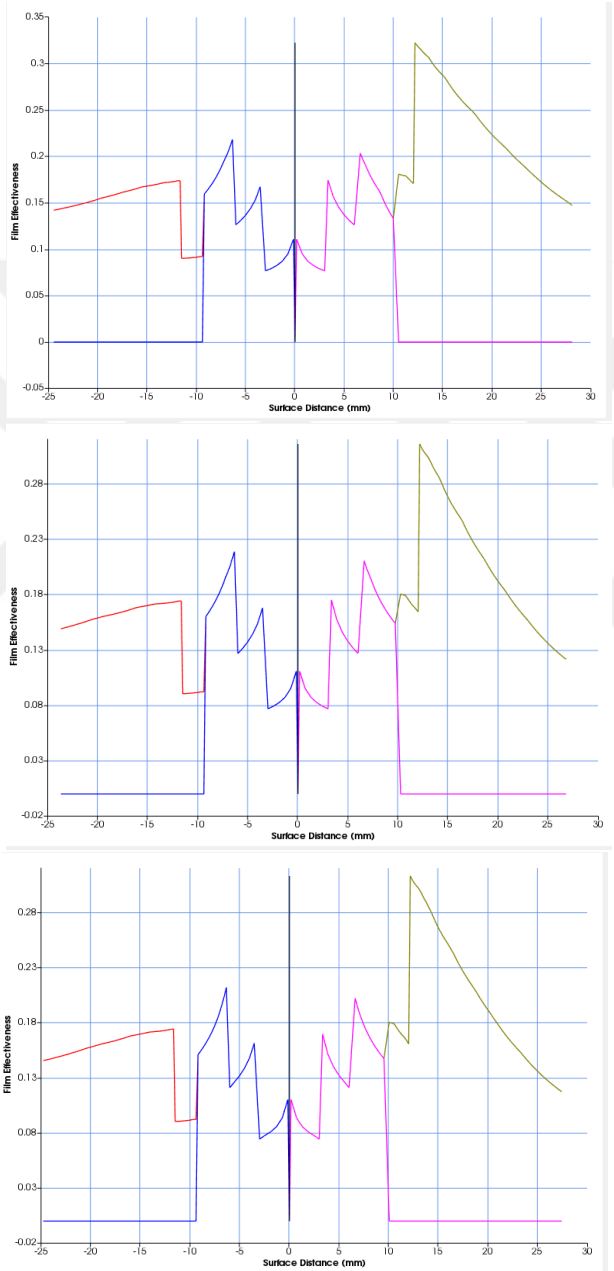

Figure 5.20 : Film Effectiveness of Tip Mid and Hub Section of The Span for 0.7mm Leading Edge Thickness 0.25mm Wall Thickness

5.4.3 0.5mm leading edge thickness and 0.35mm wall thickness

Temperature distribution plots and temperature spans of the geometry with 0.5mm leading edge thickness and 0.35mm wall thickness are in Figure 5.21 and 5.22.

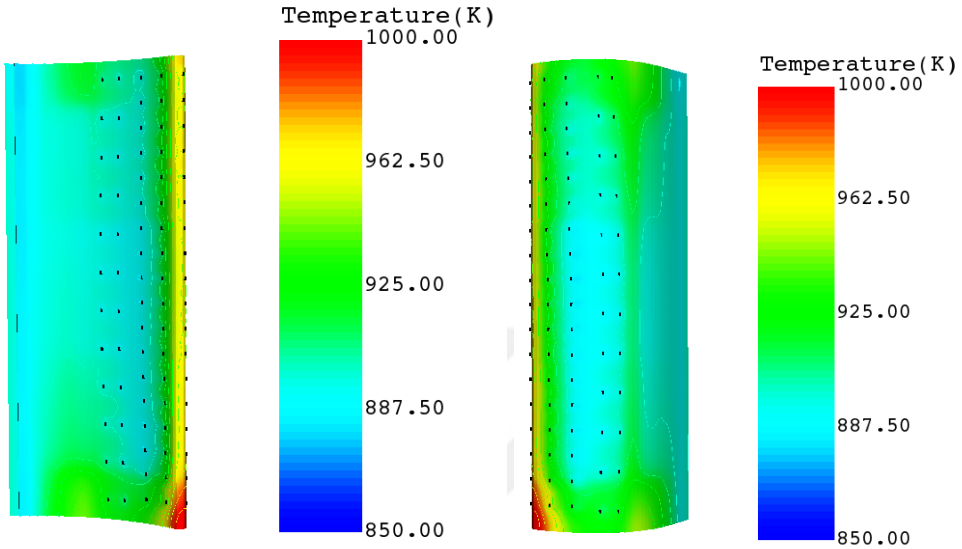

Figure 5.21 : Temperature Distribution for 0.5mm Leading Edge Thickness 0.35mm Wall Thickness

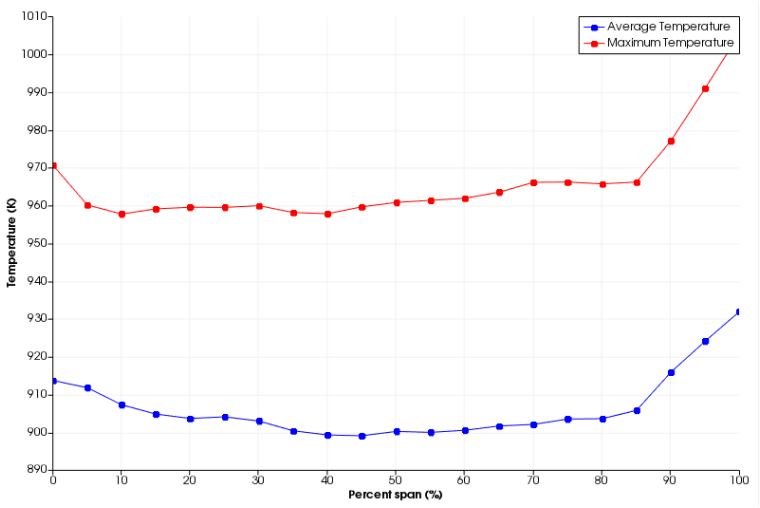

Figure 5.22 : Average and Maximum Temperature Span for 0.5mm Leading Edge Thickness 0.35mm Wall Thickness

Film effectiveness plots for tip, mid, and hub section of the geometry with 0.5mm leading edge thickness and 0.35 wall thickness are in Figure 5.23.

Red line shows the pressure side combined film effectiveness, blue line shows the pressure side of the showerhead film effectiveness, green line suction side combined film effectiveness, purple line shows the suction side of the showerhead film effectiveness.

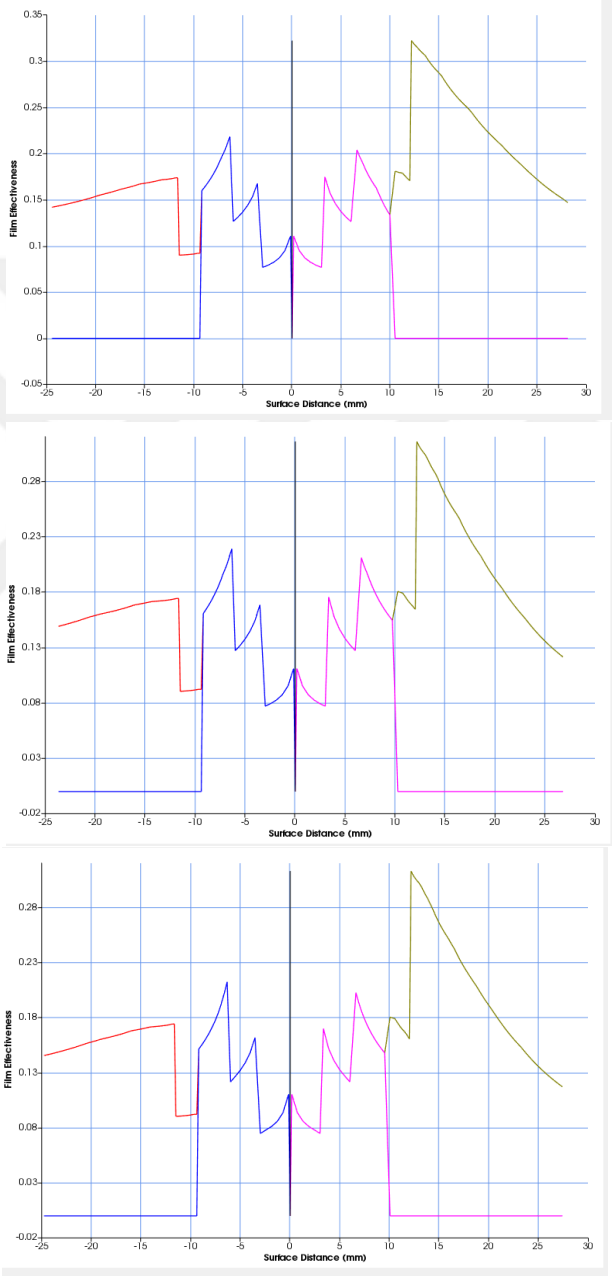

Figure 5.23 : Film Effectiveness of Tip Mid and Hub Section of The Span for 0.5mm Leading Edge Thickness 0.35mm Wall Thickness

5.4.4 0.5mm leading edge thickness and 0.3mm wall thickness

Temperature distribution plots and temperature spans of the geometry with 0.5mm leading edge thickness and 0.3mm wall thickness are in Figure 5.24 and 5.25.

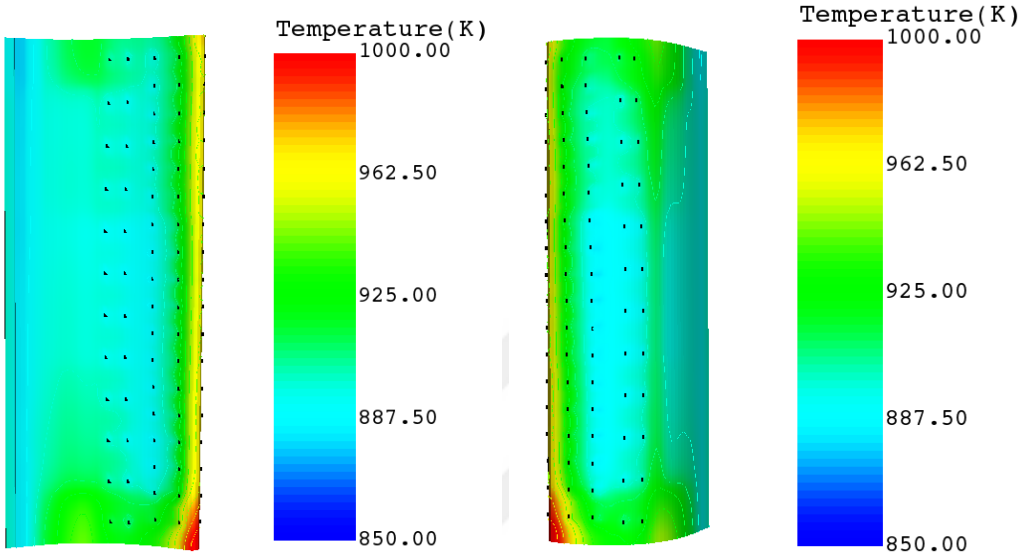

Figure 5.24 : Temperature Distribution for 0.5mm Leading Edge Thickness 0.3mm Wall Thickness

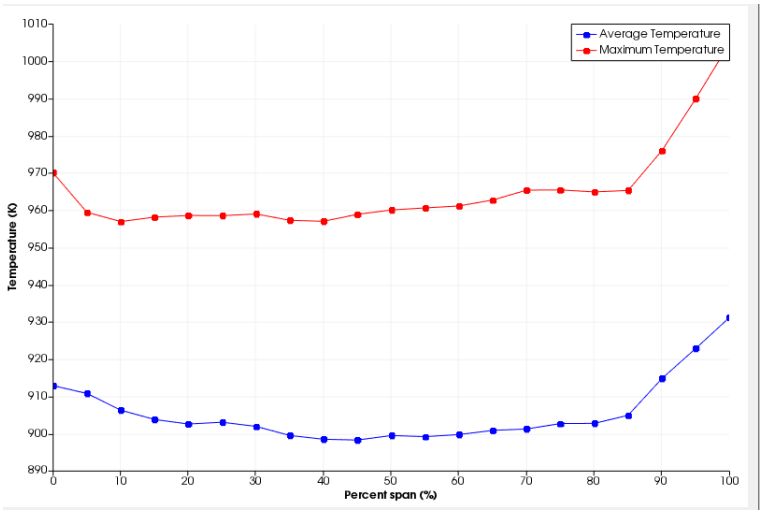

Figure 5.25 : Average and Maximum Temperature Span for 0.5mm Leading Edge Thickness 0.3mm Wall Thickness

Film effectiveness plots for tip, mid, and hub section of the geometry with 0.5mm leading edge thickness and 0.30 wall thickness are in Figure 5.26.

Red line shows the pressure side combined film effectiveness, blue line shows the pressure side of the showerhead film effectiveness, green line suction side combined film effectiveness, purple line shows the suction side of the showerhead film effectiveness.

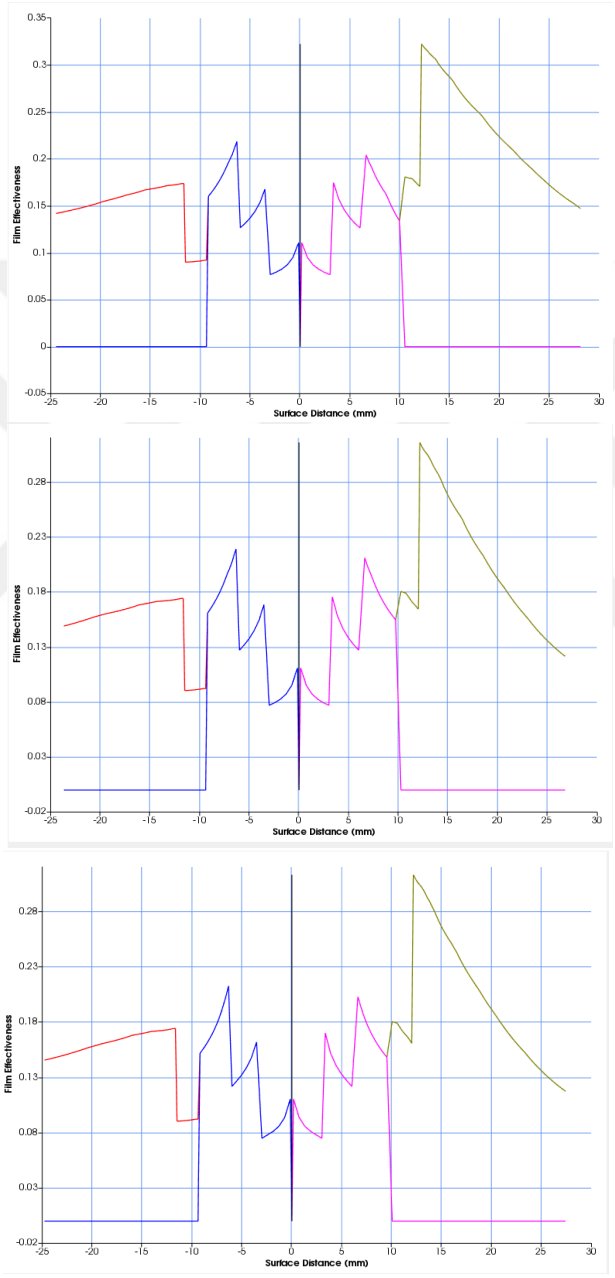

Figure 5.26 : Film Effectiveness of Tip Mid and Hub Section of The Span for 0.5mm Leading Edge Thickness 0.30mm Wall Thickness

5.4.5 Summary of thickness variation study

Thickness variation study is performed for leading edge thickness between 0.5mm - 0.7mm. Also, wall thickness study is performed between 0.25mm - 0.35mm.

When the section 5.4.1 and section 5.4.2 iterations are compared each other, there is not any significant difference between them in term of wall temperatures. The difference between the geometries is leading edge thickness. Geometry is in section 5.4.1 is colder than section 5.4.2 in terms of leading edge wall temperatures as it can be seen in table 5.1.

Table 5.1 : Leading Edge Thickness Variation

Section	Max Temperature (K)		
	% 0 Span	% 50 Span	% 100 Span
5.4.1	972	961	1006
5.4.2	974	962	1008

When the section 5.4.3 and section 5.4.4 iterations are compared each other, average and maximum temperatures of section 5.4.4 are lower than section 5.4.3 as it can be located in table 5.2. But difference is around small amounts. According to results, it is said that when the thickness is decreased, temperature is decreased. As the thickness decreases, cooling flow rate effects more temperature decreasing for the geometry.

Table 5.2 : Wall Thickness Variation

Section	Max Temperature (K)		
	% 0 Span	% 50 Span	% 100 Span
5.4.3	970	961	1006
5.4.4	970	960	1005

5.5 Film Cooling Holes

5.5.1 Film cooling holes diameter study for midchannel

Base NGV middle channel model has total 4 columns film cooling holes. 2 of them is located in suction side 2 of them is located in pressure side that is located in Figure 5.27. In section 5.5.1, it is studied how the film cooling holes on the midchannel affect the temperature.

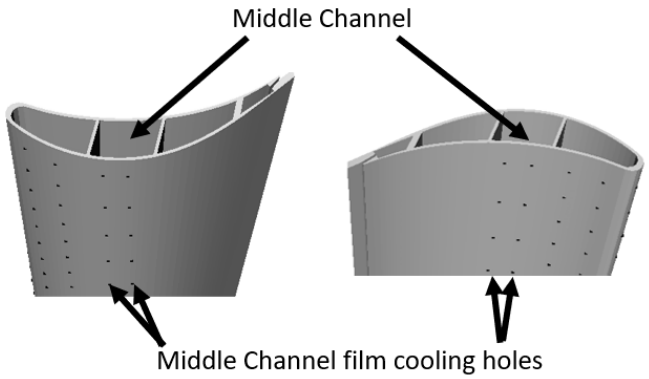

Figure 5.27 : Middle Channel Film Cooling Holes

5.5.1.1 1^{st} column of midchannel of pressure side of film cooling holes diameter is 0.4mm

Temperature distribution plots and temperature spans of the geometry within section 5.5.1.1 is shown in Figure 5.28 and 5.29.

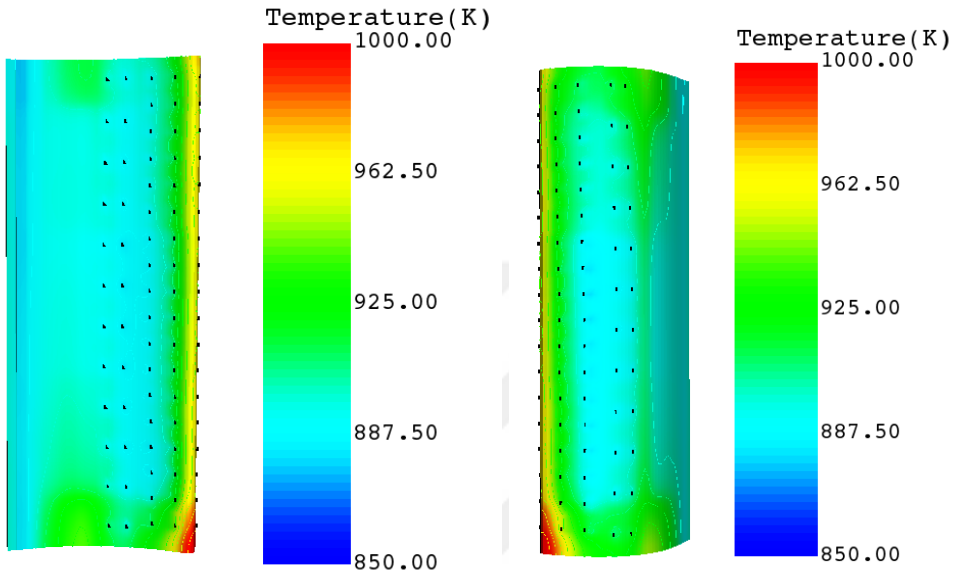

Figure 5.28 : Temperature Distribution

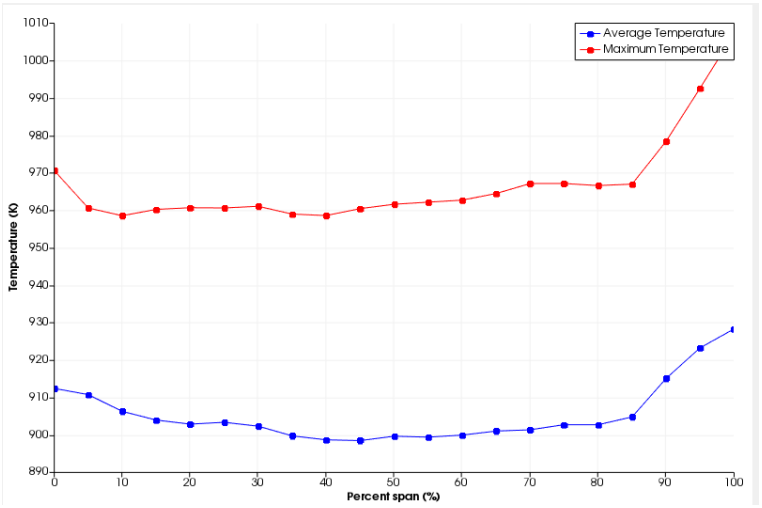

Figure 5.29 : Average and Maximum Temperature Span

Film effectiveness plots for tip, mid, and hub section of the geometry within section 5.5.1.1 is shown in Figure 5.30.

Red line shows the pressure side combined film effectiveness, blue line shows the pressure side of the showerhead film effectiveness, green line suction side combined film effectiveness, purple line shows the suction side of the showerhead film effectiveness.

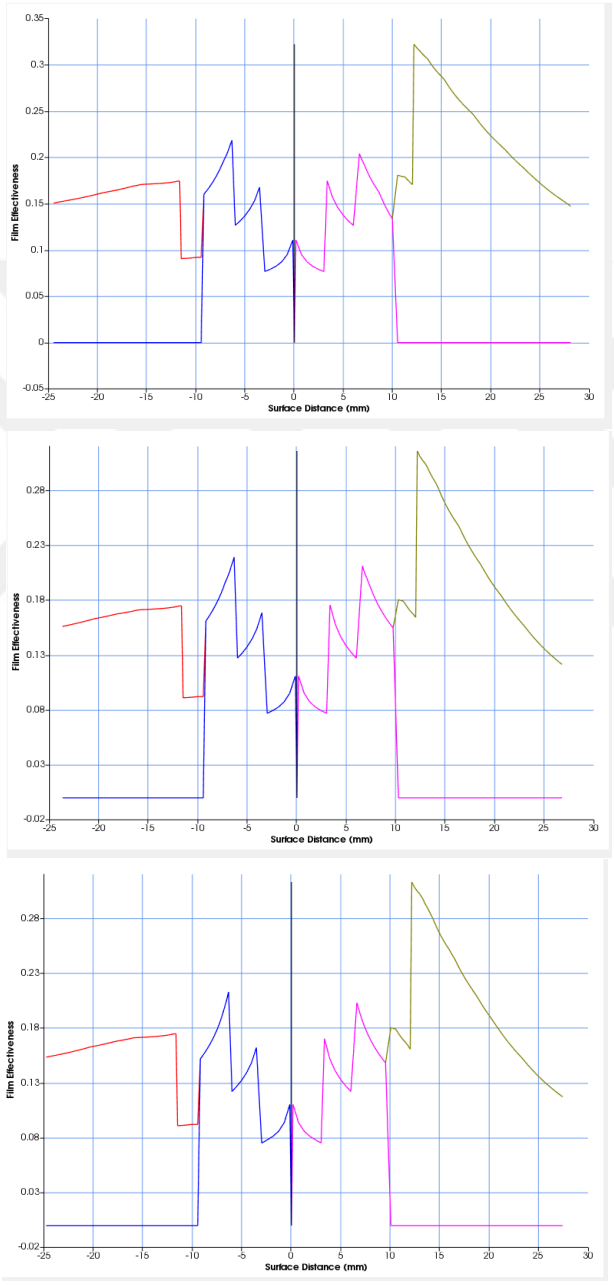

Figure 5.30 : Film Effectiveness of Tip Mid and Hub Section of The Span

5.5.1.2 1^{st} column of midchannel of pressure side of film cooling holes diameter is 0.5mm

Temperature distribution plots and temperature spans of the geometry within section 5.5.1.2 is shown in Figure 5.31 and 5.32.

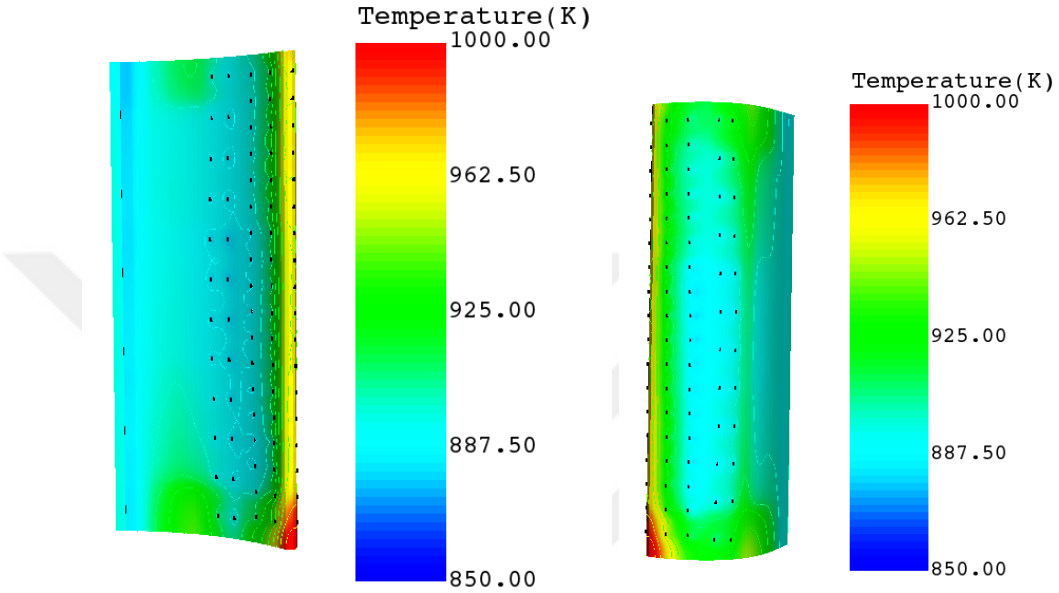

Figure 5.31 : Temperature Distribution

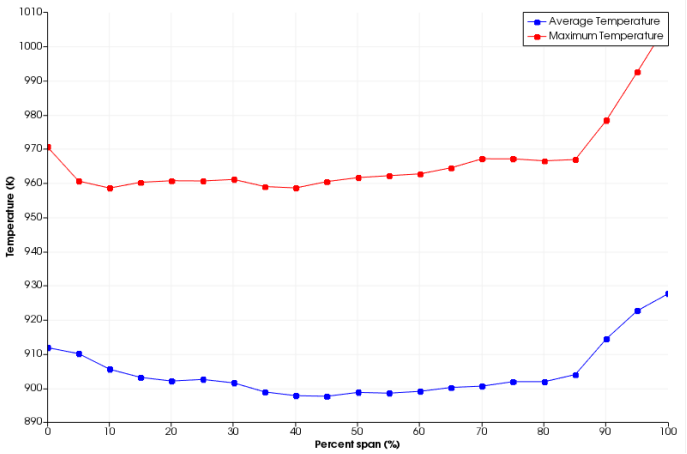

Figure 5.32 : Average and Maximum Temperature Span

Film effectiveness plots for tip, mid, and hub section of the geometry within section 5.5.1.2 is shown in Figure 5.33.

Red line shows the pressure side combined film effectiveness, blue line shows the pressure side of the showerhead film effectiveness, green line suction side combined film effectiveness, purple line shows the suction side of the showerhead film effectiveness.

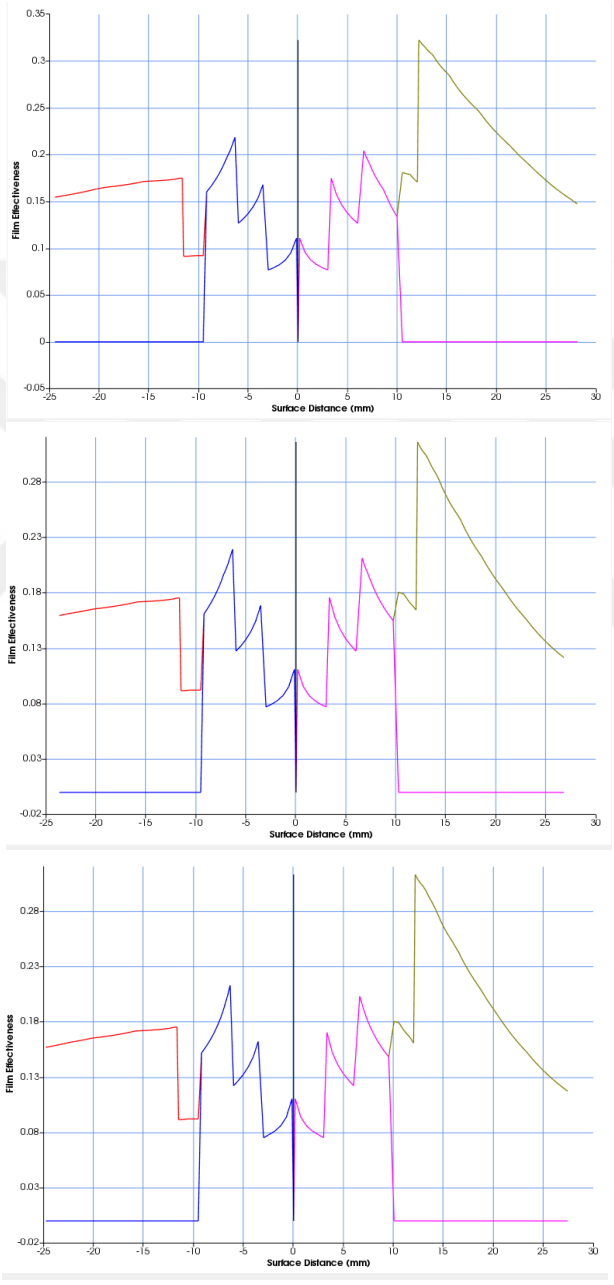

Figure 5.33 : Film Effectiveness of Tip Mid and Hub Section of The Span

5.5.1.3 2^{nd} column of midchannel of pressure side of film cooling holes diameter is 0.4mm

Temperature distribution plots and temperature spans of the geometry within section 5.5.1.3 is shown in Figure 5.34 and 5.35.

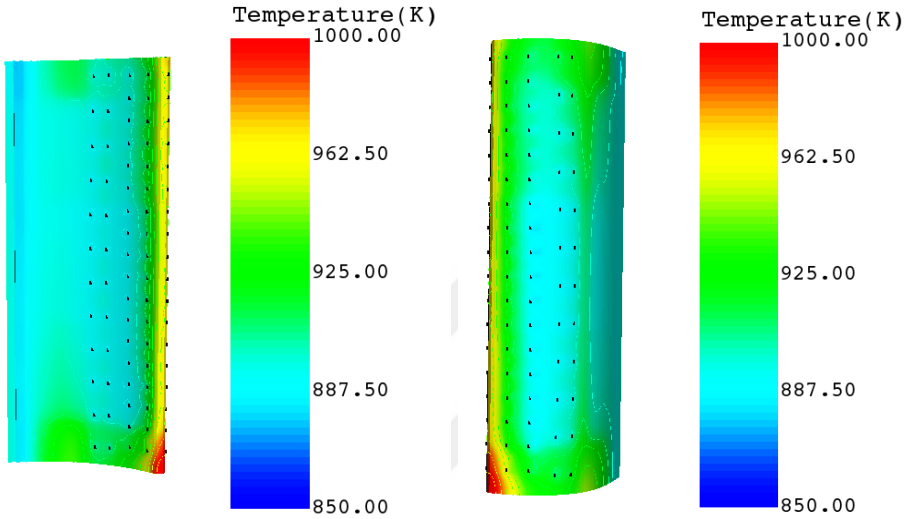

Figure 5.34 : Temperature Distribution

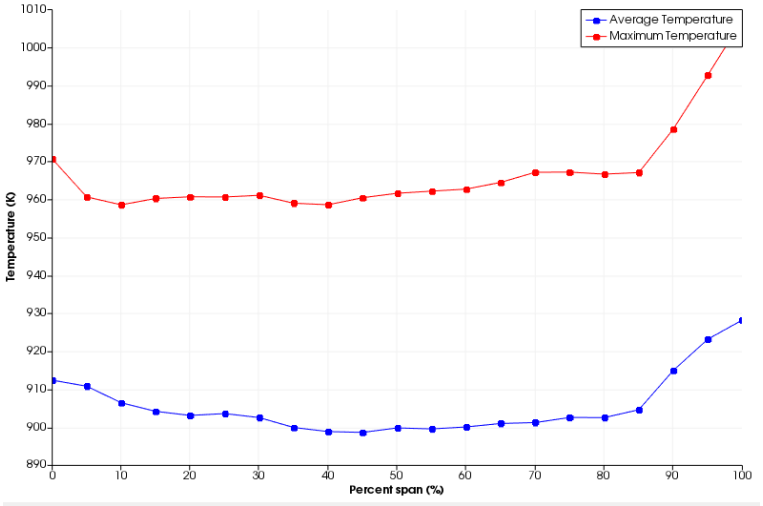

Figure 5.35 : Average and Maximum Temperature Span

Film effectiveness plots for tip, mid, and hub section of the geometry within section 5.5.1.3 is shown in Figure 5.36.

Red line shows the pressure side combined film effectiveness, blue line shows the pressure side of the showerhead film effectiveness, green line suction side combined film effectiveness, purple line shows the suction side of the showerhead film effectiveness.

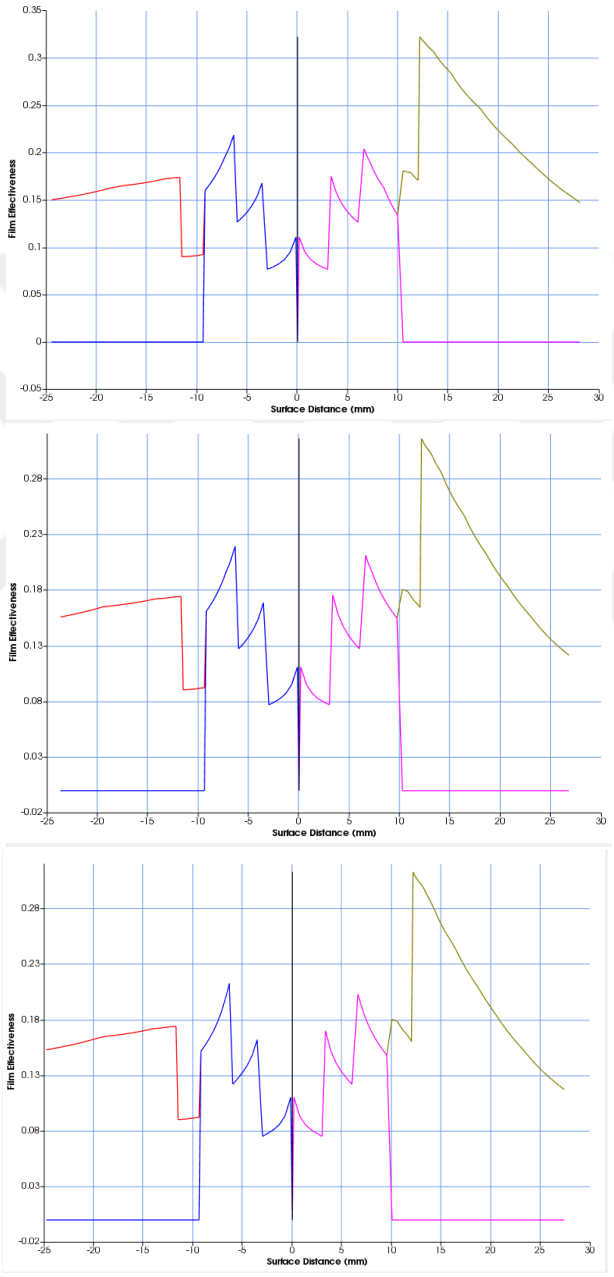

Figure 5.36 : Film Effectiveness of Tip Mid and Hub Section of The Span

5.5.1.4 2^{nd} column of midchannel of pressure side of film cooling holes diameter is 0.5mm

Temperature distribution plots and temperature spans of the geometry within section 5.5.1.4 is shown in Figure 5.37 and 5.38.

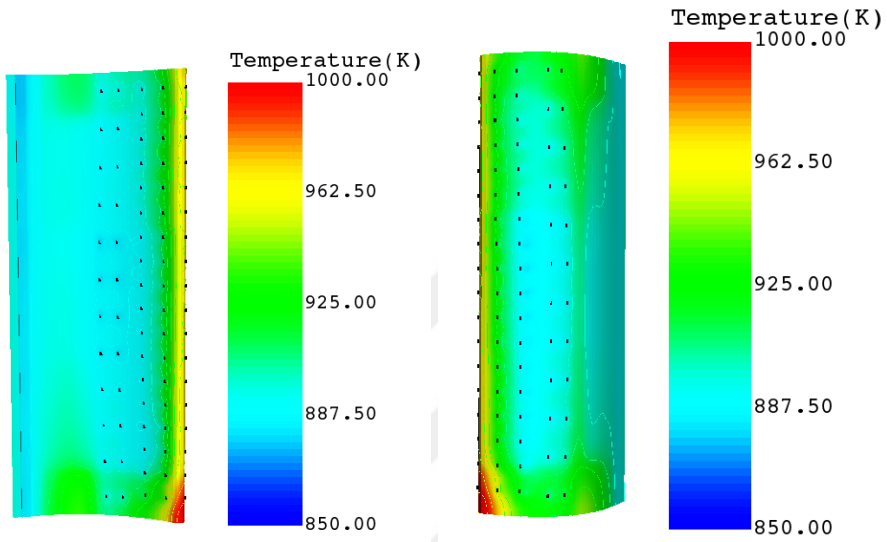

Figure 5.37 : Temperature Distribution

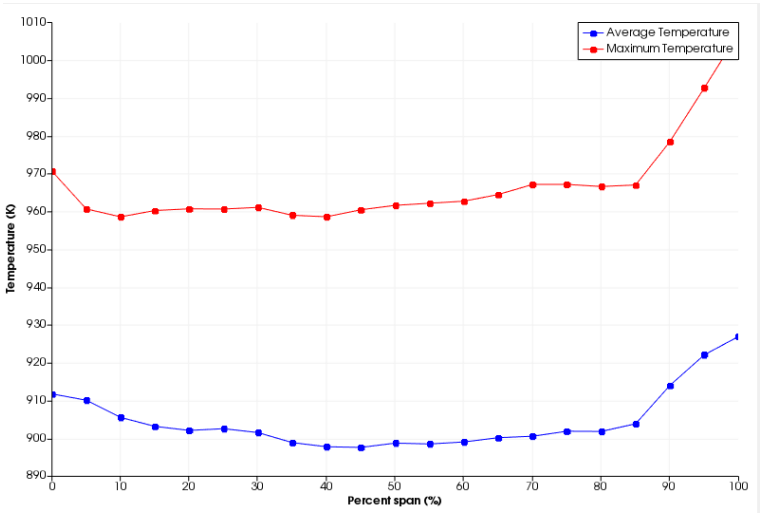

Figure 5.38 : Average and Maximum Temperature Span

Film effectiveness plots for tip, mid, and hub section of the geometry within section 5.5.1.4 is shown in Figure 5.39.

Red line shows the pressure side combined film effectiveness, blue line shows the pressure side of the showerhead film effectiveness, green line suction side combined film effectiveness, purple line shows the suction side of the showerhead film effectiveness.

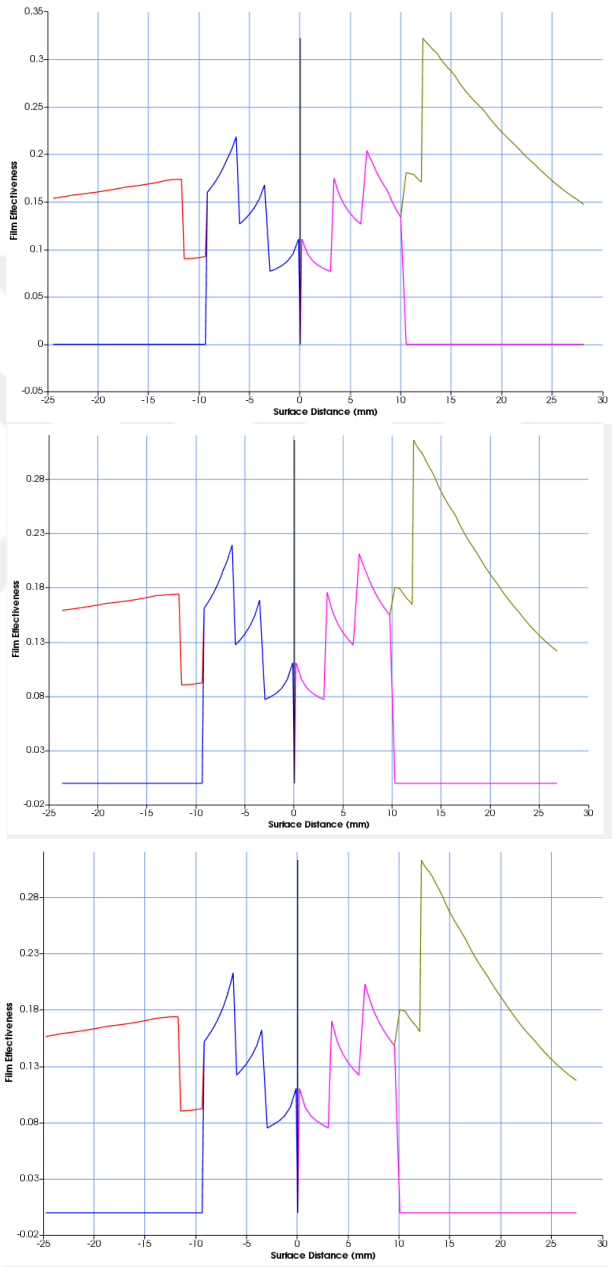

Figure 5.39 : Film Effectiveness of Tip Mid and Hub Section of The Span

5.5.1.5 1^{st} column of midchannel of suction side of film cooling holes diameter is 0.4mm

Temperature distribution plots and temperature spans of the geometry within section 5.5.1.5 is shown in Figure 5.40 and 5.41.

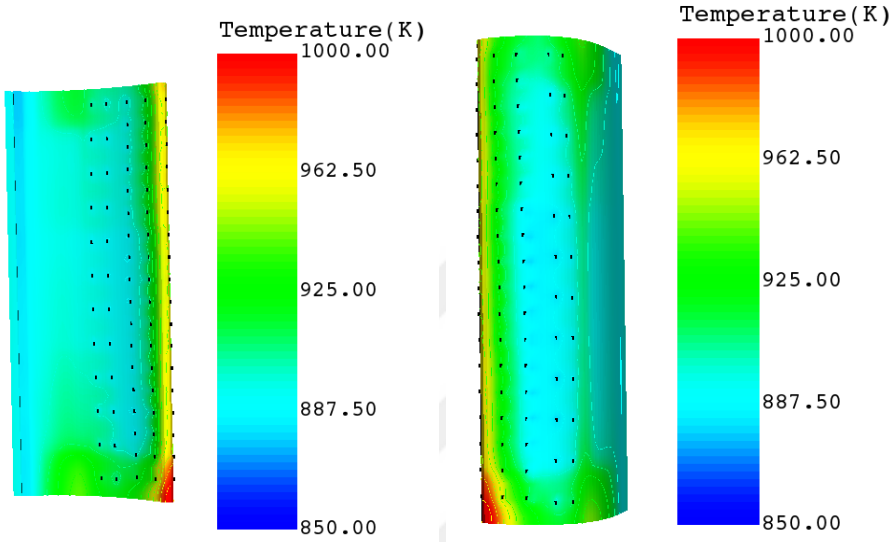

Figure 5.40 : Temperature Distribution

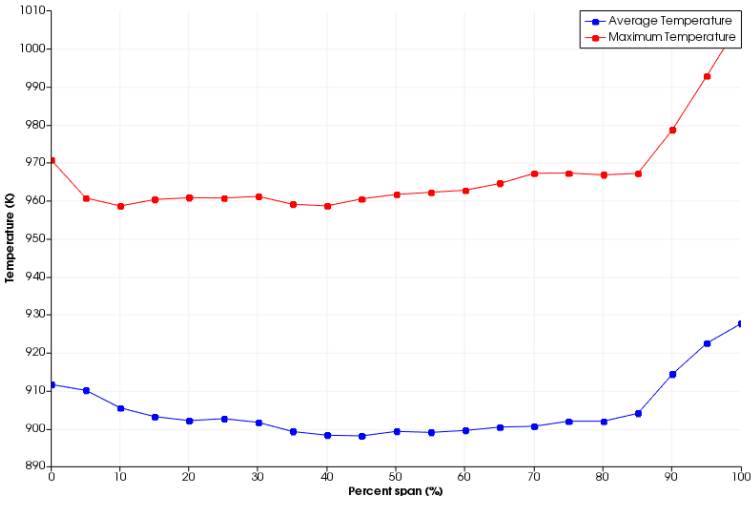

Figure 5.41 : Average and Maximum Temperature Span

Film effectiveness plots for tip, mid, and hub section of the geometry within section 5.5.1.5 is shown in Figure 5.42.

Red line shows the pressure side combined film effectiveness, blue line shows the pressure side of the showerhead film effectiveness, green line suction side combined film effectiveness, purple line shows the suction side of the showerhead film effectiveness.

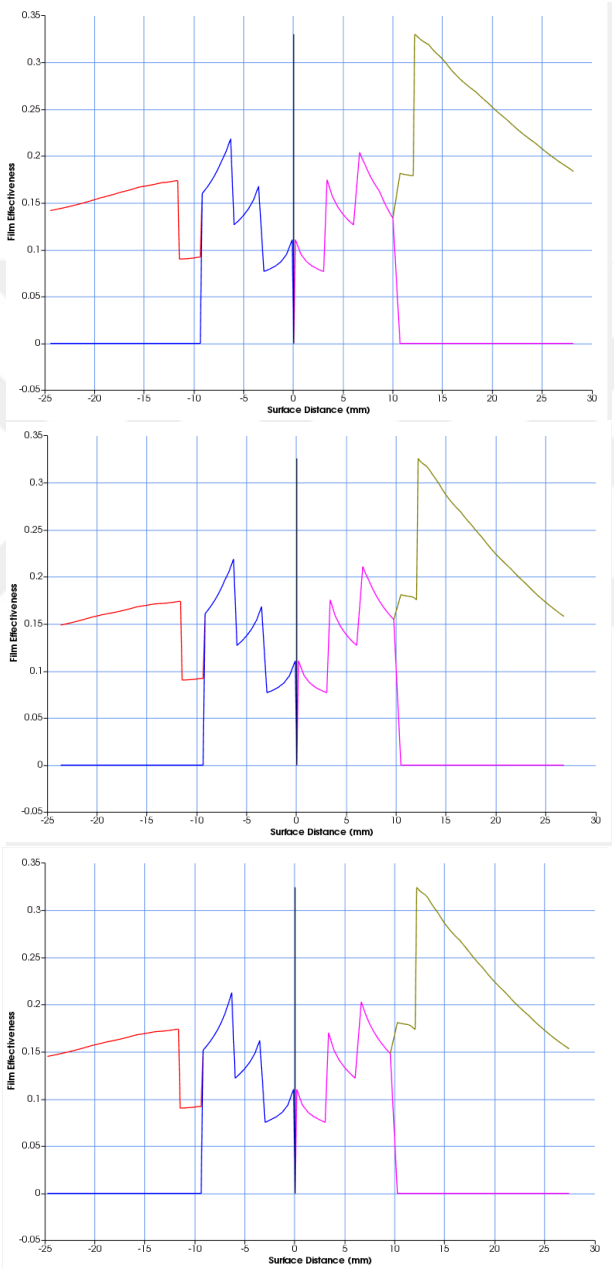

Figure 5.42 : Film Effectiveness of Tip Mid and Hub Section of The Span

5.5.1.6 1^{st} column of midchannel of suction side of film cooling holes diameter is 0.5mm

Temperature distribution plots and temperature spans of the geometry within section 5.5.1.6 is shown in Figure 5.43 and 5.44.

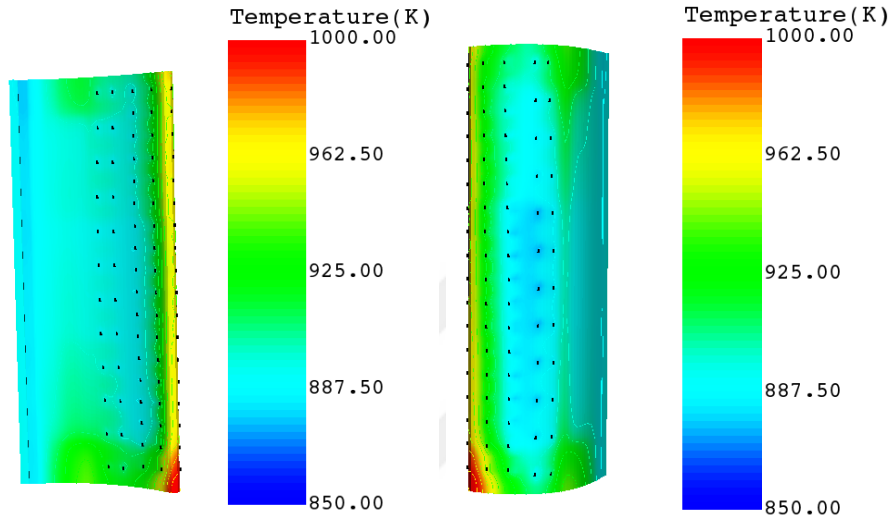

Figure 5.43 : Temperature Distribution

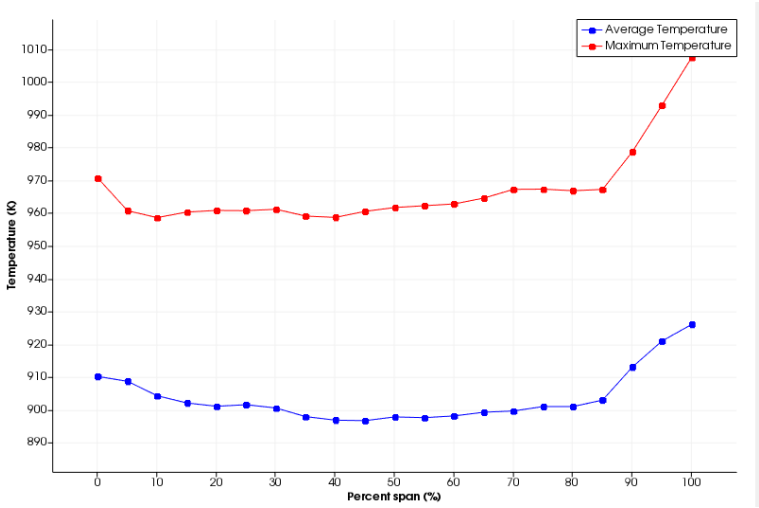

Figure 5.44 : Average and Maximum Temperature Span

Film effectiveness plots for tip, mid, and hub section of the geometry within section 5.5.1.6 is shown in Figure 5.45.

Red line shows the pressure side combined film effectiveness, blue line shows the pressure side of the showerhead film effectiveness, green line suction side combined film effectiveness, purple line shows the suction side of the showerhead film effectiveness.

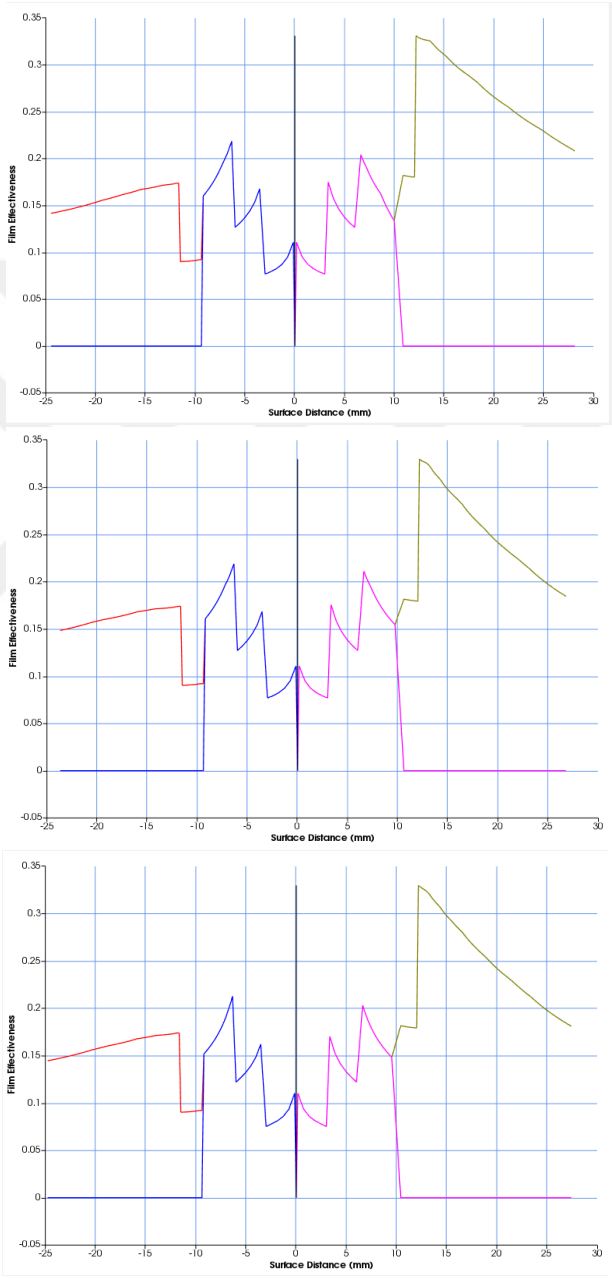

Figure 5.45 : Film Effectiveness of Tip Mid and Hub Section of The Span

5.5.1.7 2^{nd} column of midchannel of suction side of film cooling holes diameter is 0.4mm

Temperature distribution plots and temperature spans of the geometry within section 5.5.1.7 is shown in Figure 5.46 and 5.47.

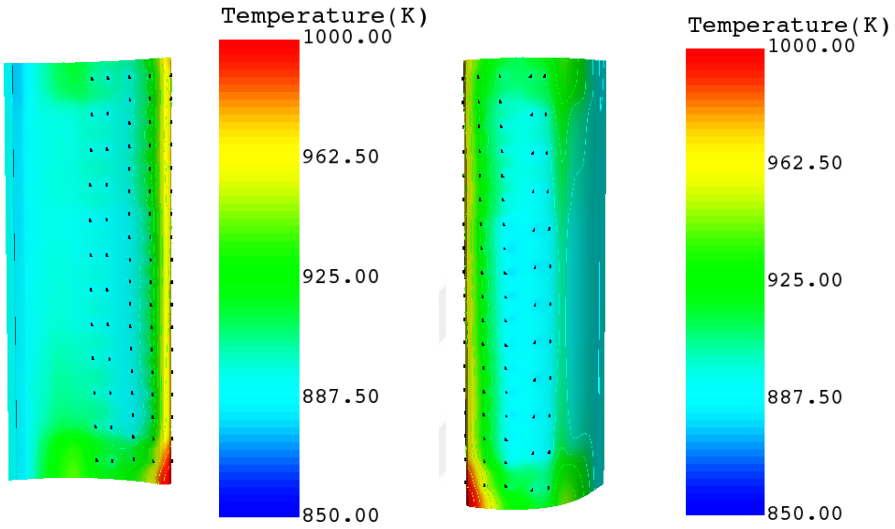

Figure 5.46 : Temperature Distribution

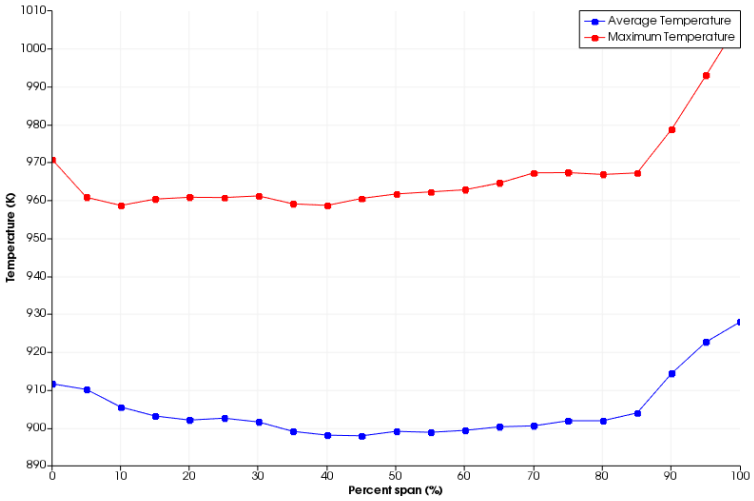

Figure 5.47 : Average and Maximum Temperature Span

Film effectiveness plots for tip, mid, and hub section of the geometry within section 5.5.1.7 is shown in Figure 5.48.

Red line shows the pressure side combined film effectiveness, blue line shows the pressure side of the showerhead film effectiveness, green line suction side combined film effectiveness, purple line shows the suction side of the showerhead film effectiveness.

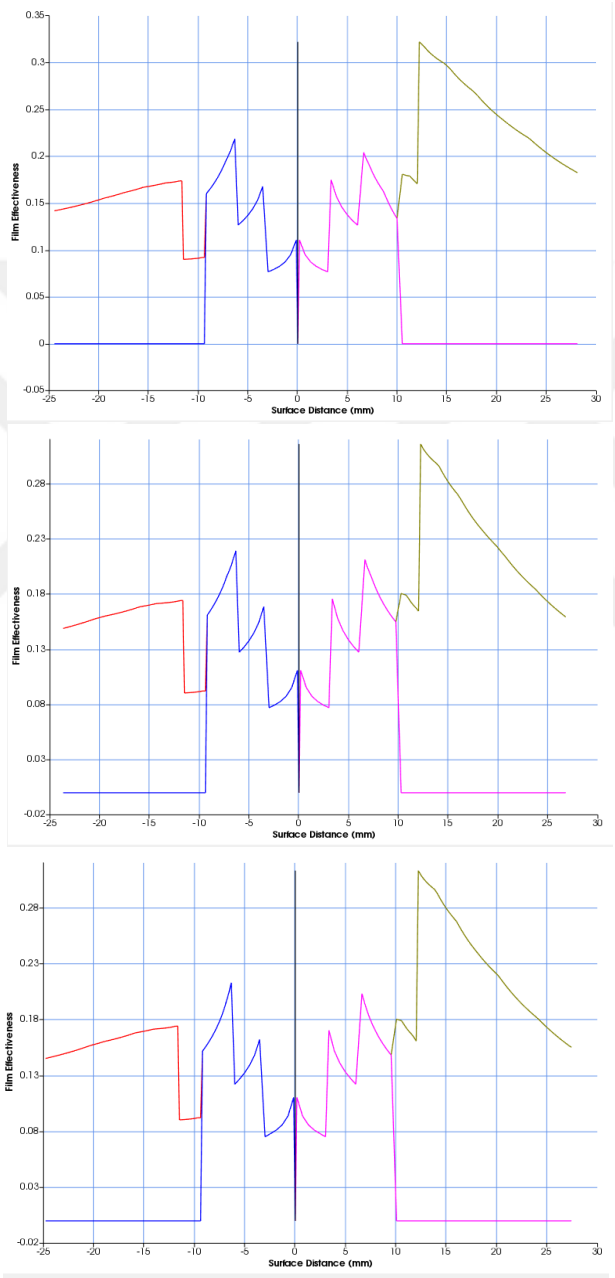

Figure 5.48 : Film Effectiveness of Tip Mid and Hub Section of The Span

5.5.1.8 2^{nd} column of midchannel of suction side of film cooling holes diameter is 0.5mm

Temperature distribution plots and temperature spans of the geometry within section 5.5.1.8 is shown in Figure 5.49 and 5.50.

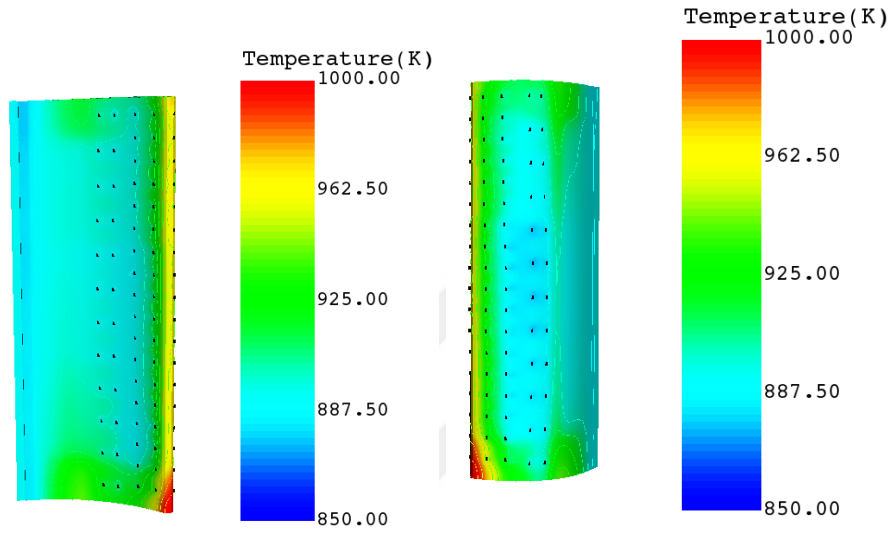

Figure 5.49 : Temperature Distribution

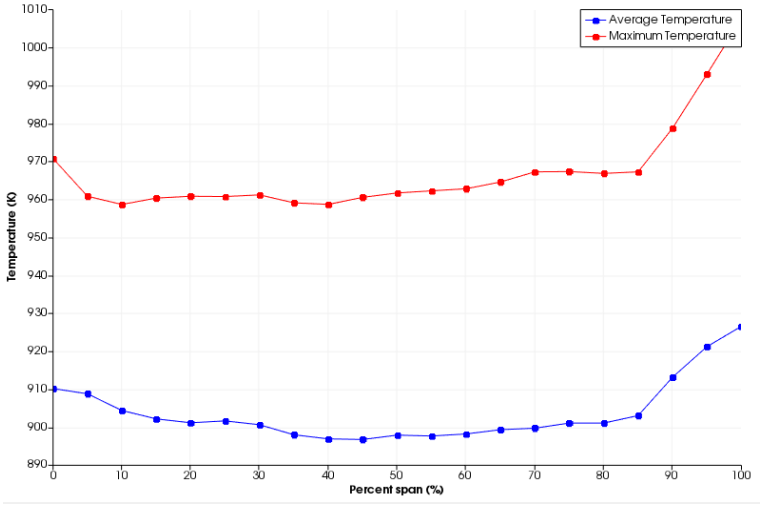

Figure 5.50 : Average and Maximum Temperature Span

Film effectiveness plots for tip, mid, and hub section of the geometry within section 5.5.1.8 is shown in Figure 5.51.

Red line shows the pressure side combined film effectiveness, blue line shows the pressure side of the showerhead film effectiveness, green line suction side combined film effectiveness, purple line shows the suction side of the showerhead film effectiveness.

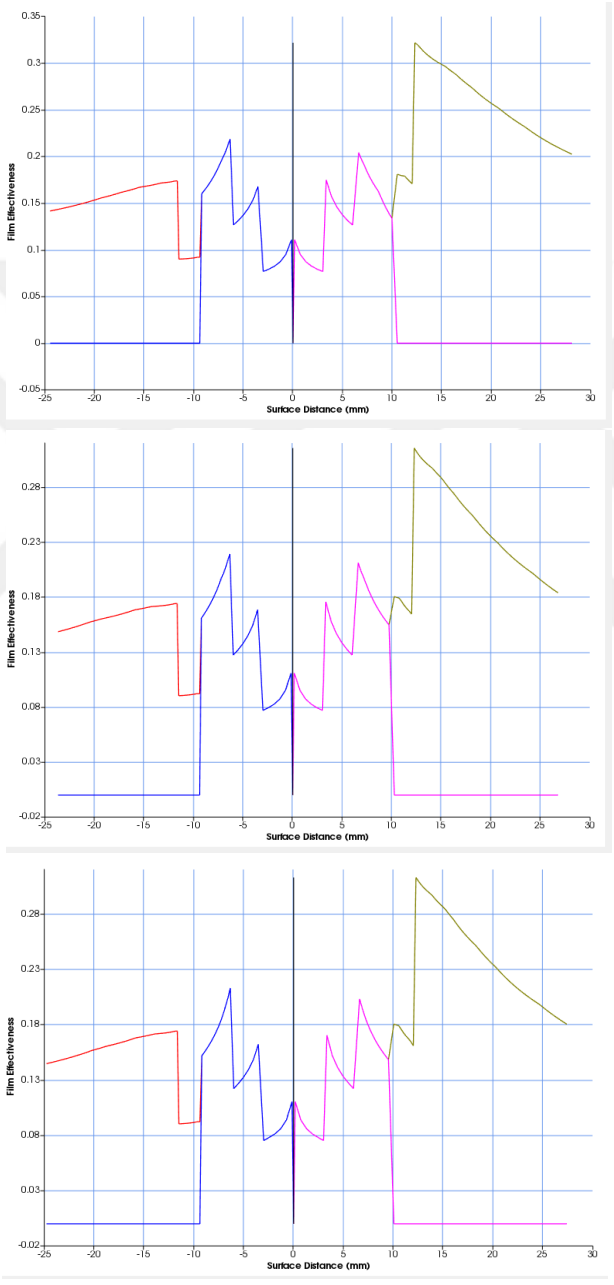

Figure 5.51 : Film Effectiveness of Tip Mid and Hub Section of The Span

5.5.1.9 Summary of midchannel film cooling diameter study

Midchannel holes diameters is studied for 0.4 and 0.5mm. When the iterations are studied it is said that max temperatures are not changed as stated in table 5.3. As, max temparatures location is in showerhead area.

Table 5.3 : Max Temperatures for Midchannel Study

Section	Max Temperature (K)		
	%0 Span	%50 Span	%100 Span
5.5.1.1	971	962	1004
5.5.1.2	971	962	1004
5.5.1.3	971	962	1004
5.5.1.4	971	962	1004
5.5.1.5	971	962	1004
5.5.1.6	971	962	1004
5.5.1.7	971	962	1004
5.5.1.8	971	962	1004

There is minor changes for average temperatures for midchannel study as it can be seen in table 5.4.

Table 5.4 : Average Temperatures for Midchannel Study

Section	Average Temperature (K)		
	%0 Span	%50 Span	%100 Span
5.5.1.1	913	900	928
5.5.1.2	912	898	927
5.5.1.3	913	900	928
5.5.1.4	912	898	927
5.5.1.5	912	899	928
5.5.1.6	910	895	925
5.5.1.7	912	898	928
5.5.1.8	910	898	925

5.5.2 Film cooling holes diameter study for showerhead and stagnation line

Base NGV showerhead model has total 5 columns film cooling holes. Two of them is located in suction side, two of them is located in pressure side and one of them is located on the stagnation line that can be seen in Figure 5.52 and 5.53. In section 5.5.2, it is studied how the film cooling holes on the showerhead affect the temperature.

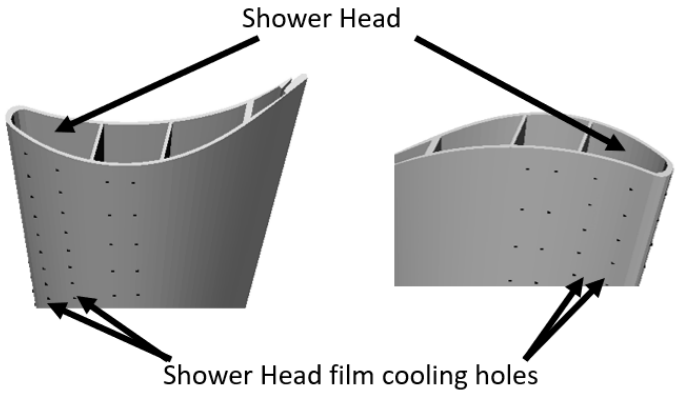

Figure 5.52 : Shower Head Film Cooling Holes

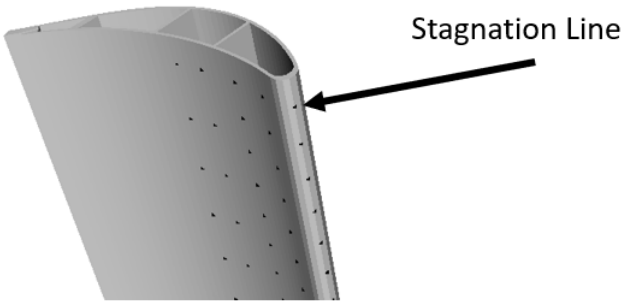

Figure 5.53 : Stagnation Line Film Cooling Holes

5.5.2.1 1^{st} column of showerhead of pressure side of film cooling holes diameter is 0.4mm

Temperature distribution plots and temperature spans of the geometry within section 5.5.2.1 is shown in Figure 5.54 and 5.55.

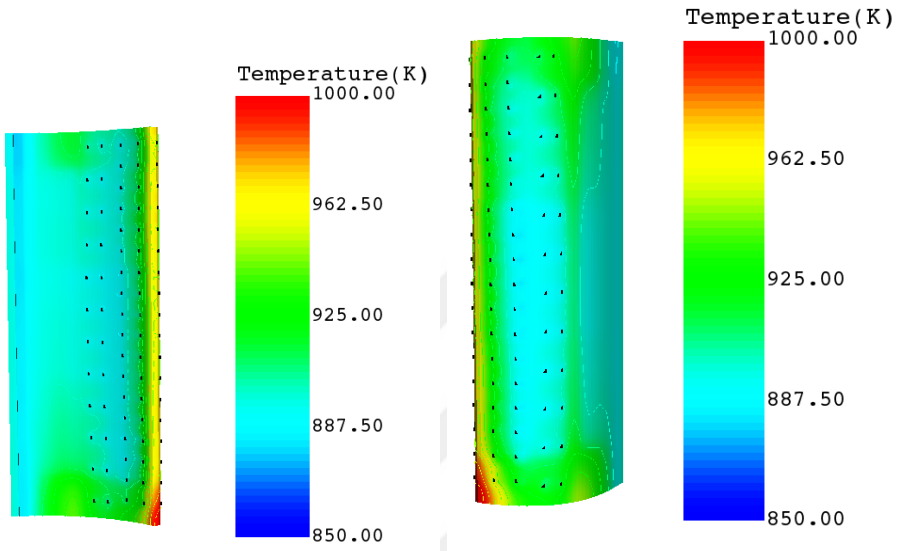

Figure 5.54 : Temperature Distribution

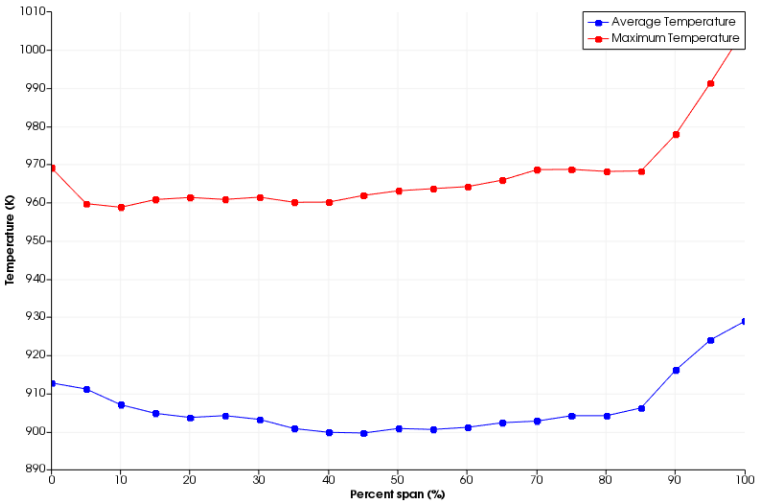

Figure 5.55 : Average and Maximum Temperature Span

Film effectiveness plots for tip, mid, and hub section of the geometry within section 5.5.2.1 is shown in Figure 5.56.

Red line shows the pressure side combined film effectiveness, blue line shows the pressure side of the showerhead film effectiveness, green line suction side combined film effectiveness, purple line shows the suction side of the showerhead film effectiveness.

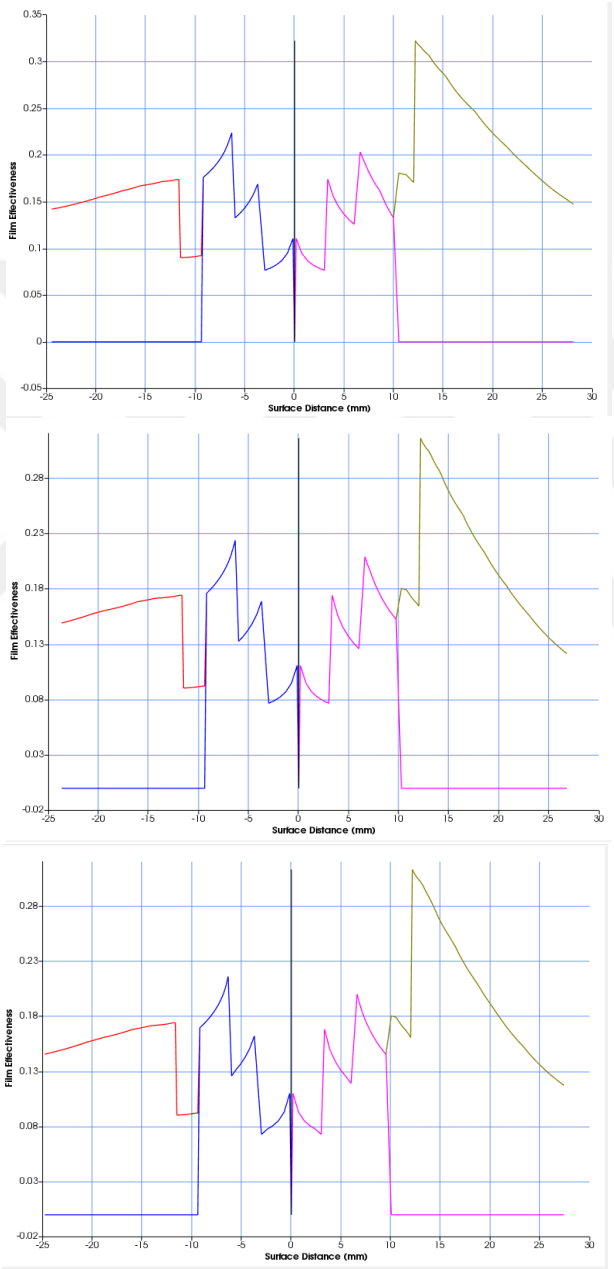

Figure 5.56 : Film Effectiveness of Tip Mid and Hub Section of The Span

5.5.2.2 1^{st} column of showerhead of pressure side of film cooling holes diameter is 0.5mm

Temperature distribution plots and temperature spans of the geometry within section 5.5.2.4 is shown in Figure 5.57 and 5.58.

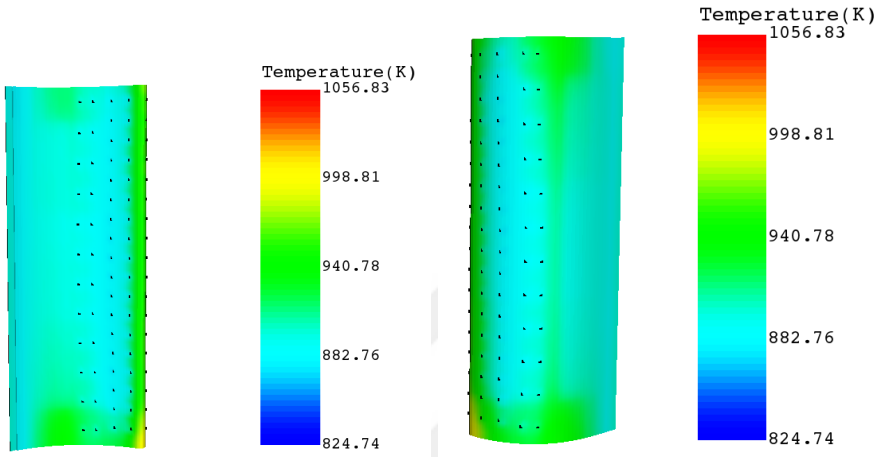

Figure 5.57 : Temperature Distribution

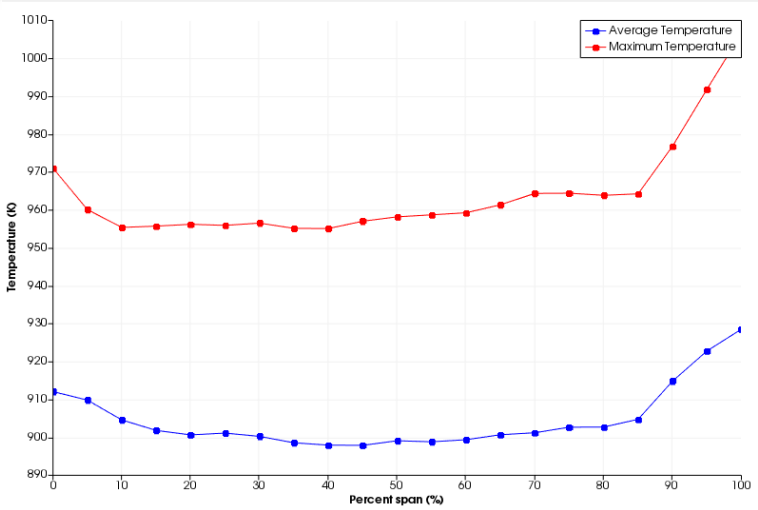

Figure 5.58 : Average and Maximum Temperature Span

Film effectiveness plots for tip, mid, and hub section of the geometry within section 5.5.2.4 is shown in Figure 5.59.

Red line shows the pressure side combined film effectiveness, blue line shows the pressure side of the showerhead film effectiveness, green line suction side combined film effectiveness, purple line shows the suction side of the showerhead film effectiveness.

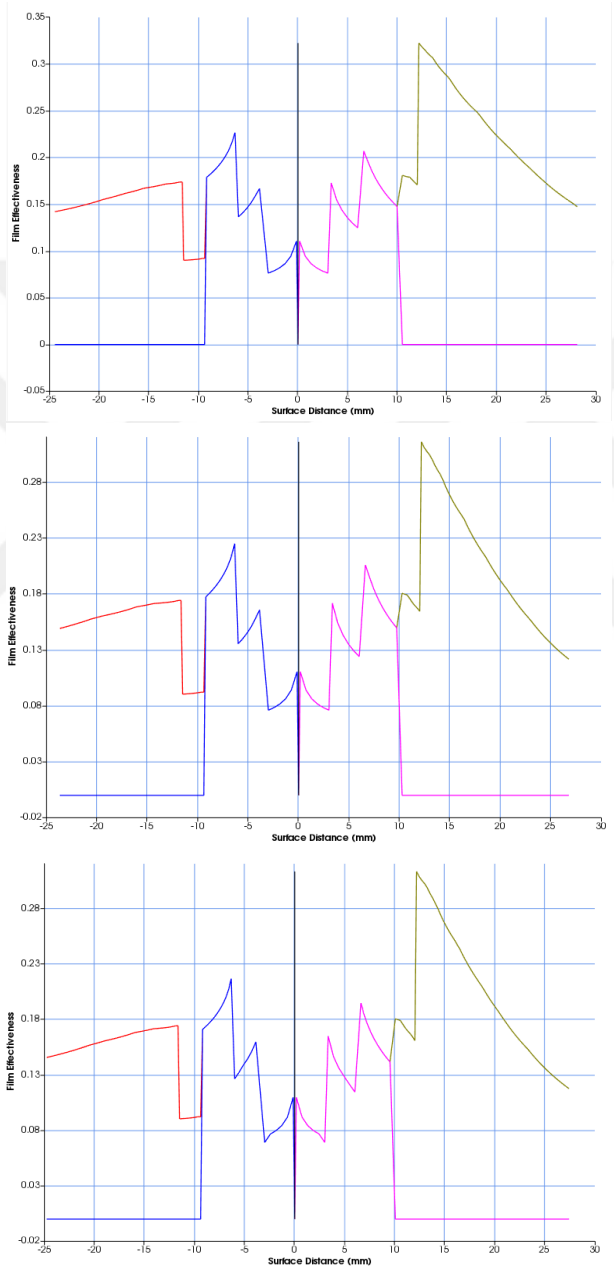

Figure 5.59 : Film Effectiveness of Tip Mid and Hub Section of The Span

5.5.2.3 1^{st} column of showerhead of suction side of film cooling holes diameter is 0.4mm

Temperature distribution plots and temperature spans of the geometry within section 5.5.2.2 is shown in Figure 5.60 and 5.61.

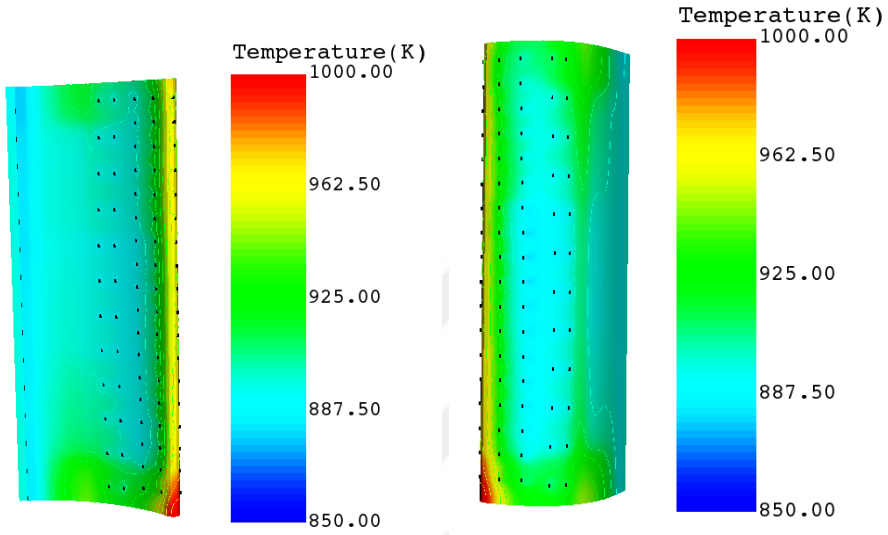

Figure 5.60 : Temperature Distribution

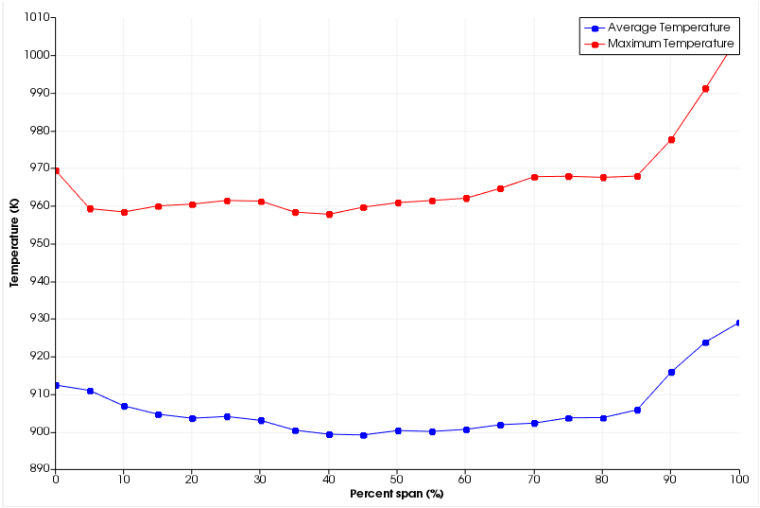

Figure 5.61 : Average and Maximum Temperature Span

Film effectiveness plots for tip, mid, and hub section of the geometry within section 5.5.2.2 is shown in Figure 5.62.

Red line shows the pressure side combined film effectiveness, blue line shows the pressure side of the showerhead film effectiveness, green line suction side combined film effectiveness, purple line shows the suction side of the showerhead film effectiveness.

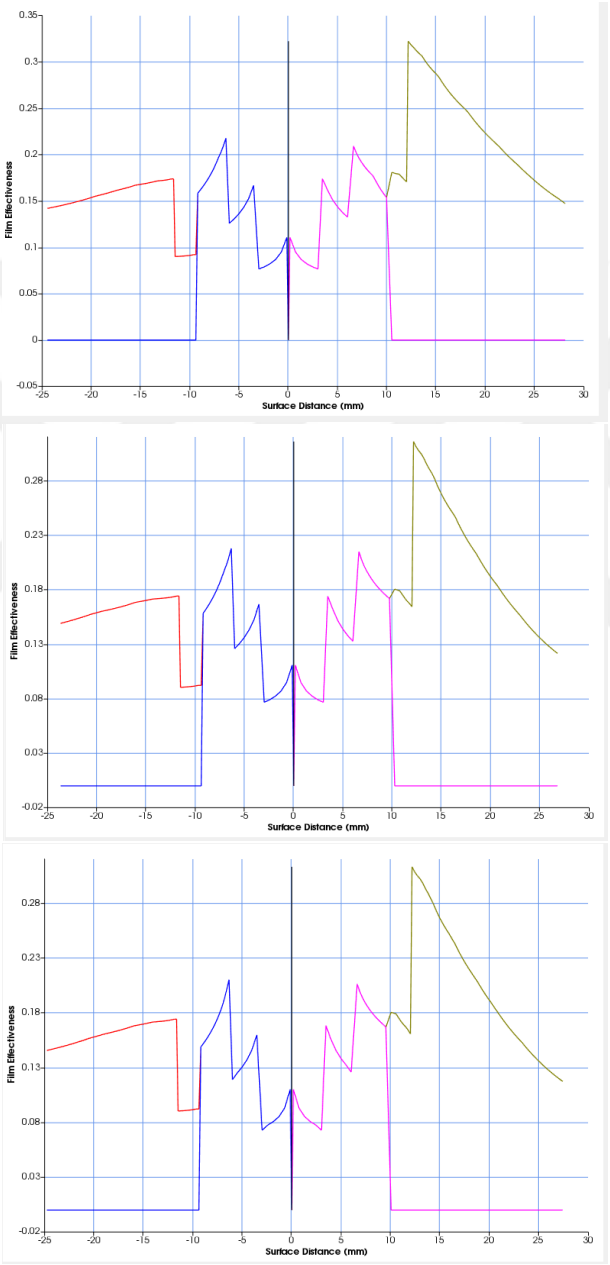

Figure 5.62 : Film Effectiveness of Tip Mid and Hub Section of The Span

5.5.2.4 1^{st} column of showerhead of suction side of film cooling holes diameter is 0.5mm

Temperature distribution plots and temperature spans of the geometry within section 5.5.2.3 is shown in Figure 5.63 and 5.64.

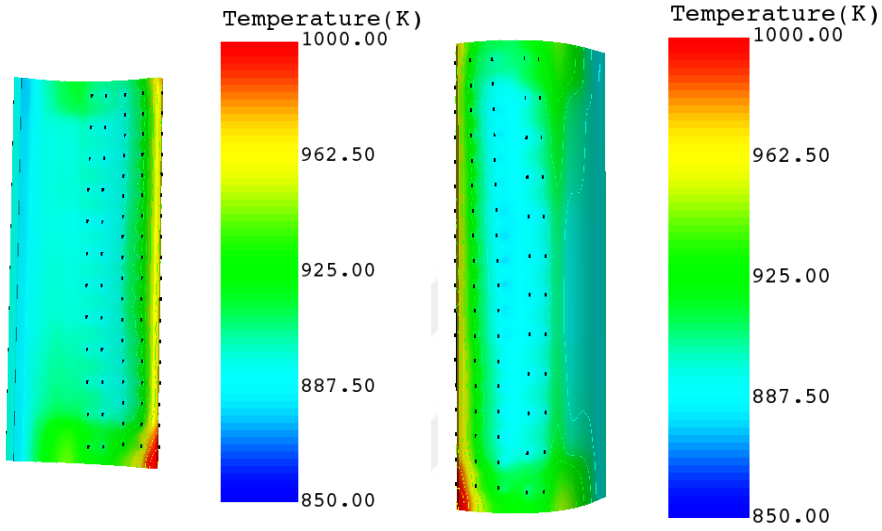

Figure 5.63 : Temperature Distribution

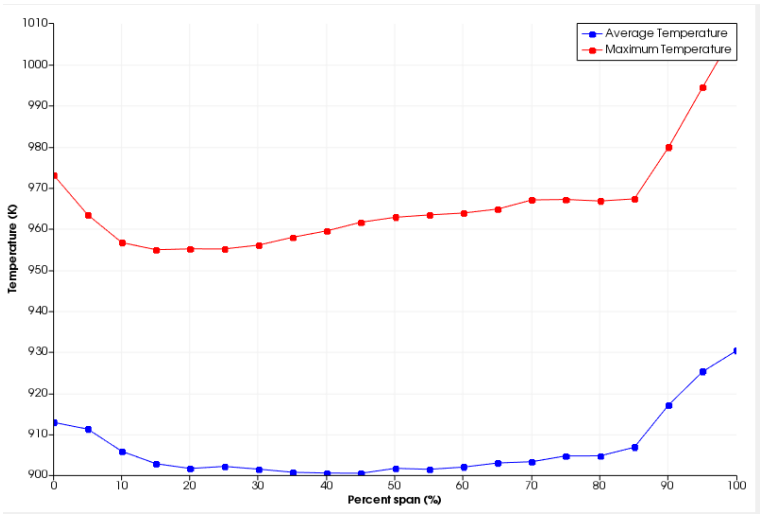

Figure 5.64 : Average and Maximum Temperature Span

Film effectiveness plots for tip, mid, and hub section of the geometry within section 5.5.2.3 is shown in Figure 5.65.

Red line shows the pressure side combined film effectiveness, blue line shows the pressure side of the showerhead film effectiveness, green line suction side combined film effectiveness, purple line shows the suction side of the showerhead film effectiveness.

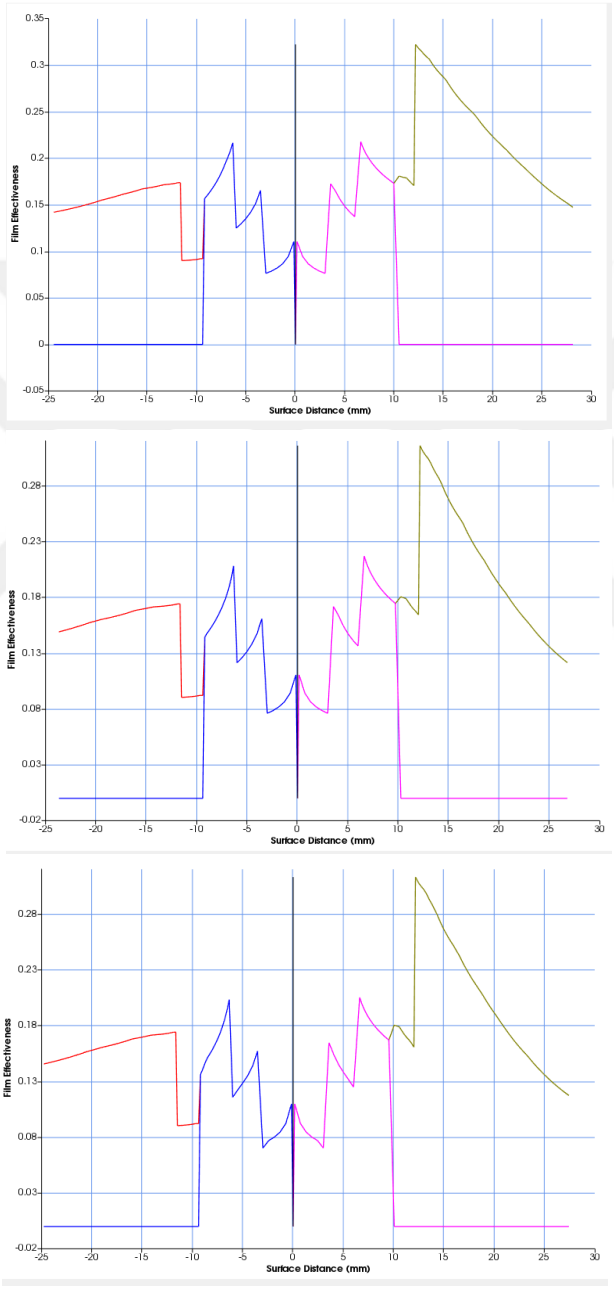

Figure 5.65 : Film Effectiveness of Tip Mid and Hub Section of The Span

5.5.2.5 2^{nd} column of showerhead of pressure side of film cooling holes diameter is 0.4mm

Temperature distribution plots and temperature spans of the geometry within section 5.5.2.5 is shown in Figure 5.66 and 5.67.

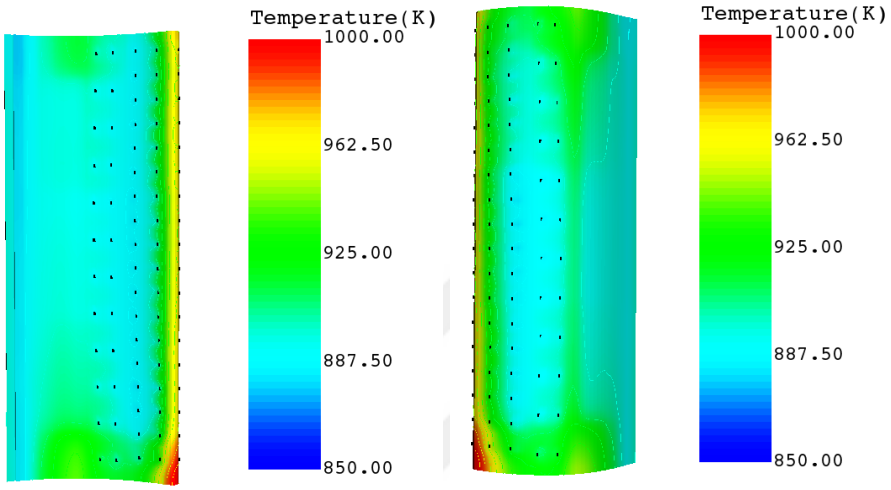

Figure 5.66 : Temperature Distribution

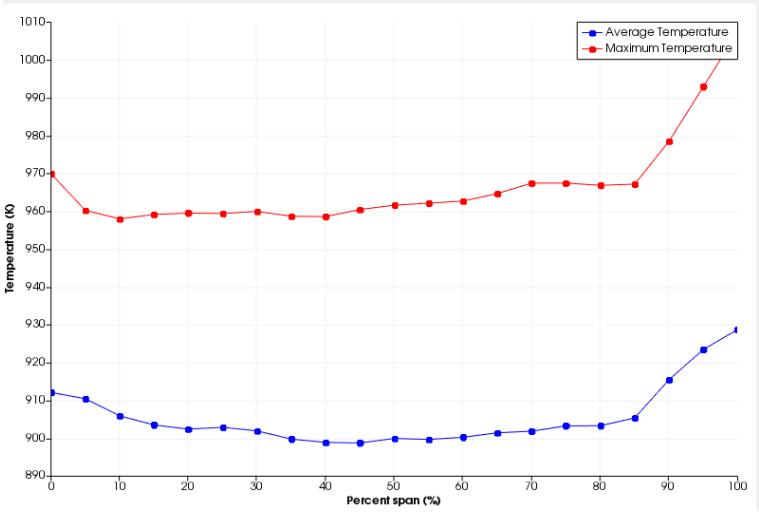

Figure 5.67 : Average and Maximum Temperature Span

Film effectiveness plots for tip, mid, and hub section of the geometry within section 5.5.2.5 is shown in Figure 5.68.

Red line shows the pressure side combined film effectiveness, blue line shows the pressure side of the showerhead film effectiveness, green line suction side combined film effectiveness, purple line shows the suction side of the showerhead film effectiveness.

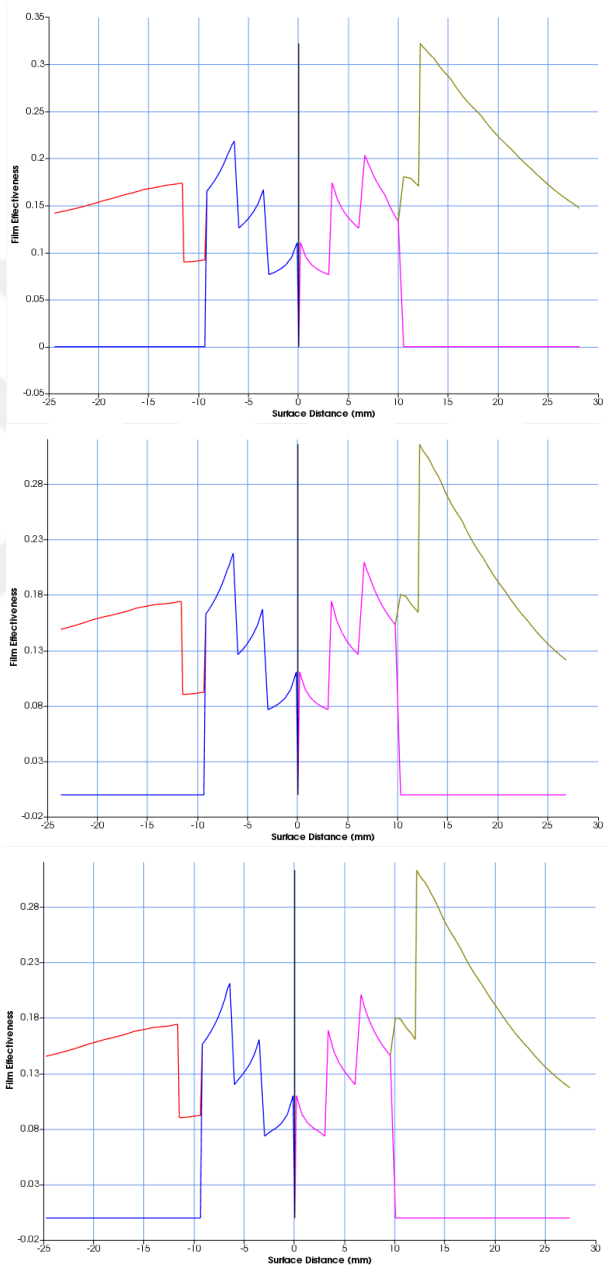

Figure 5.68 : Film Effectiveness of Tip Mid and Hub Section of The Span

5.5.2.6 2^{nd} column of showerhead of pressure side of film cooling holes diameter is 0.5mm

Temperature distribution plots and temperature spans of the geometry within section 5.5.2.6 is shown in Figure 5.69 and 5.70.

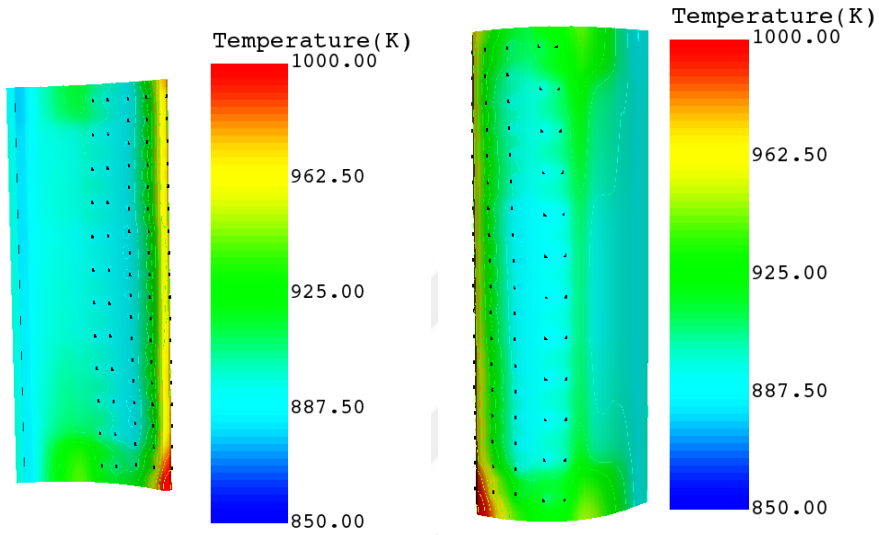

Figure 5.69 : Temperature Distribution

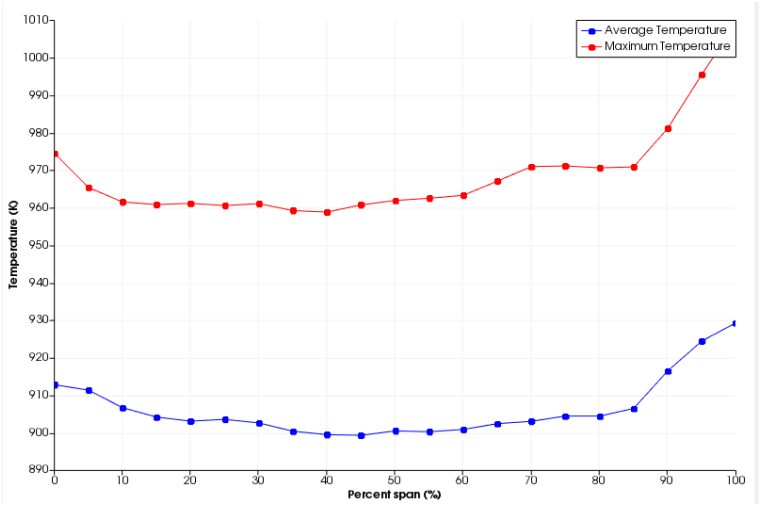

Figure 5.70 : Average and Maximum Temperature Span

Film effectiveness plots for tip, mid, and hub section of the geometry within section 5.5.2.6 is shown in Figure 5.71.

Red line shows the pressure side combined film effectiveness, blue line shows the pressure side of the showerhead film effectiveness, green line suction side combined film effectiveness, purple line shows the suction side of the showerhead film effectiveness.

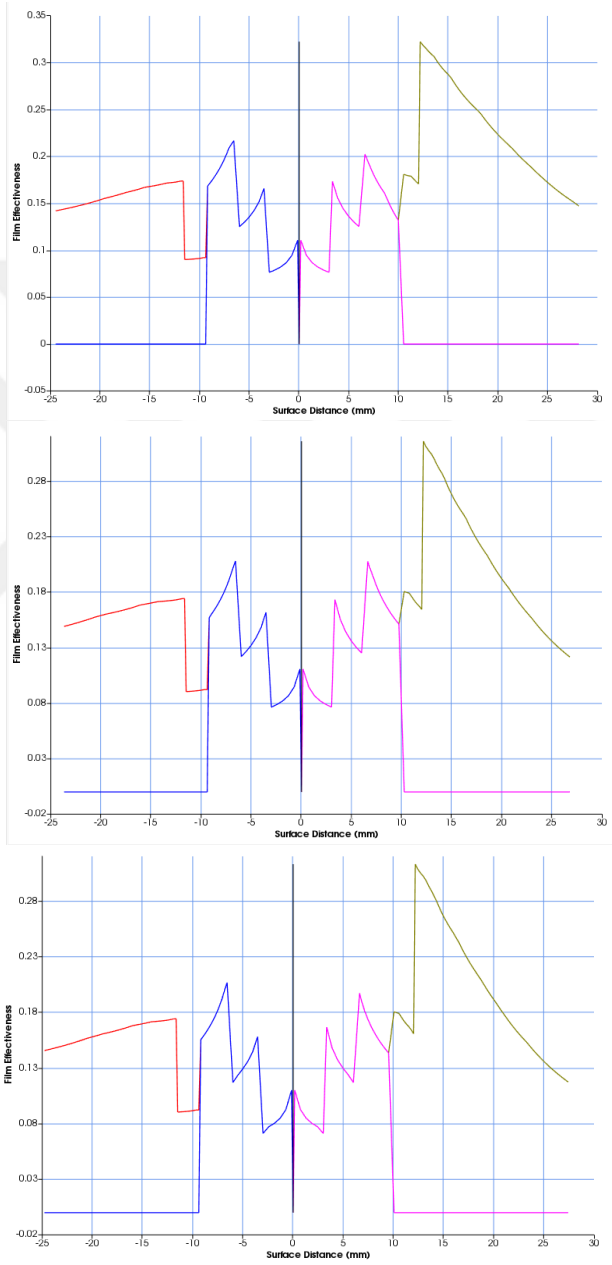

Figure 5.71 : Film Effectiveness of Tip Mid and Hub Section of The Span

5.5.2.7 Stagnation line side of film cooling holes diameter is 0.4mm

Temperature distribution plots and temperature spans of the geometry within section 5.5.2.7 is shown in Figure 5.72 and 5.73.

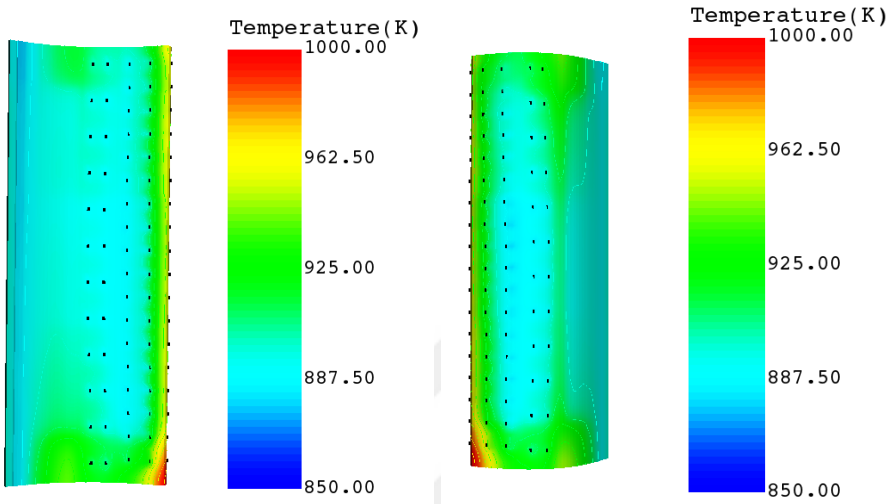

Figure 5.72 : Temperature Distribution

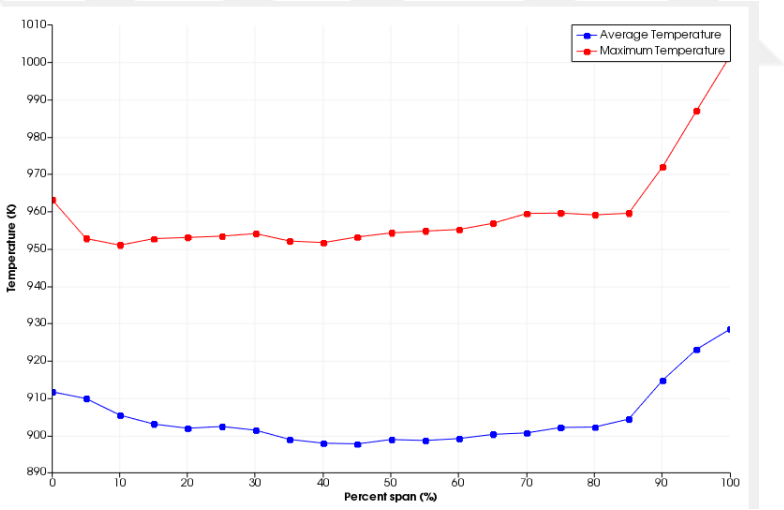

Figure 5.73 : Average and Maximum Temperature Span

Film effectiveness plots for tip, mid, and hub section of the geometry within section 5.5.2.7 is shown in Figure 5.74.

Red line shows the pressure side combined film effectiveness, blue line shows the pressure side of the showerhead film effectiveness, green line suction side combined film effectiveness, purple line shows the suction side of the showerhead film effectiveness.

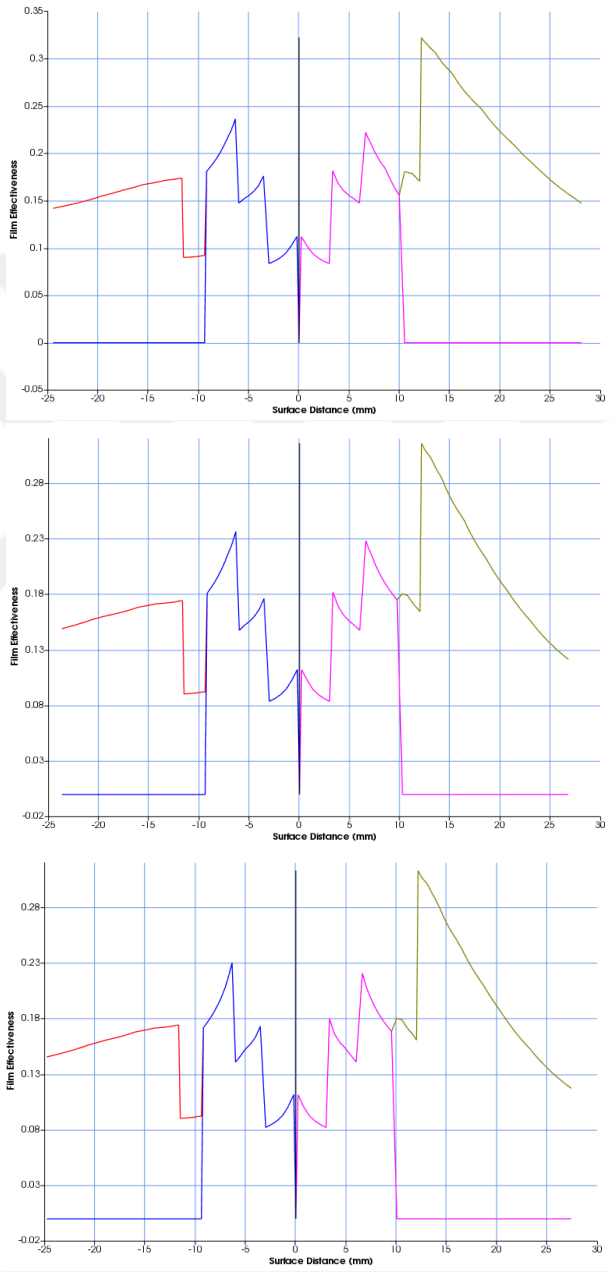

Figure 5.74 : Film Effectiveness of Tip Mid and Hub Section of The Span

5.5.2.8 Stagnation line side of film cooling holes diameter is 0.5mm

Temperature distribution plots and temperature spans of the geometry within section 5.5.2.8 is shown in Figure 5.75 and 5.76.

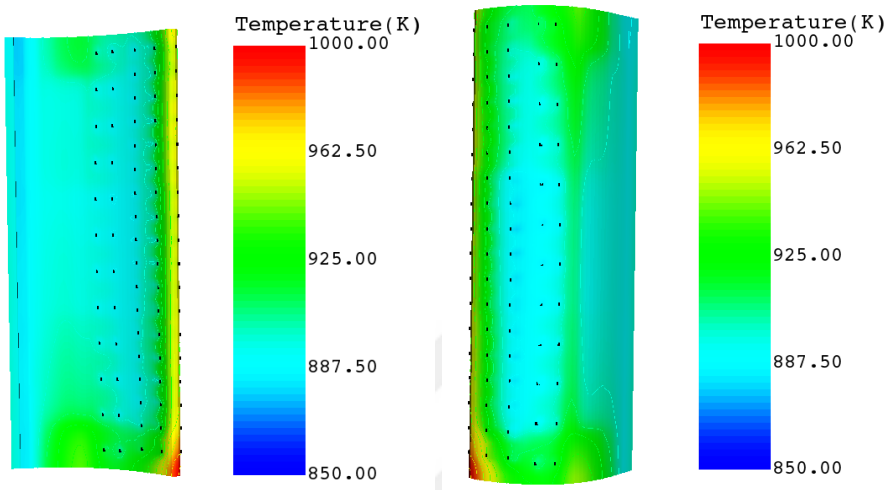

Figure 5.75 : Temperature Distribution

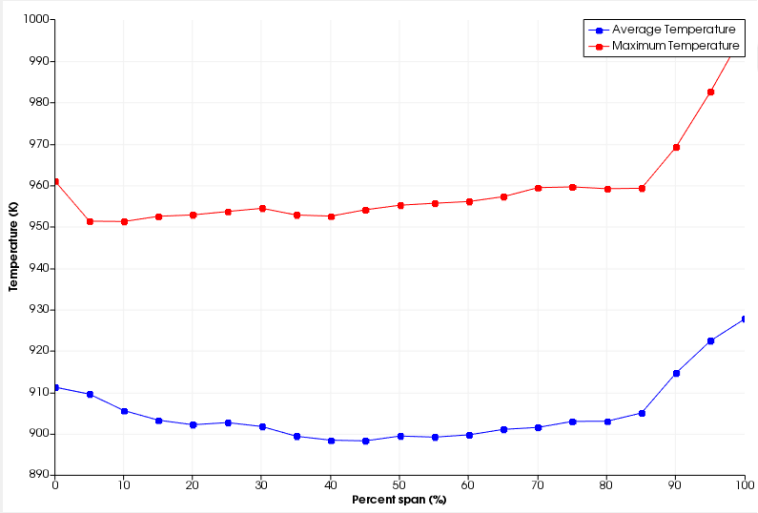

Figure 5.76 : Average and Maximum Temperature Span

Film effectiveness plots for tip, mid, and hub section of the geometry within section 5.5.2.8 is shown in Figure 5.77.

Red line shows the pressure side combined film effectiveness, blue line shows the pressure side of the showerhead film effectiveness, green line suction side combined film effectiveness, purple line shows the suction side of the showerhead film effectiveness.

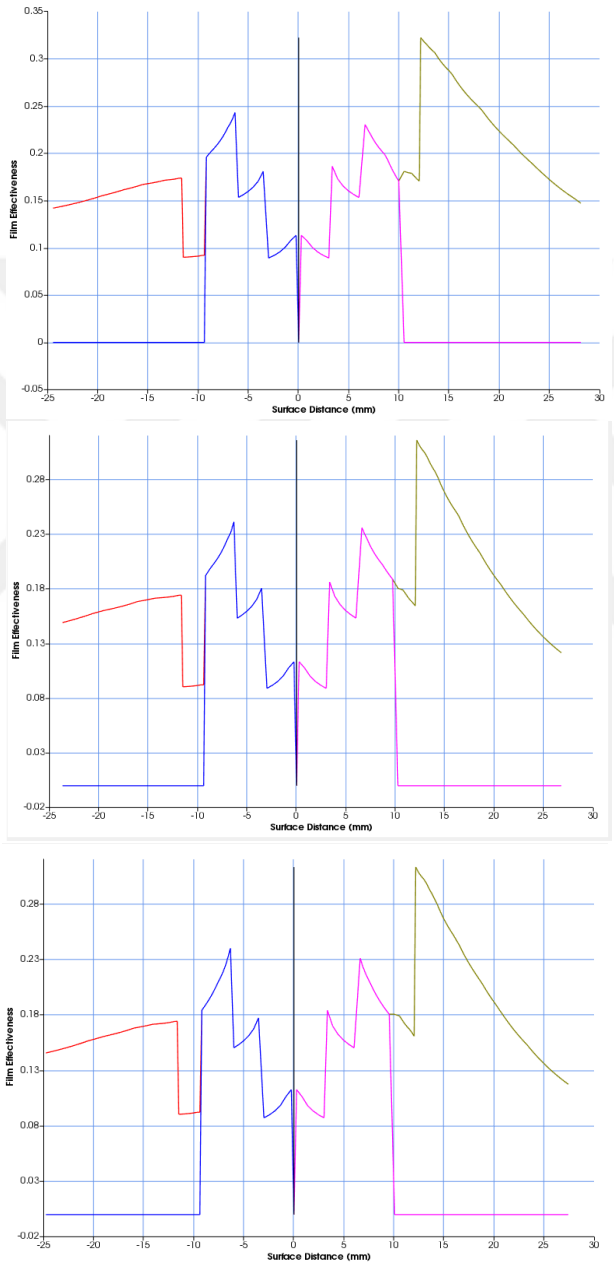

Figure 5.77 : Film Effectiveness of Tip Mid and Hub Section of The Span

5.5.2.9 Summary of showerhead and stagnation line film cooling diameter study

Showerhead holes diameters is studied for 0.4 and 0.5 mm. When the iterations are studied it is said that max temperatures are changed. As, max temparatures location is in showerhead area. Most effective results are located in stagnation line iterations. Max temperatures of the iterations are located in table 5.5.

Table 5.5 : Max Temperatures for Showerhead and Stagnation Line Study

Section	Max Temperature (K)		
	%0 Span	%50 Span	%100 Span
5.5.2.1	969	965	1005
5.5.2.2	969	961	1005
5.5.2.3	972	963	1007
5.5.2.4	971	958	1002
5.5.2.5	970	961	1003
5.5.2.6	975	961	1009
5.5.2.7	962	955	996
5.5.2.8	961	955	994

When the iterations are studied it is said that average temperatures are changed minimally. Like max temperatures, most effective results are located in stagnation line iterations. Average temperatures of the iterations are located in table 5.6.

Table 5.6 : Average Temperatures for Showerhead and Stagnation Line Study

Section	Average Temperature (K)		
	%0 Span	%50 Span	%100 Span
5.5.2.1	911	900	930
5.5.2.2	912	900	929
5.5.2.3	912	902	931
5.5.2.4	912	900	928
5.5.2.5	912	900	929
5.5.2.6	912	900	930
5.5.2.7	911	900	928
5.5.2.8	911	900	928

6. CONCLUSIONS

In this study, the cooling geometry designed for the NGV is affected by the burned gases. Selecting the most appropriate cooling configurations is numerically examined.

In the second chapter, the operation of gas turbine engines and the theoretical details of the cycle used in gas turbine engines are mentioned. Also, historical development of gas turbine engines and Brayton Cycle are explained in chapter 2.

In chapter 2, general informations about the open cycle gas turbine system is introduced. Gas turbines are classified in terms of energy input, based on cycle type, mechanical layout, used parts, and depending on the usage. Also, historical development is mentioned in section 2.2. After that, basic principles of gas turbines is introduced. Since gas turbines are operated with Brayton cycle, Brayton cycle and efficiency formulas are mentioned. Hence, Brayton Cycle with Regeneration and Brayton Cycle with Reheat and Intercooling are inspected.

In chapter 3, why cooling design is important for engines is mentioned. Advantages of cooling design is mentioned in this chapter. Basically its is said that cooling is important for gas turbines in terms of material life, lower maintenance expenses, rise of turbine output power, and turbine efficieny. Moreover, increase of turbine inlet temperatures of year by year is mentioned. Effect of the cooling techniques on the turbine inlet temperature is mentioned. Furthermore, heat transfer mechanism of gas turbines are investigated. It is imported that most of the cooling types are related with the convection type.

In chapter 4, cooling methods for gas turbine engines are studied. Basically, cooling types are divided into two sections as air cooling and liquid cooling. Liquid cooling usage are is not wide. Hence, air cooling types are various. Internal and external cooling types are detailed. Furthermore, thermal barrier coating is used for engines. TBC details are mentioned.

In chapter 5, NGV with cooling geometry is designed and analysis is made. As output, metal temperature contours are obtained. Firstly, design details are mentioned. Cooling efficiency and keeping the life maximum important for the geometry. Also 3D geometry details and nomenclature is mentioned. Mesh details and boundary conditions are mentioned. Besides, mesh independency is studied. After that iterations are located. Wall thickness effects are studied. As a result, when the geometry gets thinner, temperatures are decreased. On the other hand, manufacturing and structural concerns are also important parameters on the wall thickness. For instance, optimum cooling wall thickness may not be manufactured. In that case, wall thickness must be increased in terms of manufacturing.

When the design phase of each gas turbine engine part is completed, a technical drawing is prepared to be sent to the manufacturer. The company that will manufacture makes preparations according to this drawing. In this process, GDT symbols is defined to control the size, form, orientation and location of each element defined in the technical drawing. Sometimes, the high tolerances of some dimensions can create problems in design. The variations in the thickness variation iterations studied here can be considered as the minimum and maximum values of manufacturing tolerances. When the results are examined, there are not high differences between the temperatures.

The film cooling diameter effects on the cooling performance is studied in section 5.5.

Film Diameter variation study is performed between 0.4mm - 0.5mm. When the iterations are examined, better cooling is observed on the pressure side of the geometry. Hotter locations are seen at the end of the middle channel on the suction side. Therefore, the iterations on the pressure side are not effective in the general cooling of the geometry. Because pressure side is already colder than suction side.

Also, film effectiveness values of the geometries are located in the table 6.1.

Table 6.1 : Film Effectiveness Values

Location	Pressure Side	Suction Side
Wall	0.17	0.32
Shower Head	0.22	0.21

Better cooling is observed in the iterations on the suction side. Especially, better cooling occurs in the iterations on the middle channel side.

Hottest part of the geometry is hub and tip section of the stagnation line. Therefore, most optimum cooling is observed for the stagnation line iterations that are section 5.5.2.7 and section 5.5.2.8. The coldest geometry is obtained in 5.5.2.8 iteration.

REFERENCES

[1] **Han, J.**, **Dutta, S. and Ekkad, S.** (2012). *Gas Turbine Heat Transfer and Cooling Technology, Second Edition*, Taylor & Francis.

[2] **Cengel, Y.A.**, **Boles, M.A. and Kanoğlu, M.** (2011). *Thermodynamics: an engineering approach*, volume 5, McGraw-hill New York.

[3] **Moore, C.** (1991). Encyclopedia of chemical technology, Mass spectrometry, Wiley, New York, 4. edition.

[4] **Royce, R.** (2015). *The jet engine*, John Wiley & Sons.

[5] **Yin, F. and Rao, A.G.** (2017). Performance analysis of an aero engine with inter-stage turbine burner, *The Aeronautical Journal*, *121*(1245), 1605–1626.

[6] **Naik, S.** (2017). *Basic Aspects of Gas Turbine Heat Transfer. Heat Exchangers - Design, Experiment and Simulation*.

[7] **Wang, W.**, **Yan, Y.**, **Zhou, Y. and Cui, J.** (2022). Review of Advanced Effusive Cooling for Gas Turbine Blades, *Energies*, *15*(22), 8568.

[8] **Bergman, T.**, **Lavine, A. and Incropera, F.** (2011). *Fundamentals of Heat and Mass Transfer, 7th Edition*, John Wiley & Sons, Incorporated.

[9] **Rasimarzabadi, F.**, **Kamalimoghadam, R.**, **Najafi, M.**, **Mohammadi, M. and Sahranavard Fard, N.** (2020). Cooling Improvement of Gas Turbine Rotary Blades, *Volume 7C: Heat Transfer*, V07CT14A019.

[10] **Froissart, M. and Ochrymiuk, T.** (2021). Thermal-Fluidndash;Solid Couplingm-dash;Parametrical Numerical Analysis of Hot Turbine Nozzle Guide Vane, *Materials*, *14*(23).

[11] **Hossain, A.**, **Ameri, A. and Bons, J.** (2021). Conjugate Heat Transfer Study of Innovative Pin-Fin Cooling Configuration, *Journal of Propulsion and Power*, *37*, 1–11.

[12] **R.K. Matta, G.D. Mercer, R.T.** Power Systems for the 21st Century – “H” Gas Turbine Combined-Cycles.

[13] **Bunker, R.S.**, **Dees, J.E. and Palafox, P.** (2014). Impingement Cooling In Gas Turbines:Design, Applications, And Limitations, *WIT Transactions on State-of-the-art in Science and Engineering*, *76*.

[14] **Bathie, W.** (1996). *Fundamentals of Gas Turbines*, Wiley.

[15] **Ekkad, S. and Han, J.C.** (2013). A Review of Hole Geometry and Coolant Density Effect on Film Cooling, volume 6.

[16] **G. James Van Fossen, J. and Stepka, F.** (April, 1979). Review and Status of Liquid-Cooling Technology for Gas Turbines, *National Aeronautics and Space Administration, Scientific and Technical Information Office*.

[17] **Robert D. Thulin, D.C.H. and Singer, I.D.** (January, 1982). High-Pressure Turbine Detailed Design Report, *National Aeronautics and Space Administration, Lewis Search Center*.

[18] **Halila, E. E., L.D.T. and Thomas, T.T.** (June 1, 1982). Energy Efficient Engine: High-Pressure Turbine Test Hardware Detailed Design Report, *National Aeronautics and Space Administration, Lewis Search Center*.

[19] **Özkan, D.** (2009). *GAZ TÜRBİNİ ÇALIŞMA DONANIMLARININ İNCELENMESİ, AxSTREAM PROGRAMI İLE EKSENEL AKIŞLI KOMPRESÖR VE TÜRBĠN DİZAYNI - ANALİZİ*.

[20] **Frey, H. and Zhu, Y.**, (2012). 11 - Techno-economic analysis of combined cycle systems, **A.D. Rao**, editor, Combined Cycle Systems for Near-Zero Emission Power Generation, Woodhead Publishing Series in Energy, Woodhead Publishing, pp.306–328.

[21] **Lopez, P.F.** (1994). Aerodynamic aspects of film cooling.

[22] **Öztürk, E.** (1997). Türbin Motorların Aerotermodinamiği ve Mekaniği, *Birsen Yayınevi, İstanbul*.

[23] **Suo, M.** (1985). Turbine cooling, *Aerothermodynamics of Aircraft Engine Components*, 275–328.

[24] **El-Jummah, A.M.** (2014). *Impingement and impingement/effusion cooling of gas turbine components: conjugate heat transfer predictions*, University of Leeds.

[25] **Saravanamuttoo, H.I.H.**, **Rogers, G.F.C.**, **Cohen, H. and Straznicky, P.V.** (2009). *Gas Turbine Theory*, Pearson Prentice Hall, Harlow, England; New York, 6 edition.

[26] **Lakshminarayana, B.** (1995). *Fluid dynamics and heat transfer of turbomachinery*, John Wiley & Sons.

[27] **Altorairi, M.** (2003). Film Cooling From Cylindrical Holes In Transverse Slots.

[28] **Sultanian, B.** (2018). Review of Thermodynamics, Fluid Mechanics, and Heat Transfer, Cambridge Aerospace Series, Cambridge University Press, p.34–142.

[29] **Nelson, W.A.**, **Orenstein, R.M.**, **DiMascio, P.S. and Johnson, C.A.** (1995). Development of Advanced Thermal Barrier Coatings for Severe Environments, *Volume 4: Heat Transfer; Electric Power; Industrial and Cogeneration*, V004T10A011.

[30] **Han, J.C.** (2004). Recent Studies in Turbine Blade Cooling, *International Journal of Rotating Machinery*, *10*.

[31] **Bredberg, J.** (2002). Turbulence Modelling for Internal Cooling of Gas-Turbine Blades.

[32] **Sundberg, J.** (2006). Heat Transfer Correlations for Gas Turbine Cooling.

[33] **Polezhaev, J.** (1997). The transpiration cooling for blades of high temperatures gas turbine, *Energy Conversion and Management*, *38*(10), 1123–1133, international Symposium on Advance Energy Conversion Systems and Related Technologies.

[34] **Sundaram, N. and Thole, K.A.** (2008). Bump and Trench Modifications to Film-Cooling Holes at the Vane-Endwall Junction, *Journal of Turbomachinery*, *130*(4), 041013, https://doi.org/10.1115/1.2812933.

[35] **Koç, İ.** (2006). *Gaz Türbin Kanadı Üzerinde Film Soğutmanın Sayısal Ve Deneysel İncelenmesi*, Fen Bilimleri Enstitüsü.

[36] **Hironori Takahashi, Chayut Nuntadusit, H.K.H.I.T.U.K.T.** (2006). Characterisctic of Various Film Cooling Jets Injected in a Conduit.

[37] **NREC, C.** (2003). *CTAADS Tutorial*.

[38] **Herbert Martin Hofmann, Rafael Kaiser, M.K. and Martin, H.** (2007). Calculations of Steady and Pulsating Impinging Jets—An Assessment of 13 Widely used Turbulence Models, *Numerical Heat Transfer, Part B: Fundamentals*, *51*(6), 565–583.

[39] **Kannan B.T. and Sundararaj, S.** (2015). Steady State Jet Impingement Heat Transfer from Axisymmetric Plates with and without Grooves, *Procedia Engineering*, *127*, 25–32, iNTERNATIONAL CONFERENCE ON COMPUTATIONAL HEAT AND MASS TRANSFER (ICCHMT) - 2015.

[40] **Sharif, M.A.R. and Mothe, K.K.** (2009). Evaluation of Turbulence Models in the Prediction of Heat Transfer Due to Slot Jet Impingement on Plane and Concave Surfaces, *Numerical Heat Transfer, Part B: Fundamentals*, *55*(4), 273–294.

[41] **Dutta, R.**, **Dewan, A. and Srinivasan, B.** (2013). Comparison of various integration to wall (ITW) RANS models for predicting turbulent slot jet impingement heat transfer, *International Journal of Heat and Mass Transfer*, *65*, 750–764.

[42] **Torroba, A.**, **Köser, O.**, **Calba, L.**, **Maestro, L.**, **Carreno-Morelli, E.**, **Rahimian, M.**, **Milenkovic, S.**, **Sabirov, I. and Llorca, J.** (2014). Investment casting of nozzle guide vanes from nickel-based superalloys: part I—thermal calibration and porosity prediction, *Integrating Materials and Manufacturing Innovation*, *3*, 25.

APPENDICES

APPENDIX A : Material Details

APPENDIX A :

Ni	C	Cr	Co	Mo	W	Ta	Al	Ti	Hf
Base	0.15	8.4	10	0.7	10	3.1	5.5	1.05	1.4

Figure A.1 : Chemical Composition of Mar-M247 [42]

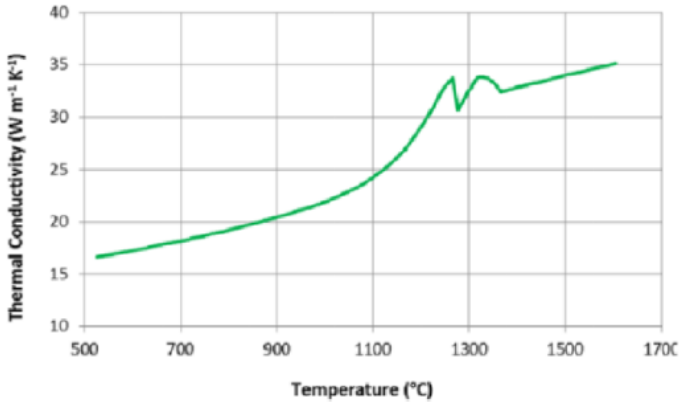

Figure A.2 : Thermal Conductivity of Mar-M247 [42]

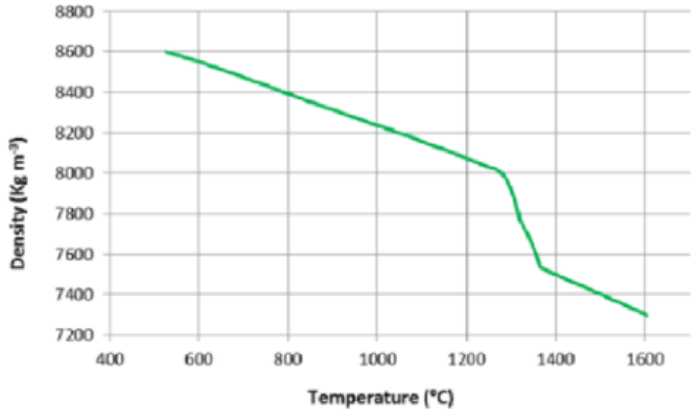

Figure A.3 : Density of Mar-M247 [42]

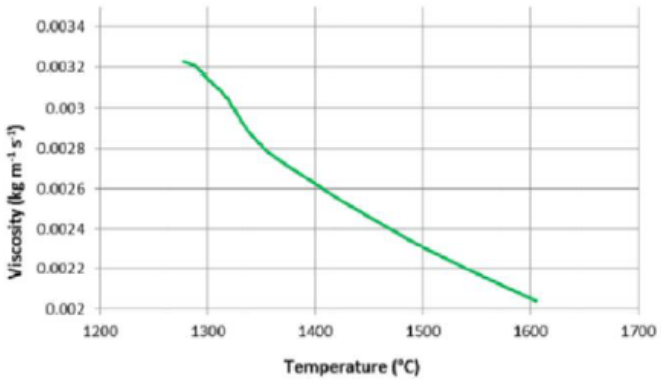

Figure A.4 : Viscosity of Mar-M247
[42]

CURRICULUM VITAE

Name SURNAME : Alparslan HALAÇ

EDUCATION :

- **B.Sc.:** 2020, Istanbul Technical University, Faculty of Mechanical Engineering, Mechanical Engineering Department

PROFESSIONAL EXPERIENCE AND REWARDS:

- **Halac A.,** Gunes H. (2024). NOZZLE GUIDE VANE COOLING DESIGN FOR THE GAS TURBINE ENGINES. INTERNATIONAL GRADUATE RESEARCH SYMPOSIUM IGRS'24, 8-10 May 2024 Istanbul, Turkey.